

FLIGHT PERFORMANCE IN BATS AND ITS ECOMORPHOLOGICAL
IMPLICATIONS

BY

JOSÉ IRIARTE-DÍAZ

B.Sc. UNIVERSIDAD DE CHILE 1998

M. Sc. UNIVERSIDAD DE CHILE 2002

A DISSERTATION SUBMITTED IN PARTIAL FULFILLMENT OF THE
REQUIREMENTS FOR THE DEGREE OF DOCTOR OF PHILOSOPHY IN THE
DIVISION OF BIOLOGY AND MEDICINE AT BROWN UNIVERSITY

PROVIDENCE, RHODE ISLAND

MAY 2009

© Copyright 2009 by José Iriarte-Díaz

This dissertation by José Iriarte-Díaz is accepted in its present form by the Department of Ecology and Evolutionary Biology as satisfying the dissertation requirement for the degree of Doctor of Philosophy.

Date _____

Sharon M. Swartz, Advisor

Recommended to the Graduate Council

Date _____

Kenneth S. Breuer, Reader

Date _____

Stephen M. Gatesy, Reader

Date _____

Duncan J. Irschick, Reader

Date _____

Thomas J. Roberts, Reader

Approved by the Graduate Council

Date _____

Sheila Bonde, Dean of the Graduate School

CURRICULUM VITAE

DATE AND PLACE OF BIRTH

08 October, 1976
Santiago, Chile

EDUCATION

- 2002 – present Doctoral candidate
Department of Ecology and Evolutionary Biology
Brown University
- 2000 – 2002 Master of Science
Departamento de Ciencias Ecológicas, Facultad de Ciencias
Universidad de Chile
- 1995 – 1998 Licenciatura en Ciencias con mención Biología
Facultad de Ciencias
Universidad de Chile

PUBLICATIONS

- Riskin, D. K., Willis, D. J., Iriarte-Diaz, J., Hedrick, T. L., Kostandov, M., Chen, J., Laidlaw, D. H., Breuer, K. S. & Swartz, S. M.** (in press) Quantifying the complexity of bat wing kinematics. *J. Theor. Biol.*
- Iriarte-Diaz, J., Bozinovic, F. & Vasquez, R. A.** (2006) What explains the trot-gallop transition in a small mammal? *J. Exp. Biol.* **209**: 4061-4066.
- Tian, X., Iriarte-Diaz, J., Middleton, K., Galvao, R., Israeli, E., Roemer, A., Sullivan, A., Song, A., Swartz, S. M. & Breuer, K.** (2006) Direct measurements of the kinematics and dynamics of bat flight. *Bioinspiration & Biomimetics* **1**: S10-S18.
- Canals, M., Atala, C., Grossi, B. & Iriarte-Diaz, J.** (2005). Relative size of hearts and lungs of small bats. *Acta Chiropt.* **7**: 65-72.
- Canals, M., Grossi, B., Iriarte-Diaz, J. & Veloso, C.** (2005). Biomechanical and ecological relationships of wing morphology of eight Chilean bats. *Rev. Chil. Hist. Nat.* **78**: 215-227.
- Saavedra, B., Quiroz, D., Iriarte, J.** (2004). Past and present: small mammals of Isla Mocha (Chile). *Mammal. Biol.* **68**: 365-371.
- Iriarte-Diaz, J.** (2002). Differential scaling of locomotor performance in small and large terrestrial mammals. *J. Exp. Biol.* **205**: 2897-2908.

- Iriarte-Díaz, J., Novoa, F. F. & Canals, M.** (2002). Comparative wing morphology of two species of Chilean bats *Tadarida brasiliensis* and *Myotis chiloensis*, and their biomechanic consequences. *Acta Theriol.* **47**: 193-200.
- Bacigalupe, L. D., Iriarte-Díaz, J. & Bozinovic, F.** (2002) Functional morphology and geographic variation in the digging apparatus of cururos (*Spalacopus cyanus*, octodontidae). *J.Mammal.* **83**: 145-152.
- Canals, M., Iriarte-Díaz, J., Olivares, R. & Novoa, F. F.** (2001) Comparación de la morfología alar de los quirópteros *Tadarida brasiliensis* (Chiroptera: Molossidae) y *Myotis chiloensis* (Chiroptera: Vespertilionidae), representantes de dos diferentes patrones de vuelo. *Rev. Chil. Hist. Nat.* **74**: 699-704.

PUBLISHED ABSTRACTS

- Riskin, D. K., Iriarte-Díaz, J., Middleton, K. Breuer, K. S. & Swartz, S. M.** (2008) Effects of body size on the wing kinematics of bats. *Comp. Biochem. Physiol. A* **150**: S78.
- Swartz, S.M., Galvao, R., Iriarte-Díaz, J., Israeli, E., Middleton, K., Roemer, R., Tian, X. & Breuer, K.** (2005) Unique characteristics of aerodynamics of bat flight evidence from direct visualization of patterns of airflow in the wakes of naturally flying bats. *Integ. Comp. Biol.* **45**: 1080.
- Iriarte-Díaz, J. & Lee, M. –M.** (2004) Kinematics of slow turning maneuvering in bats. *Integ. Comp. Biol.* **44**: 575.
- Swartz, S.M., Middleton, K.M., Iriarte-Díaz, J., Lee, M., Wofford, J.M., Breuer, K.S. & Ritter, D.A.** (2004) Can bats actively control the mechanical properties of the wing membrane? *Integ. Comp. Biol.* **44**: 751.
- Iriarte-Díaz, J., Vásquez, R. A. & Bozinovic, F.** (2004) Trot-gallop transition in a small mammal. *Integ. Comp. Biol.* **43**: 1030.
- Sartori, D, Iriarte, J., Cecchi, C., Veloso, C. & Vásquez, R. A.** (2000) Reconocimiento de parentesco en el roedor caviomorfo *Octodon degus*. *Biol. Res.* **33**: R53.
- Iriarte-Díaz, J. & Canals, M.** (2000) Predictores morfológicos del desempeño locomotor en mamíferos terrestres. *Biol. Res.* **33**: R75.
- Iriarte, J., Atala, C., Novoa, F. F. & Canals, M.** (1999) Morfometría comparada de dos especies de murciélagos chilenos y su correlación con la conducta de vuelo. *Biol. Res.* **32**: R151.
- Iriarte, J.** (1998) Escalamiento diferencial de la velocidad máxima estandarizada en mamíferos terrestres. *Noticiero de Biología* **6**: 119.

Iriarte, J., Moreno, K., Rubilar, D. & Vargas, A. (1999) A titanosaurid from quebraba La Higuera (late cretaceous), III Region, Chile. *Ameghiniana* **36**: 102.

INVITED SEMINARS

2008 Department of Organismal Biology and Anatomy, University of Chicago
2008 Graduate Program in Organismal and Evolutionary Biology, University of Massachusetts, Amherst
2006 Facultad de Ciencias, Universidad de Chile

HONORS AND AWARDS

2007 John J. Peterson Fellow, Brown University
2007 Dean's Teaching Excellence Award, The Warren Alpert Medical School of Brown University
2001 Partial Financing of Thesis grant, Departamento de Postgrado y Postítulo de la Vicerrectoría de Asuntos Académicos, Universidad de Chile
1998 Academic Excellent Scholarship, Facultad de Ciencias, Universidad de Chile

TEACHING EXPERIENCE

At Brown University

2004 – 2007 Teaching assistant. Human Morphology (BI 181)
2003 – 2004 Teaching assistant. Comparative Biology of Vertebrates (BI 188)
2002 Teaching assistant. Biological Design (BI 040)

At Universidad de Chile

2001 Guest lecturer. Vertebrate Biology (EC 410)
2000 – 2001 Lecturer. Biostatistics (EC 530)
1999 Teaching assistant. Biostatistics (EC 530)
1996 Teaching assistant. Developmental Biology (BC 220)

RESEARCH EXPERIENCE

2001 Research assistant. Use of time and energy of small endotherms in natural conditions: physiological constraints, behavioral processes, and ecological consequences (Francisco Bozinovic, PI), Pontificia Universidad Católica de Chile
1999 -2001 Research assistant. Plasticity and trade-offs in behavioral ecology: use of information, time and energy in fluctuating environments (Rodrigo A. Vásquez, PI), Facultad de Ciencias, Universidad de Chile

SERVICE

Reviewer for

Revista Chilena de Historia Natural
Physiological and Biochemical Biology

ACKNOWLEDGMENTS

This dissertation could have not been possible without the help of many people. I would like to start by thanking my advisor, Sharon M. Swartz, who so warm-heartedly received me in her lab. She provided me with a great environment for my development as a scientist. Her expertise and ideas helped shape my dissertation and affected profoundly my view of how to approach the study of functional systems. I thank my committee, Kenny Breuer, Steve Gatesy, Duncan Irschick, and Tom Roberts for insightful discussion and for inputs to my research. In particular, Kenny Breuer for helping me understand the complex aerodynamics of compliant membranes and for discussions of the turning mechanics of bats, Steve Gatesy for always challenging me to think out-of-the-box, Tom Roberts for sharing his expertise in biomechanical systems, and Duncan Irsichick for providing valuable insight into my work from an ecomorphological perspective. I would like to thank the entire Morphology group at Brown University, by being so generous with their time and by providing incredible helpful discussions and comments on projects and manuscripts. I am in debt to Carol Casper, Shannon Silva, Bonnie Horta, Adella Francis, and Trina Pappadia for making disappear every little, tiny problem that I would encounter. Because of their incredible efficiency I had no excuse but to blame myself for not progressing enough on my dissertation.

I would like to thank Andy Biewener who allowed us to use the Concord Field Station's facilities for all our experiments, providing space, equipments, and technical support. In the same vein, I would like to thank his students (Chris Richards, Angie Berg, Russell Main, Carlos Moreno, Ed Yoo, Craig McGowan, Ivo Ros) and postdocs (Dave Lee, Polly McGuigan, Andrew Carroll) for making the Field Station such a fun and scientifically inspiring environment. In particular, Ty Hedrick, that first as a graduate student at the Field Station, and after as a visiting researcher in our lab, was a constant source of technical support, whose vast expertise was absolutely essential at several points in this dissertation. Pedro Ramírez deserves special consideration for taking such a wonderful care of our bats. And to Peg, Lisa, and Ken, for invaluable logistic support.

The people of the Bat Lab are worthy of special recognition. The work presented in this thesis could have never being obtained and analyzed without the help and

extremely hard work provided by fantastic undergraduate and graduate students, postdocs and friends. Because all the experiments were carried out at the Concord Field Station, our summers were constantly on the road, up and down I-95 between Providence and Bedford. Without them this work would have been brutal. Special thanks to Kevin Middleton, Allyce Sullivan, Joe Bahlman, Rachel Roemer, Arnold Song, Ming-Ming Lee, Joe Wolford, Ann xx, Xiadong Tian, and Claudio Hetz for the long hours spent driving, setting up and running experiments. I have been incredibly fortunate to have a group of colleagues with such a diverse interests and expertise. Kevin Middleton, Tatjana Hubel, Dave Willis, Arnold Song, Joe Bahlman, and Nick Hristov provided fun and really helpful discussions throughout my dissertation. In particular, I will be always in debt to Dan Riskin. He was kind enough to read, correct, and offer suggestions on incredibly long, and many times absolutely horrible manuscripts. But beyond the scientific support provided, Dan also brought to the lab Frisbee-golf and an incredibly positive attitude, making it a wonderful and fun place to work. Thanks dude!

During my time in Providence I had a very nomadic life, moving from place to place on a daily basis looking for that perfect working spot. I am grateful to everybody that housed me during my working hours. In this respect I owe a lot to the Sala Lab for welcoming in their lair. I spent many, many hours in coffee shops, and a large portion of this work was done enjoying either a cup of mocha or hot chocolate. In particular, I would like to express my gratitude to the people of Coffee Exchange, The Edge, Blue State Café, and Starbucks for allowing me to hog their tables.

I believe that the only way to maintain a certain level of sanity during grad school is to have a strong group of friends. In this sense I have been extremely lucky. I had the opportunity to meet and share with amazing people and cannot thank enough the 'latin gang' for being there for me. They became my family away from home. Pedro and Lucía, Maggy and Angel, Lara and Paco, Omer and Judith, Jen and Guille, Ruben and Maya, Julia and Luca, Isa and Dave, Ana y Andrés, Jota y Andrés, and last but not least, Laureano, that, with their friendship and kindness have made living in Providence a constant celebration. I also thank my roommates, Ronan, Lole and Mike, Pauline (cra-

cra) and Jeremy, for bearing with my weird working hours and for their friendship throughout this time, and specially for not getting mad at me for drinking all their beers.

I would like to thank the undying support of my family. They have gone through a lot to give me the opportunity to pursue my dreams. My mom sacrificed plenty to put me through school and to provide me with an environment where I could develop as a person and as a scientist. She believed in me when I told her that I wanted to study biology, in a country where, most of the time, studying sciences means a very likely position in the list of unemployment. She supported me when I told her that I wanted to study abroad and she continued doing so from far. I would like to thank my brother, who has been a constant source of inspiration and admiration, for his support through this journey. My nieces, Casandra, Zoe, Bruna, and Aurelia, have been always in my thoughts. It has been hard to see them grow in the distance but it makes me very happy to see how they became such beautiful persons.

Finally, I would like to thank my *pb*, Valentine Baud, who despite all we have gone through has been always there, supporting me even in difficult situations. Many portions of this dissertation were only possible because of her love, encouragement, and patience. She lifted me when I was down and for that I will be always grateful.

TABLE OF CONTENTS

<i>Curriculum vitae</i>	iv
Acknowledgment	viii
List of illustrations	xiv
List of tables	xviii
Chapter 1: Kinematics of slow turning maneuvering in the fruit bat <i>Cynopterus brachyotis</i>	1
Abstract	2
Introduction	3
Materials and methods	6
Results	17
Discussion	26
Acknowledgments	36
List of symbols	36
References	38
Supplementary figure 1	41
Chapter 2: Modulation of wingbeat kinematics with flight speed in the fruit bat <i>Cynopterus brachyotis</i>	42
Abstract	43
Introduction	44
Material and methods	45
Results	55

Discussion	62
List of symbols	69
Acknowledgments	70
References	70
Chapter 3: No net thrust on the upstroke: whole-body kinematics of a fruit bat reveal the influence of wing inertia on body accelerations	74
Abstract	75
Introduction	76
Material and methods	79
Results	84
Discussion	86
List of symbols	91
Acknowledgments	91
References	92
Chapter 4: The effect of loading on the loading kinematics of a fruit bat	94
Abstract	95
Introduction	96
Material and methods	98
Results	108
Discussion	112
List of symbols	118
Acknowledgments	119

References	119
Chapter 5: Ecomorphological approach to the study of flight in bats	124
Introduction	125
What is ecomorphology?	126
Ecomorphology of the flight of bats: wing shape, flight performance and ecology	127
Case studies	136
Conclusions	144
References	146

LIST OF ILLUSTRATIONS

Chapter 1

Figure 1	Diagram showing two types of turning mechanisms	4
Figure 2	Superior view of turning portion of the flight corridor, indicating the position of the calibrated space and the high-speed cameras ...	7
Figure 3	Schematic of marker positions on the ventral side of a bat	8
Figure 4	Orientation and body angles used in this study	10
Figure 5	Schematic of the mass distribution model used to calculate the CoM of the bat	12
Figure 6	Dorsal view of a flying bat showing the relationship between bearing angle (ϕ) and heading angle (ψ) in the global coordinate system for a bat at three time points during the turn	14
Figure 7	Lateral and dorsal view of a flapping bat, indicating vertical (γ_v) and horizontal (γ_h) stroke plane angle in the body coordinate system	16
Figure 8	Plot of the orientation angles and body angles for a representative right turn	18
Figure 9	Angles, angular velocities and angular accelerations for the orientation angles and the body angles (yaw, pitch and roll)	19
Figure 10	Angle and angular velocity for heading and bearing throughout a stroke cycle, measured in a global coordinate system	21
Figure 11	Speed of wrist marker and wingtip marker in the body coordinate system over a standardized wingstroke	21
Figure 12	Angle of attack and wrist angle over a standardized wingbeat cycle	22

Figure 13	Relationship between heading angular velocity and bank angle with the bearing angular velocity	23
Figure 14	Effect of bank angle and heading on the estimation of the expected centripetal acceleration due to the banked orientation of the body	25
Figure 15	Distance of the wingtip to the midline of the body in the horizontal plane X_g-Y_g	26
Figure 16	Forward velocity profiles for the wingtip and wrist markers in a global coordinate system that has been rotated in the Z_g axis to align the X axis component to the bearing velocity vector and thus, the forward velocity represents the marker velocity in the direction of flight	32
Figure S1	Position and velocity for the wingtip and wrist marker in the body coordinate system	41
 Chapter 2		
Figure 1	Ventral view diagram of a bat indicating the position of the wing and body markers and the triangular segmentation used to calculate surface area, vertical force coefficient (C_{vF}), and the angles of attack	46
Figure 2	Lateral and ventral view of a bat, indicating body pitch angle (θ), stroke angles (γ) and excursion of the wingtip	49
Figure 3	Lateral projection of the wingtip with respect of still air and with respect to the bat's body, for a representative bat flying at different speeds	55
Figure 4	Wingbeat frequency, wingbeat amplitude, downstroke ratio, and stroke plane angle as a function of speed, for both flight corridor and wind tunnel flights	57
Figure 5	Body pitch angle as a function of flight speed, for wind tunnel experiments only	57

Figure 6	Forward, vertical, and lateral velocity of the wingtip with respect to the body, as a function of flight speed, for both flight corridor and wind tunnel trials	58
Figure 7	Forward, vertical, and lateral excursion of the wingtip with respect to the body, as a function of flight speed, for wind tunnel trials only	59
Figure 8	Angle of attack as a function of flight speed, for the proximal and distal portion of the wing. Values from wind tunnel flights only ...	60
Figure 9	Mean wing camber during downstroke as a function of flight speed. Values are from wind tunnel flights only	60
Figure 10	Mean extension angle for the downstroke and the upstroke portions of the wingbeat cycle for the elbow and wrist joints, as a function of flight speed	60
Figure 11	Mean coefficient of lift during downstroke as a function of flight speed, for wind tunnel flights only	61
Figure 12	Reduced frequency (A) and Strouhal number (B) as a function of flight speed, for wind tunnel flights only	61
Figure 13	Comparison between the measured wingbeat frequency (f) and amplitude (ϕ_v) and the predicted values derived from Bullen and McKenzie (2002) for all <i>C. brachyotis</i>	67
Chapter 3		
Figure 1	Effect of the oscillation of the wings on the position of the CoM and accelerations of the body	78
Figure 2	Schematic of the experimental setup of the wind tunnel and the dorsal view of a bat indicating the position of the body and wing markers used to calculate kinematic parameters	80
Figure 3	Schematic of the mass distribution model used to calculate the CoM of the bat	82

Figure 4	Lateral projection of the trace of the wingtip over two wingbeats for a bat flying at different speeds, with respect to still air and with respect to its own body	84
Figure 5	Acceleration profiles over a standardized wingbeat cycle for the CoM, estimated from the mass-model, and for the body-fixed sternum and pelvis markers at three speeds representing slow, intermediate and fast flights for a representative individual	85
Figure 6	Horizontal and vertical accelerations during downstroke and upstroke for the sternum marker and the CoM	86

Chapter 4

Figure 1	Ventral view diagram of a bat indicating the position of the wing and body markers and the triangular segmentation used to calculate surface area, vertical force coefficient (C_{vf}), and the angles of attack	100
Figure 2	Wing motion parameters of bats in unloaded and loaded treatments	108
Figure 3	Relationship between forward, vertical, and lateral wingtip velocity with respect to the body with flight speed for unloaded and loaded flights	110
Figure 4	Wing shape parameters of bats in unloaded and loaded treatments	111
Figure 5	Relationship between the vertical force coefficient, C_{vf} , and flight speed for unloaded and loaded flights	112

Chapter 5

Figure 1	Scatter plot of the second and third principal components of the wing morphology in bats, identified as measures of wing loading and aspect ratio, respectively	130
Figure 2	Schematic of a typical banked turn	137

LIST OF TABLES

Chapter 2

Table 1	Morphological measurements of the individuals used in this study	45
Table 2	Slopes of the linear relationships between kinematic variables and flight speed	56

Chapter 4

Table 1	Morphological measurements of the three individuals used in this study	99
Table 2	Body mass of experimental subjects for wind tunnel and flight corridor experiments, prior to the experiment, immediately injection and approximately one hour subsequent to the experiment	99
Table 3	Summary of ANCOVA analyses of kinematic variables in response to loading and speed as a covariate	109

Chapter 1

Kinematics of slow turn maneuvering in the fruit bat *Cynopterus brachyotis*

José Iriarte-Díaz & Sharon M. Swartz

Department of Ecology and Evolutionary Biology, Brown University

Abstract

Maneuvering abilities have long been considered key factors that influence habitat selection and foraging strategies in bats. To date, however, very little experimental work has been carried out to understand the mechanisms that bats use to perform maneuvers. Here we examined the kinematics of slow-speed turning flight in the lesser short-nosed fruit bat, *Cynopterus brachyotis*, to understand the basic mechanics employed to perform maneuvers and to compare them with previous findings in bats and other flying organisms. Four individuals were trained to fly in L-shaped flight enclosure that required them to make a 90-degree turn midway through each flight. Flights were recorded with three low light, high-speed videocameras, allowing the three-dimensional reconstruction of the body and wing kinematics. For any flying organisms, turning requires changes of the direction of travel and the reorientation of the body around the center of mass to maintain the alignment with the flight direction. In *C. brachyotis*, changes in body orientation (i.e., heading) took place during upstroke and preceded the changes in flight direction, which were restricted to the downstroke portion of the wingbeat cycle. Mean change in flight direction was significantly correlated to the mean heading angular velocity at the beginning of the downstroke and to the mean bank angle during downstroke, although only heading velocity was significant when both variables were considered. Body reorientation previous to changes in direction might be a mechanism to maintain the head and body aligned with the direction of travel and thus maximizing spatial accuracy in three-dimensionally complex environments.

Introduction

Flight maneuverability in bats is subject to strong selective pressures. Many bats inhabit and navigate rapidly through cluttered environments and the ability to perform quick and sharp changes in flight direction are likely to play an important role in their survival in natural environments. Accordingly, it has been hypothesized that variation in maneuvering performance strongly influences habitat selection and foraging strategies in bats (Norberg and Rayner, 1987). Most studies of the morphological basis of bird and bat maneuvering, however, have been restricted to analyses based on fixed-wing aerodynamics (Rayner and Aldridge, 1985; Aldridge, 1987; Warrick, 1998), even though flying animals turn using unsteady dynamics, violating the assumptions of steady-state aerodynamic theory. Although the degree to which assuming fixed-wing models introduces error in analysis is unknown, predictions derived from steady-state models have been applied extensively in the bird and bat research communities, particularly when looking for morphological correlates of flight performance and its ecological implications (e.g., Aldridge, 1986a; Norberg and Rayner, 1987; Kalcounis and Brigham, 1995). Recent information on maneuvering flight of birds (Warrick and Dial, 1998; Warrick et al., 1998; Hedrick and Biewener, 2007; Hedrick et al., 2007) and insects (Fry et al., 2003; Card and Dickinson, 2008) has expanded the discussion beyond the assumption of fixed wings. These studies emphasize the importance of temporal sequences of wing movements to understand the mechanical basis of turning behavior. Although bats are believed by some to be as the most maneuverable flying animals for their size, no analogous studies have been performed for bats. Here, we evaluate the

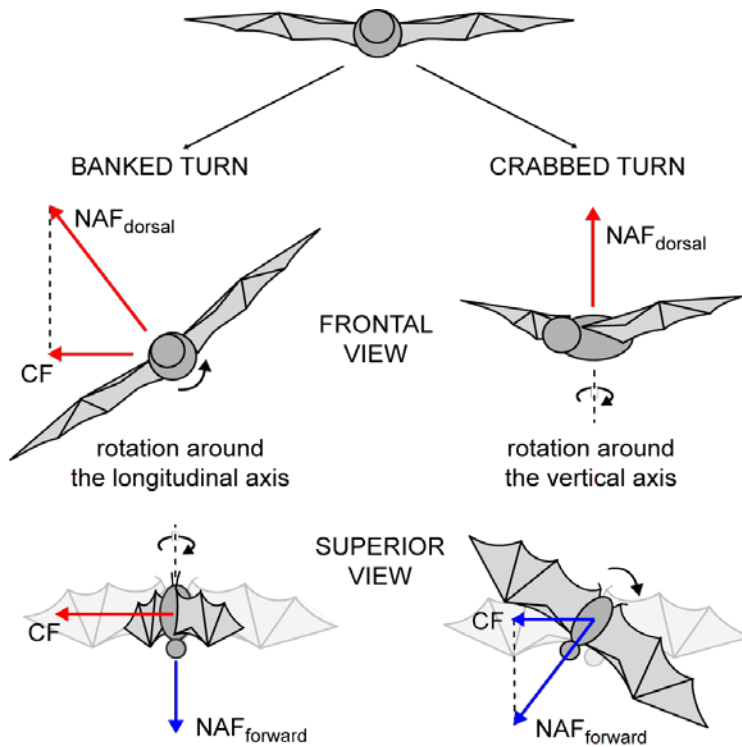


Fig. 1: Diagram showing two types of turning mechanisms. (A) In a banked turn a bat rolls into the turn. By banking the body, a bat reorients the vector of dorsal component with respect of the body of the net aerodynamic force (NAF_{dorsal}) towards the center of the turn producing a centripetal force (CF). (B) In a crabbed turn a bat yaws into the turn. The forward component of the net aerodynamic force ($NAF_{forward}$) produced during downstroke now will have a centripetal component that will drive the bat through the turn.

morphological and aerodynamic mechanisms used by bats to carry out 90-degree turns at slow speed by analyzing wing and body kinematics in detail.

To successfully complete a turn, an animal must translate its center of mass (CoM) along the flight path (i.e., change its flight direction) and rotate its body around its CoM to align its body orientation with the new direction. The magnitude of change in direction of flight is a function of the impulse (force \cdot time) perpendicular to the original direction of movement. Impulse is the result of the centripetal force produced by the change of the orientation of the net aerodynamic force generated by the body and wings. Two basic strategies to produce a turning force include banked and crabbed turns (Fig. 1). In a banked turn, the animal rolls around its cranio-caudal axis, tilting the vector of the vertical component of the net aerodynamic force (i.e., lift in level flight) laterally and towards the center of the turn (Fig. 1). These turns are used by most fixed-wing aircraft

(Filippone, 2006). In contrast, in a crabbed turn the animal yaws into the turn, orienting the forward component of the net aerodynamic force (i.e., thrust in level flight) towards the center of the turn, without need of adjusting the vertical component vector (Fig. 1). In both cases, the reorientation of aerodynamic forces produces a laterally-oriented force that drives the organism into a turn. Both banked and crabbed turning mechanisms require the rotation of the body around its CoM.

Banked turns appear more common in animal flight. They have been described for organisms as diverse as fruit flies (Fry et al., 2003), locusts (Berger and Kutsch, 2003), dragonflies (Alexander, 1986), gliding frogs (McCay, 2001) gliding mammals (Bishop and Brim-DeForest, 2008) and birds (Warrick and Dial, 1998; Hedrick and Biewener, 2007). Crabbed turns are also phylogenetically widespread, however, having been described in some dipterans (see Dudley, 2002), dragonflies (Alexander, 1986), gliding frogs (McCay, 2001), and gliding mammals (Bishop and Brim-DeForest, 2008).

For both banked or crabbed turns, body rotation results from an asymmetry in aerodynamic forces between left and right wings, an asymmetry in the inertial forces produced by the two wings, or a combination of both. Aerodynamically generated force asymmetries can be expected as the result of differential changes in wing shape, such as changes in wing surface area, angle of attack, or camber, or maybe due to differences between left and right wings in kinematic parameters, such as relative velocity (see Dudley, 2002). In contrast, inertially generated force asymmetries can be produced by differences in motion between left and right wings. Inertial forces can produce net changes in body orientation over a wingbeat cycle even when no external torques are applied due to conservation of angular momentum (Hedrick et al., 2007).

Moreover, little is known about the kinematics and aerodynamics of turning in bats, including whether they use primarily one, the other, or both turning mechanisms. While aerial maneuvers have been qualitatively described for two bat species (Norberg, 1976), and kinematics of the CoM have been analyzed for six other species performing 180-degree turns (Rayner and Aldridge, 1985; Aldridge, 1987), no detailed analysis of body orientation and/or wing kinematics has yet been carried out for bats.

Photographs of bats performing flying maneuvers sometimes show the body rolled toward the direction of turning (Norberg, 1976). Based on this evidence and the widespread use of banked turns in organisms as morphologically and phylogenetically diverse as insects, amphibians, birds and mammals, we predicted that bats would also use banked turning, and therefore maneuver by rolling their body to reorient the lift force vector.

Materials and methods

Experimental animals and flight corridor

The study animals were non-reproductive adult female lesser short-nosed fruit bats (*Cynopterus brachyotis*), loaned by the Lube Bat Conservancy (Gainesville, FL, USA), housed at the Harvard University Concord Field Station (Bedford, MA, USA). Animals were provided with food and water *ad libitum* and kept in a large cage that allowed them to perform short flights. Four bats (body mass 32.8 to 41.7 g, $N=4$) were selected from among the captive population based in their consistent flight ability and cooperation during training sessions. Experimental subjects were trained to fly through an

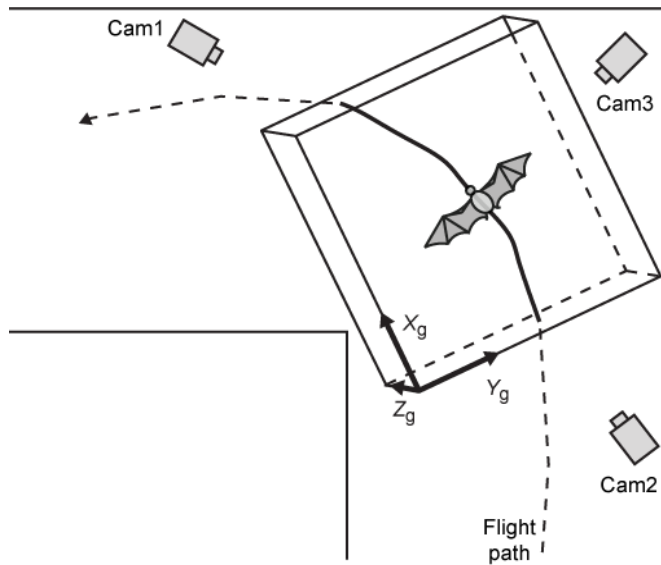


Fig. 2: Superior view of turning portion of the flight corridor, indicating the position of the calibrated space and the high-speed cameras. Three cameras were placed on the floor pointing upward to capture the ventral side of the bat body and wing. As the bat passed through the calibrated volume, the position of several anatomical markers were tracked in the global coordinate system $X_g Y_g Z_g$. Figure not to scale.

L-shaped flight corridor (7 m length x 1 m width x 2 m height) making a 90-degree turn midway through each flight (Fig. 2). Bats were hand-released approximately 1.5 m above the floor on either side of the corridor, performed either a right or a left turn, depending on release site, and landed on the ceiling at the other end of the corridor.

Three-dimensional coordinate mapping

Each turn was recorded with three synchronized, high-speed digital video cameras: either three infrared-sensitive Redlake PCI 1000 cameras (320×280 pixel resolution; Redlake Inc., San Diego, CA, USA) or two Redlake cameras and one Photron Fastcam-X 1280 PCI camera (1024×1024 pixel resolution; Photron USA Inc., San Diego, CA, USA). Flights were recorded at 500 frames s^{-1} with shutter speeds of 1/1000th of a second. The cameras were placed on the floor of the flight corridor in such a way that at least one camera provided a cranioventral view and another a caudoventral view (Fig. 2). Bats typically prefer low levels of visible light, so illumination was provided by a series

of infrared lights for the Redlake cameras and by a high-power red LED light for the Photron camera. The video files were calibrated by a modified direct linear transformation (DLT), a technique that computes 3D coordinates from multiple known 2D views, using a 25-point calibration frame (0.45×0.45×0.55 m) captured on video at the beginning of each series of flight (Hatze, 1988).

Lightweight spherical beads covered with reflective tape were attached to the pelvis, on the skin overlying the pubic symphysis (*pvs* marker) and just lateral to the sternum (*Rch* and *Lch*, right and left chest markers, respectively). Chest markers were placed medial to the glenohumeral joint to ensure they remained in the field of view of the cameras as much as possible throughout the wingbeat cycle. Three additional anatomical landmarks on each wing: the wrist, and the distal part of the distal phalanges of the 3rd and 5th digit (*wst*, *d3* and *d5*, respectively; Fig. 3) were marked with small circular pieces of reflective tape.

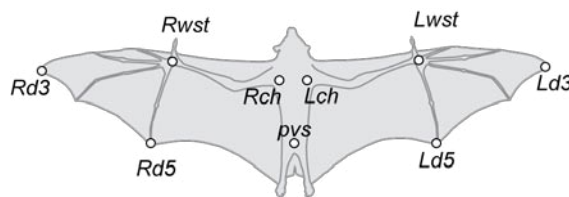


Fig. 3: Schematic of marker positions on the ventral side of a bat. Prefixes *R* and *L* refer to right and left, and *pvs*, *ch*, *wst*, *d3* and *d5* to pelvis, chest, wrist, end of the third digit and end of the fifth digit, respectively.

A trade-off exists between maximizing the size of the cameras' field of view and maximizing spatial resolution of estimates of each marker's three-dimensional coordinates. Here, cameras were positioned to capture between 2 and 4 wingbeat cycles, depending on the flight speed of the bat in a particular trial. Sequences where all markers were visible for at least one complete wingbeat were digitized using custom-designed

software (Hedrick, 2007). The three-dimensional position of each marker was reconstructed from the two-dimensional video files using the DLT coefficients derived from the calibration frame. Because of the great range of motion of the wing during flight, in some cases markers were not visible in at least two cameras and the spatial position of the marker could not be resolved, resulting in gaps in the data. This was the case for the *wst* and *d5* markers at the beginning and at the end of the downstroke, in particular. Gaps, however, were relatively short and the curves were interpolated and filtered with the ‘Generalized Cross Validatory Spline’ (GCVSPL) software (Woltring, 1986). The spline smoothing coefficients were adjusted to produce a filter cut-off frequency of approximately 45 Hz, nearly five times greater than the wingbeat frequency. The quintic spline method also allows the direct calculation of higher-order derivatives, and therefore provides greater accuracy in calculating velocities and accelerations (Walker, 1998). First and second derivatives of positional data were calculated from the spline coefficients, assuming no error and hence without further filtering.

To test the accuracy of our experimental setup, a spherical marker bead was thrown in a parabolic path through the calibrated space in front of the camera. Our calculation of its downward acceleration based on kinematic reconstruction was within 0.5% of 9.81 m s^{-1} . We also moved a rigid card with attached reflective markers at known separation distances similar to the intermarker distances on our bats’ wings. Measurement error based on kinematic reconstruction was no more than 3% from the actual distances, with mean absolute errors ranging from 0.3 mm to 1.2 mm.

Frames of reference, coordinate systems and body orientation angles

We employed two frames of reference to describe the positions of kinematic markers during turning (Fig. 4). First, an earth-fixed, global coordinate system $X_g Y_g Z_g$ was defined, with X_g and Y_g describing the horizontal plane and with $+Z_g$ pointing in the direction of gravity. Second, we used a dynamic, body-based coordinate system $X_b Y_b Z_b$, centered on the pelvis marker, where $+X_b$ points cranially along the body axis, $+Y_b$ points laterally toward the right wing, and $+Z_b$ points downward and lies in the plane of symmetry of the body. This frame of reference was defined by three coplanar body

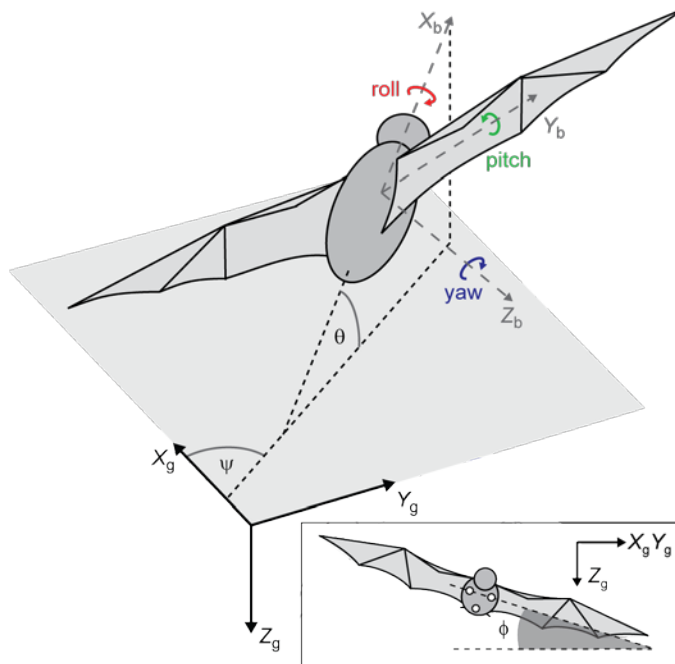


Fig. 4: Orientation and body angles used in this study. The heading angle (ψ) was defined as the angle between the projection of the longitudinal axis of the body on the horizontal plane (X_g - Y_g) and the X_g axis; the elevation angle (θ) was defined as the angle between the longitudinal axis of the body and the horizontal plane (X_g - Y_g); and the bank angle (ϕ) was defined as the angle between the line connecting both chest markers and the horizontal plane (X_g - Y_g) (see inset). Body angles were defined as the deviation around the body-fixed axes in a body coordinate system. Arrows define the positive rotation direction of the body angles.

landmarks (*pvs*, *Rch* and *Lch*), and changed relative to the global coordinates as a bat moved through space. The body coordinate system was calculated from the global coordinate system using a series of Euler rotations for each time step. In an Euler angle system, three successive rotations around non-orthogonal axes define a unique attitude or general orientation of a rotated object with respect to a reference coordinate system. The two first Euler rotation angles described

the heading (ψ) and elevation (θ) of the body with respect to the global coordinate system (Fig. 4). Because of these rotations, however, the last rotation angle does not accurately represent the bank orientation of the body with respect to the global coordinate system. Therefore, bank angle (ϕ) was calculated as the angle between the line connecting the two chest markers and the horizontal (X_g - Y_g) plane (Fig. 4, inset).

Body angles: yaw, pitch and roll

Rotations around the body-centered X_b , Y_b , and Z_b axes were designated roll, pitch and yaw, respectively (Fig. 4), following aerodynamic conventions (Phillips, 2004). Body angular velocities were calculated by applying a classical transformation from the angular velocities of the Euler angles, commonly used in rigid body dynamics (Phillips, 2004). Because bats were recorded mid-turn, they already had an initial ‘pitch’ and ‘roll’ angles relative to the global coordinate system. These angles were added to the angular velocity cumulative sum and represent the angular body position with respect to the beginning of the recorded portion of the turn. Yaw initial orientation was arbitrary, but because it has no systematic effect on flight control, all trials started with zero degree yaw angle (following Card and Dickinson, 2008). Body angular accelerations were calculated as the first derivative of the body angular velocities over time.

Determination of CoM

Although the wings of the bat comprise a relatively small fraction of the overall weight of the bat (Thollesson and Norberg, 1991), the motions and accelerations associated with wing flapping may produce substantial inertial effects. As a result of these morphing motions, the CoM of the bat will not correspond to a fixed anatomical

location on the bat during flight. To account for the wing displacements in the determination of the location of the center of mass, we constructed a mass model representation of the bat.

The mass model is a time varying, discrete mass approximation of the bat mass distribution, based on the location of the markers. To develop the discrete mass system representing the bat, we partitioned total body mass into individual components or regions. The wing membrane, wing bones and trunk were treated as separate masses which were combined to form the total mass model.

To model the mass distribution of the membrane, we constructed a triangulation of the wing geometry at each time step. The large-scale, base triangulation was developed using the location of the marker positions at any given time, and a subsequent subdivision of those triangles was performed to give a mesh of fine-scale triangular elements (Fig. 5).

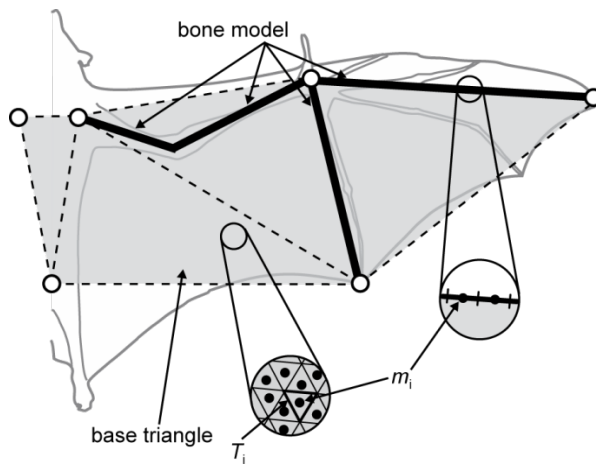


Fig. 5: Schematic of the mass distribution model used to calculate the CoM of the bat. The blue lines represent the modeled masses of the bone. The shaded triangle patches represent the base triangles of the skin mass model, and insets show detailed subdivisions of bone and skin masses (m_i) and individual triangular elements (T_i) of the model.

Each triangle element (T_i) on the membrane was assigned a constant thickness (1×10^{-4} m) and density (1×10^3 kg m⁻³), based on measured characteristics of bat wing membrane skin (Swartz et al., 1996). A resulting discrete point mass (m_i) for each triangular membrane element was computed based on the volume of that triangular membrane and assigned a

position at the centroid of the triangle element. To model the distribution of mass among and within each of the wing bones, we constructed a curve between the markers at the endpoints of the bones. The curve for each bone in the wing was defined from the location of the markers, and the mass of the fourth digit, that we did not track, was divided equally between the third and fifth digit. Given the tapered shape of bat bones (Swartz, 1997), the cross-sectional radius of each bone element of the model was defined by a quadratic function with respect to the length of the bone. We assigned a constant density to the bones ($2 \times 10^3 \text{ kg m}^{-3}$). Using the distribution of bone radii distribution and the location of the bone elements in space, the line was subdivided into smaller line-elements, from which discrete mass points were defined. The mass of the wings was scaled such that the constructed distribution represents the 16% of the total body mass, according to measurements of bats of similar size (Thollesson and Norberg, 1991). The mass and moment of inertia of the wing with respect to the shoulder was compared to measured values (Thollesson and Norberg, 1991) to ensure that the model represents the physical reality. Finally, the bat's body was defined as a three-dimensional ellipsoid divided into discrete mass points.

The discrete mass representation of the membranes, bones and body was combined with detailed kinematic records of motion of each landmark to determine the center of mass of each one of the mass elements, m_i , using the equation

$$\vec{r}_{CoM} = \frac{\sum \vec{r}_i m_i}{m_T}, \quad (1)$$

where \vec{r}_{CoM} represents the position vector of the CoM, \vec{r}_i represents the position vector of the i -th discrete point mass and m_T represents the total mass of the bat.

Calculation of kinematic parameters

Velocity, acceleration, changes in heading, and curvature

Net body velocity (\mathbf{V}_b) and acceleration (\mathbf{A}_b) vectors were calculated as the first and second derivatives of the position vector of the CoM in the global coordinate system. The global trajectory of the bat (i.e., the flight direction) in the horizontal plane was defined as the bearing angle (φ) and it was calculated as the angle between the horizontal component of the net body velocity vector ($\mathbf{V}_{b,xy}$) and the X_g axis (Fig. 6). Changes in heading can be described as a rate of turning known as curvature (κ). Curvature is defined as the inverse of the radius of the curved path and is calculated by the equation

$$\kappa = \frac{|\mathbf{V}_{b,xy} \times \mathbf{A}_{b,xy}|}{|\mathbf{A}_{b,xy}|^3}, \quad (2)$$

where $\mathbf{V}_{b,xy}$ and $\mathbf{A}_{b,xy}$ are the velocity and acceleration of the body in the horizontal plane X_g - Y_g , respectively.

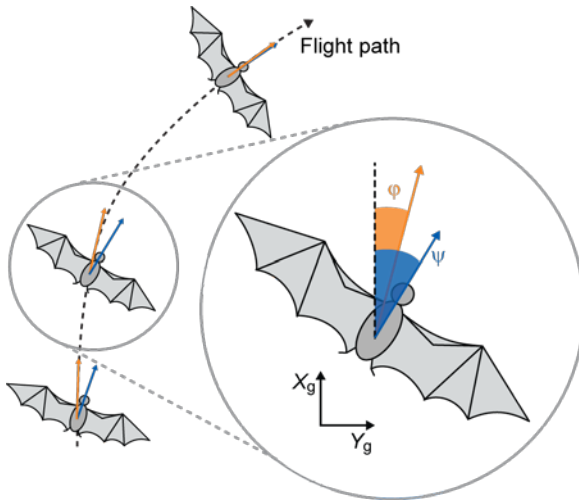


Fig. 6: Dorsal view of a flying bat showing the relationship between bearing angle (φ) and heading angle (ψ) in the global coordinate system for a bat at three time points during the turn. Bearing angle is calculated from the body velocity vector (\mathbf{V}_b , orange arrows) obtained as the derivative of the position vector of the CoM.

Angle of attack and wing surface area

Differences in the angle of attack of the two wings during a wingbeat cycle could have aerodynamic influence that results in turning. Angle of attack was calculated for each wing as the angle between the relative incident air velocity of the wrist marker (*wst*) and the plane of the hand wing, defined by the markers on the wrist (*wst*), fifth digit (*d5*) and the wingtip (*d3*). The exact calculation of angle attack requires the estimation of the induced velocity on the wing (i.e., wake and wing-bound vortex velocities) (Aldridge, 1986b) but we ignored induced velocity, because our analyses focus on comparisons between left and right wings, and induced velocities are similar for the two wings.

The difference in the surface area between left and right wing was estimated by calculating the wrist angle, a measure of the flexion/extension of the wing as a proxy. Wrist angle was defined as the interior angle of the triangle formed by the chest (*ch*), wrist (*wst*) and wingtip (*d3*) markers for each wing. Thus, when wrist angle is large, wing surface area is also large.

Downstroke, upstroke, and stroke plane angle

Downstroke and upstroke phases of the wingbeat were defined by positive and negative velocities of the wrist in the Z_b direction, respectively. The vertical (γ_v) and horizontal (γ_h) stroke plane angles were defined as the major axis of the projection of the wingtip with respect to the body on the X_b-Z_b and X_b-Y_b planes, respectively (Fig. 7). These major axes were estimated by fitting a least-square line for each wingbeat.

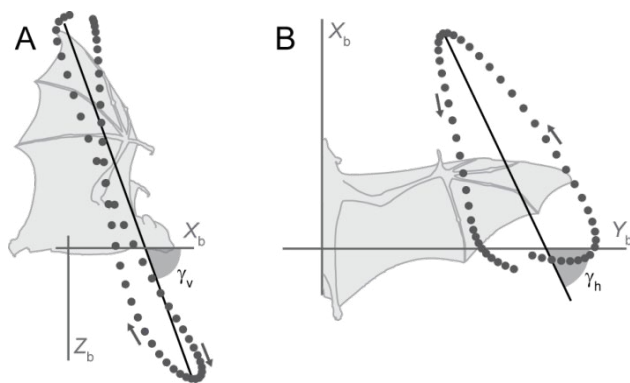


Fig. 7: Lateral (A) and dorsal view (B) of a flapping bat, indicating vertical (γ_v) and horizontal (γ_h) stroke plane angle in the body coordinate system. Continuous line corresponds to an actual trace of the right wingtip (*d3* marker) throughout a representative stroke cycle.

Lateral projection of the wings

Changes in body rotations could be potentially explained by differences in profile drag produced between the two wings. A possible mechanism to modulate drag is to alter the wing area exposed to the airflow. Lateral projection of the wing can be used as a proxy for wing area exposed, where wings that are more extended should present larger wing areas. We estimated the lateral projection as the distance of the wingtip marker to the midline of the body in the global coordinate system.

Wingbeat consolidation and statistical analyses

To avoid the problem of autocorrelation and pseudoreplication among wingbeats, kinematic parameters were calculated from one representative wingbeat per trial. We defined the representative wingbeat as the one with a heading angle the closest to 45 degree from the initial orientation of the flight. This wingbeat represented a mid-turn wingbeat and usually presented the maximum rate of change in heading angle and in body angular velocities. In some cases, these variables peaked ± 1 wingbeat from the wingbeat defined by the heading angle criterion and the former was used. For most of the analyses, a sample size of 32 trials was used and values are reported as mean \pm s.e.m.

unless specifically indicated. Statistical analyses were conducted using JMP 6 (SAS Institute, Cary, NC, USA) and MATLAB R2006a (The Mathworks, Inc., Natick, MA, USA). Regression analyses were performed with general linear models (GLM) to control for differences among individuals.

Results

General description of the turn

When turning, bats flew consistently at low forward speeds of $2.0 \pm 0.1 \text{ m s}^{-1}$ ($N=53$) and maintained relatively constant speed in the X_b direction throughout the calibrated volume, though for some trials, flight speed decreased at the end of the sequence. In a typical turn, bats gained altitude during the first half of the turn ($0.12 \pm 0.04 \text{ m}$, $N=53$) and then maintained their height after turning, thereby increasing their net altitude during the turn.

Changes in bearing occurred almost entirely during the downstroke (Fig. 8), with an average change of 16.0 ± 0.8 degrees per wingbeat. We captured, depending on the flight speed, between 2 and 4 wingbeats within the calibrated space. Extrapolating the mean change in heading during a wingbeat cycle to the whole turn, *C. brachyotis* would complete a 90-degree turn in about 6-7 wingbeats. This is likely to be an overestimation, as the change in heading tends to peak towards the middle of the turn. From a preliminary study of *C. brachyotis* performing the same task, a 90-degree turn was completed in about 6-9 wingbeats (J. Iriarte-Diaz, unpublished). Bats reached maximum changes in bearing of 416.9 ± 26.4 degrees s^{-1} near mid-downstroke, producing turns with a minimum

turning radius of 0.290 ± 0.031 m (curvature of 5.53 ± 0.62 m^{-1}), about 0.8 wingspans.

Mean curvature during downstroke was 3.36 ± 0.33 m^{-1} .

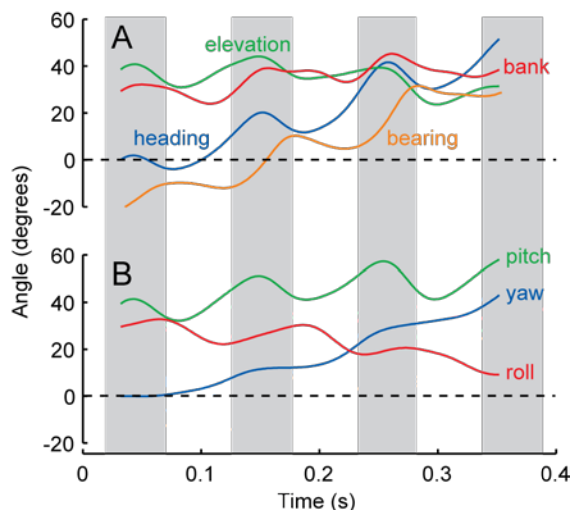


Fig. 8: Plot of the orientation angles (A) and body angles (B) for a representative right turn. Bearing angle (orange line) was included to the orientation angles plot for comparison of body attitude with the changes in flight direction. Shaded bars correspond to downstroke periods.

Changes in body orientation

Bats consistently changed their body orientation throughout the wingbeat cycle in a sinusoidal fashion with a frequency equal to the wingbeat frequency (Fig. 8). Bats rolled into a bank at the beginning of the turn. Average bank angle over a wing stroke was 25.8 ± 2.0 degrees with a maximum of 56.3 degrees. Bank angle reached a maximum at mid-downstroke and a minimum at mid-upstroke with an absolute change of 10.6 ± 1.1 degrees per half-stroke. Despite the apparent variation within a wingstroke, average bank angle did not change among wingbeats within each trial (paired t -test, $t_{31}=0.84$, $P>0.1$; Fig. 9A). Similarly, elevation angle showed changes within the wingbeat cycle, with an average difference of 10.6 ± 1.1 degrees per half-stroke, reaching a maximum at mid-downstroke and a minimum at mid-upstroke, but with no significant changes between wingbeats (paired t -test, $t_{31}=-1.55$, $P>0.1$; Fig. 9A). Mean elevation angle was 25.7 ± 2.5 degrees. Heading angle, however, showed a significant between-wingbeat component

(paired t -test, $t_{31}=13.58$, $P<0.0001$), as expected in a turn, as bats have to continuously change their body orientation to keep it aligned with their bearing (Fig. 9A). During upstroke, bats increased their heading angle an average of 20.8 ± 1.9 degrees, rotating towards the direction of the turn.

Angular velocity and angular acceleration profiles were very similar for all three angles (Fig. 9B,C). During upstroke, angular velocities increased reaching a peak around the upstroke-downstroke transition of 363.5 ± 23.7 , 217.2 ± 20.5 and 104.3 ± 23.3 degrees s^{-1} for heading, elevation and bank angles, respectively (Fig. 9B). Angular accelerations showed a clear pattern of positive acceleration for all three angles throughout upstroke

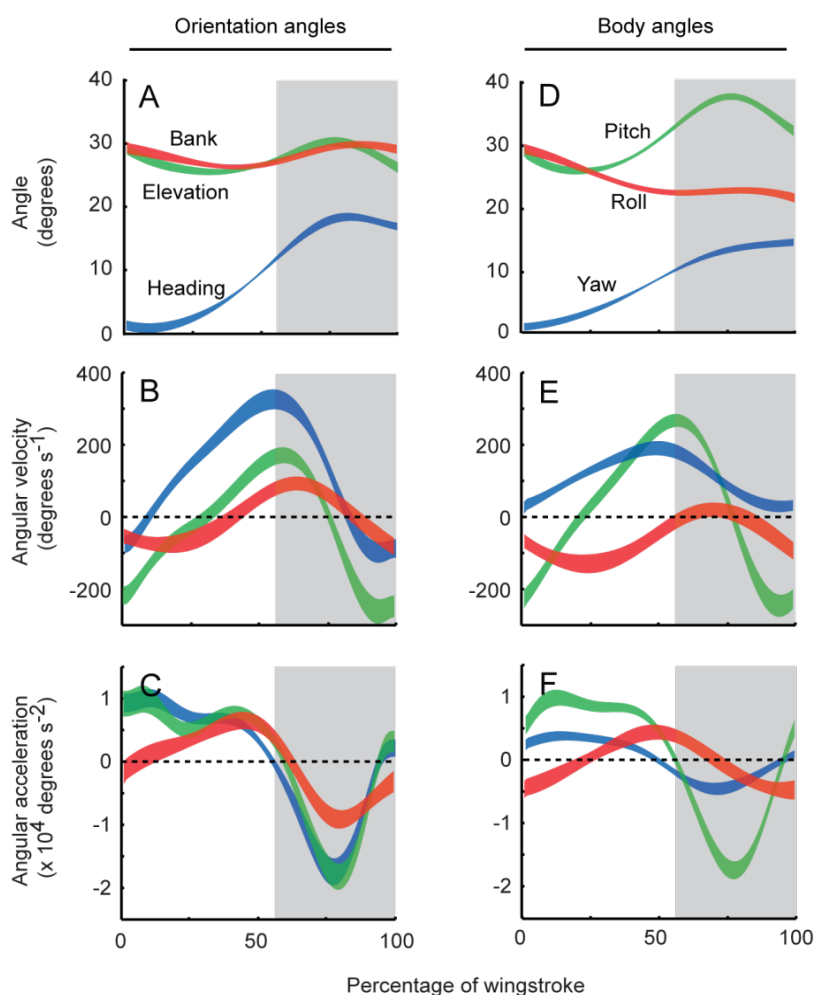


Fig. 9: Angles, angular velocities and angular accelerations for (A-C) the orientation angles (heading, elevation and bank) and (D-F) the body angles (yaw, pitch and roll). The width of the traces represents the mean \pm s.e.m.. Shaded bars correspond to downstroke periods. Because bats performed both right and left turns, all turns were standardized to a right turn, and both heading and yaw angles started at zero degrees. Body angles were obtained as the cumulative sum of the body angular velocities obtained from the angular velocities of the Euler angles. For pitch and roll angles, the cumulative sum was added to the initial elevation and bank angle, respectively, for each trial.

and a very strong negative acceleration around the middle of the downstroke (Fig. 9C).

Changes in body angles

Pitch angle showed high within-wingbeat variation, reaching a minimum at mid-upstroke and a maximum at mid-downstroke, with an average change of 12.1 ± 0.9 degrees per half-stroke (Fig. 9D). Yaw angle increased constantly throughout the wingbeat (Fig. 9D), and showed a difference of 13.7 ± 1.0 degrees between the end and the beginning of the wingbeat (paired *t*-test, $t_{31}=12.4$, $P<0.0001$) that resulted from positive yaw angular velocities throughout the wingbeat (Fig. 9E). In contrast, roll angle decreased over the wingbeat, decreasing during the upstroke and remaining constant during downstroke (Fig. 9D). Over a wingbeat cycle, roll angle decreased -4.3 ± 1.1 degrees (paired *t*-test, $t_{31}=-4.0$, $P<0.0001$). Yaw angular velocity was positive throughout the wingbeat, in contrast to roll angular velocity, which was mostly negative (Fig. 9E).

Pattern of change in heading and flight direction

Heading and bearing angle varied in a similar fashion throughout the wingbeat cycle, with changes of similar magnitude, but with a clear offset between them (Fig. 8A,10A). Heading angular velocity peaked at the upstroke-downstroke transition, although bats changed bearing the most at the middle of the downstroke (Fig. 10B), indicating that changes in heading preceded changes in flight path during the turn. The difference between heading and bearing angle peaked at the upstroke-downstroke transition, and reached a minimum at the end of the downstroke (Fig. 10A).

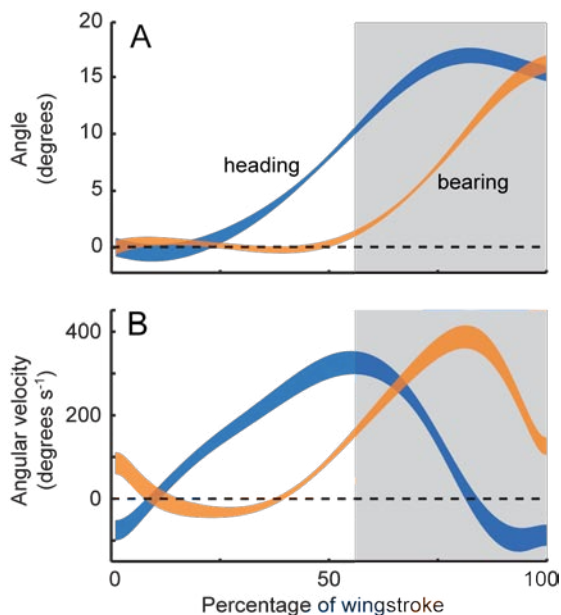


Fig. 10: Angle and angular velocity for heading (blue trace) and bearing (orange trace) throughout a stroke cycle, measured in a global coordinate system. Shaded bars correspond to downstroke periods. The width of the traces represents the mean \pm s.e.m.

Wingbeat kinematic parameters

Bats flew using wingbeat frequencies of 9.2 ± 0.1 Hz, with upstrokes comprising $56\pm 2\%$ of the stroke cycle. Wingtip speed with respect to the body showed a sinusoidal variation with a frequency of nearly half of wingbeat frequency (Fig. 11A). Wingtip speed reached a minimum of 4 m s^{-1} at mid-upstroke and a maximum of about 8 m s^{-1}

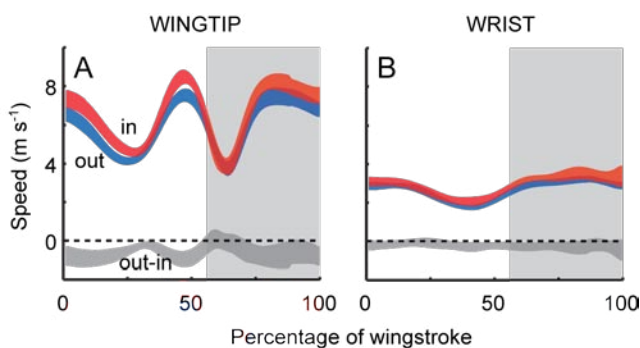


Fig. 11: Speed of wrist marker and wingtip marker in the body coordinate system over a standardized wingstroke. Red, blue and grey traces represent the inside and the outside wing and the difference between them, respectively. The width of the traces corresponds to the 95% CI. Shaded bars correspond to downstroke periods.

near the end of upstroke and at mid-downstroke (Fig. 11A). Wrist velocity showed less variation during the stroke cycle, with a mean speed near 3 m s^{-1} (Fig. 11B). Mean downstroke speed was 6.31 ± 0.11 and $2.97\pm 0.10\text{ m s}^{-1}$, for the wingtip and wrist, respectively. During a half-

stroke, angle of attack changed from around 50 degrees at the beginning of downstroke to about 20 degrees at the end of downstroke, with a mean of 26.7 ± 0.7 degrees. Vertical stroke plane angle, γ_v , was 52.7 ± 4.8 degrees.

Wing kinematics in the body coordinate system were very similar for the inside and outside wings, although small but statistically significant asymmetries were observed. Mean wingtip speed of the inside wing was 7% faster (a difference of $0.27 \pm 0.15 \text{ m s}^{-1}$; paired t -test, $t_{31}=1.82$, $P=0.08$), particularly during the upstroke (Fig. 11A). No significant differences in speed between the two wings were observed at the wrist (Fig. 11B). These differences are mostly due to higher wingtip lateral velocities of the inside wing during the beginning and the end of the upstroke (see supplementary material Fig. S1F).

The angle of attack of the inside wing during downstroke was 9% larger (a difference of 2.7 ± 0.9 degrees, paired t -test, $t_{31}=3.15$, $P<0.01$) than the outside wing (Fig. 12A). Also, the wrist angle, a measure of the extension of the hand, and likely of the surface area of the wing, was larger in the inside wing by 3.3 ± 0.7 degrees (paired t -test,

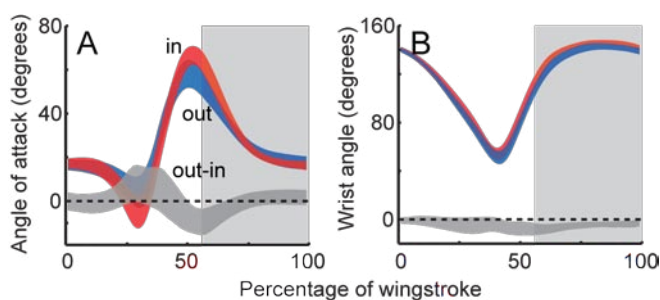


Fig. 12: Angle of attack (A) and wrist angle (B) over a standardized wingbeat cycle. Red, blue and grey traces correspond to the inside and the outside wing and the difference between them, respectively. The width of the traces corresponds to the mean \pm 95% CI. Shaded areas correspond to downstroke periods.

$t_{31}=4.18$, $P<0.001$; Fig. 12B). Even though elbow angle was not measured, we believe that this angle reflects overall wing extension, as we also found no major differences in the distance of the wingtip to the midline of the body throughout the

wingbeat (see supplementary material Fig. S1A,E,I). The largest kinematic difference was found in the horizontal stroke plane angle γ_h . The asymmetry in γ_h during turning was 10.8 ± 2.8 degrees (paired t -test, $t_{31}=3.86$, $P<0.001$), indicating that the outside wing moved more parallel to the body than the inside wing, which had an overall direction more oriented towards the midline.

Kinematic correlations with changes of direction

In a roll-based maneuver, the centripetal force that produces the turn depends on the roll angle. The greater the roll, greater the centripetal force and tighter the turn. In such a case, the rate of change in direction angle is expected to be proportional to the roll angle (McCay, 2001). On the other hand, in a yaw-based maneuver, the change in direction should be related to the rate of change in yaw rather than yaw orientation (Warrick et al., 1998; Hedrick and Biewener, 2007). Both heading angular velocity and mean bank angle during the downstroke are significantly correlated with the peak rate of change in direction (GLM, $r^2_{\text{adj}}=0.88$, $F_{4,44}=92.7$, $P<0.0001$ and GLM, $r^2_{\text{adj}}=0.72$, $F_{4,44}=32.48$, $P<0.0001$, respectively; Fig. 13). In a multiple regression model, controlling for

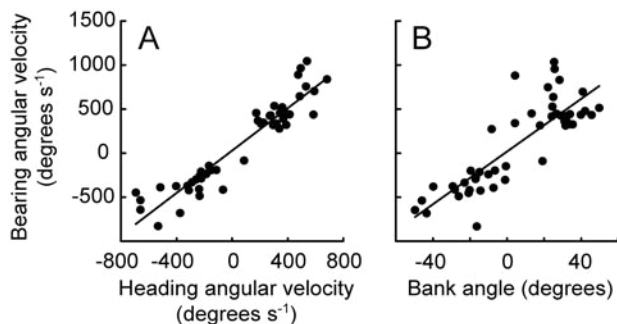


Fig. 13: Relationship between heading angular velocity (A) and bank angle (B) with the bearing angular velocity.

individual effects, only heading angular velocity was significant (GLM, $r^2_{\text{adj}}=0.89$ for the whole model; heading angular velocity effect: $\beta=0.82$, $F_{1,43}=63.5$, $P<0.0001$; bank angle effect: $\beta=0.13$, $F_{1,43}=1.6$, $P>0.2$). The partial correlation

between heading rate and bearing rate while controlling for bank angle was

$r_{\text{heading|bank}}=0.80$ (two-tailed t -test, $P<0.0001$), while the partial correlation between bank angle and bearing rate when controlling for heading angular velocity was $r_{\text{bank|heading}}=0.14$ (two tailed t -test, $P>0.05$).

Based on the instantaneous acceleration of the CoM estimated from the mass model (see Methods, above), it is possible to calculate the total instantaneous centripetal acceleration ($\mathbf{A}_{c,\text{total}}$) necessary to produce a turn with a radius $1/\kappa$ using

$$\mathbf{A}_{c,\text{total}} = \left(\mathbf{V}_{b,xy} \right)^2 \kappa, \quad (3)$$

where $\mathbf{V}_{b,xy}$ is the forward speed of the estimated CoM in the horizontal plane of the lab X_g - Y_g , and κ is the curvature of the turn. Given the symmetry in the wing kinematics in the body coordinate system, we can estimate the centripetal component produced by the banked orientation of the body, by assuming that the net aerodynamic force is oriented perpendicular to the bank angle (Fig. 14A). Thus, the bank component of the centripetal acceleration was estimated as

$$A_{c,\text{bank}} = \left(A_{\text{CoM},z} + \mathbf{g} \right) \tan \phi \cos(\psi - \phi), \quad (4)$$

where $A_{\text{CoM},z}$ corresponds to the vertical acceleration calculated from the position of the CoM, and \mathbf{g} corresponds to the acceleration of gravity (Fig. 14A,B). On average, $A_{c,\text{roll}}/A_{c,\text{total}}$, the estimated centripetal acceleration produced by the degree of bank relative to the centripetal acceleration necessary to produce the observed change in flight direction, accounted for only $74.0 \pm 4.9\%$ of the total acceleration required (Fig. 14C). In some cases, the bank contribution was as small as 10% of the necessary centripetal

acceleration, but in a few others, bank angle accounted for almost all of the acceleration needed to produce the turn.

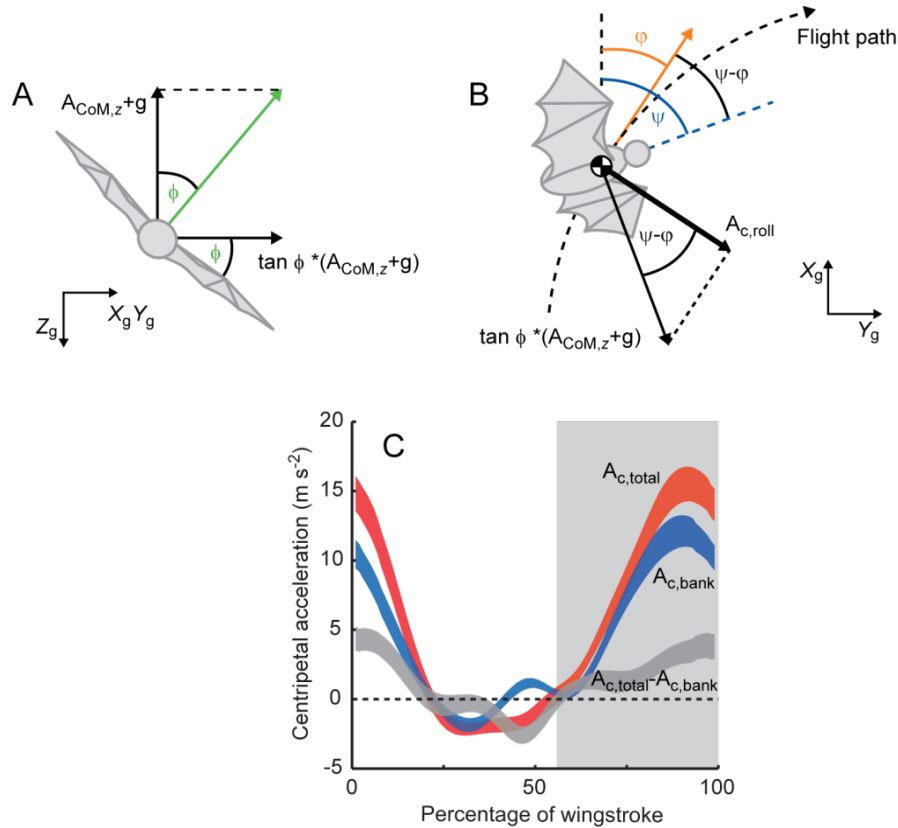


Fig. 14: Effect of bank angle and heading on the estimation of the expected centripetal acceleration due to the banked orientation of the body. (A) Posterior view of a bat performing a right turn. The net aerodynamic force (green vector) was estimated based on the bank angle (ϕ), the total vertical acceleration produced by the bat ($A_{CoM,z}$), and assuming that the net aerodynamic force is produced perpendicular to the bank angle. (B) Superior view of a bat performing a right turn. Because the heading orientation of the body (blue line) does not necessarily match the direction of flight (orange vector), the centripetal acceleration due to the bank ($A_{c,bank}$) must be corrected by the difference between heading and bearing angle ($\psi-\phi$). (C) Observed ($A_{c,total}$, red trace) and the estimated centripetal acceleration from bank ($A_{c,bank}$, blue trace) throughout a standardized wingstroke. Grey trace corresponds to the difference $A_{c,total}-A_{c,bank}$. The width of the traces represents the mean \pm 95% CI ($N=32$) and the shaded bar corresponds to the downstroke period.

Lateral projection of the wings

The lateral projection of the wing was maximal during downstroke for both wings (Fig. 15). The wingtip of the inside wing started to move laterally during the second half of the downstroke, while the outside wing was extended during downstroke as a

consequence of the bank of the body during the turn. During the second half of the upstroke, the inside wing projected further than the outside wing, which could have created greater drag on the inside wing due to a larger wing area (Fig. 15). Accordingly, the difference of the lateral projection of the wingtip between wings significantly predicts the observed changes in global yaw angular velocity at the upstroke-downstroke transition (GLM, whole model: $r^2_{\text{adj}}=0.56$; distance effect: $F_{1,24}=12.0$, $P=0.002$).

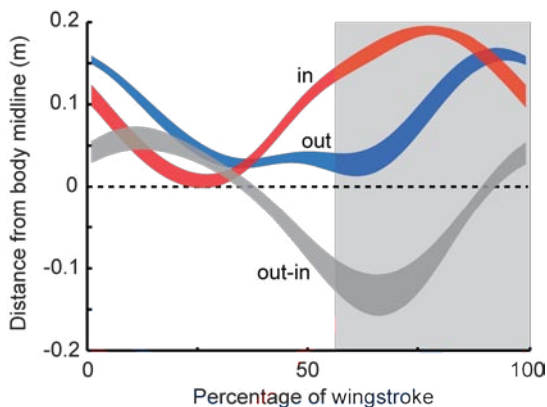


Fig. 15: Distance of the wingtip to the midline of the body in the horizontal plane X_g-Y_g . Red, blue and grey traces correspond to the inside and the outside wing and the difference between them, respectively. The width of the traces corresponds to the 95% CI. Shaded bar corresponds to the downstroke period.

Discussion

Bats carried out low speed 90-degree turns by primarily using a crabbed mechanism to redirect their net aerodynamic force and thus produce centripetal force towards the direction of the turn. We found that turns can be divided into two functionally different components associated with the portions of the wingstroke cycle. In the first part of the turn, during upstroke, bats rotated their bodies horizontally into the turn without significant changes in flight direction. As a result, at the onset of downstroke, the body was already oriented toward the direction of the turn, so that forward component of the net aerodynamic force was also oriented towards the center of the turn. In the second part, which occurred during downstroke, bats changed their flight

direction. The centripetal force necessary to change the heading of the CoM, however, was produced by a combination of the forward and the dorsal component of the net aerodynamic force. The dorsal component, which is parallel to the mid-sagittal plane of the bat's body, arose from the banked attitude of the body through which the vertical component of the net aerodynamic force was reoriented toward the center of the turn. The forward component was modulated by the heading rotation of the body that occurred during the first part of the turn. The analyses presented here do not support our prediction that bats use a banked turning mechanism, like those described for other flying organisms. However, they also indicate that turning in bats is aerodynamically and kinematically complex, and includes a distinctive use of the upstroke phase, usually ignored in studies of animal flight.

Kinematic mechanisms affecting change in heading

Discussions of turning in flying vertebrates have focused almost exclusively on the reorientation of the lift vector by rolling the body into a bank as the mechanism for the generation of the centripetal force (Norberg, 1990; Dudley, 2002). Our results, however, demonstrate that for *C. brachyotis*, change in heading was the best predictor of the change in flight direction. By rotating their bodies horizontally during upstroke, bats reoriented their major body axis in the direction of the turn. As a consequence, when aerodynamic force was produced during downstroke, the thrust vector was already oriented in the direction of the turn (Fig. 1). Although the bank angle did not significantly explain changes in flight direction when changes in heading are considered, the banked orientation of bats observed during downstroke will likely produce centripetal forces nonetheless. Our estimations of the centripetal accelerations produced by the banked

orientation suggested that bats produced about 70% of the necessary force required to generate the observed turn. This figure, however, is likely to be an overestimate. We assumed that the net aerodynamic force was perpendicular to the horizontal plane of the bat, but the larger angle of attack of the inside wing compared with the outside wing during the downstroke, would likely displace the net aerodynamic force vertically, reducing the role of banking with respect to changes in heading. Thus, we hypothesize that there will be a synergistic effect of the changes in heading during upstroke and the banked attitude of the body that will increase the amount of centripetal force produced by either a banked or crabbed turning alone.

Uncoupling of body rotations and generation of aerodynamic forces

It has been suggested that, when a flying organisms does not bank, changes in bearing in crabbed turns are functionally linked to changes in heading angles such that flight trajectory would change only when yaw angles changes (Warrick et al., 1998). This assumes, however, that the yaw moment is produced by differential generation of thrust between the left and right wings during downstroke. This is clearly not the case for *C. brachyotis*. Changes in heading occurred mainly during upstroke, and the aerodynamic forces that produced changes in bearing occurred mostly during downstroke (Fig. 10A). We hypothesize that the temporal uncoupling of the rotation of the body and the generation of aerodynamic force would increase the magnitude of useful aerodynamic force and thus increasing its contribution to the changes in flight direction. This assumes that there is a trade-off between generation of asymmetrical forces to produce body rotation and the generation of lift and thrust. Such uncoupling could be particularly important for turns during slow flight, in which air flow over the wings is relatively

slower and thus contributes less to lift generation than in high-speed flight. Accordingly, *C. brachyotis* produced maximal centripetal forces during mid-downstroke (Fig. 14). Moreover, downstroke showed little kinematic asymmetry, which was instead predominantly confined to the upstroke (Fig. 11, and see supplementary material Fig. S1).

Changes in body orientation prior to changes in heading may also improve the ability of a flying animal to orient the head to the direction of travel, therefore improving spatial orientation. Insectivorous bats clearly orient the head toward the insect when pursuing maneuverable or erratic prey, and change their flight direction accordingly to keep the body aligned with the head direction (Ghose and Moss, 2006). In this case, rotating the body before changing heading would facilitate alignment of the head and body to increase prey location and obstacle avoidance success (Ghose and Moss, 2003; Ghose et al., 2006). The fact we observe alignment of the body with flight direction on a non-echolocating, fruit-eating bat suggests that this phenomenon would be important not only when emitting echolocation calls and listening for returning echoes and when capturing prey, but simply to maneuver successfully in three-dimensionally complex environments.

Effect of body-based rotation angles (yaw, pitch and roll) on turning

Because bats adopt a banked attitude during the turn, changes in heading angle require changes in both pitch and yaw. Our results indicated that pitch is particularly relevant, showing significant variation throughout the wingbeat cycle, and higher angular accelerations than yaw. This suggests that a significant portion of the change in heading

derives from changes in pitch. This in turn, informs our understanding of the forces necessary to rotate the body. A body's rotation about its CoM depends on its mass moments of inertia and on the moments about each axis. In organisms with elongated bodies, it is assumed that the moment of inertia around the roll axis is smaller than the moment of inertia around yaw and pitch axis (e.g., Dudley, 2002), suggesting a faster rotational response to roll than to yaw or pitch. Rolling moments in these bats, however, seem to be mostly compensatory, with changes in the opposite direction to the turn, resulting in an approximately constant bank angle (Fig. 9A,D).

There are advantages of employing modulation of pitch to perform turns. Assuming that there is a trade-off between bilateral wing motion asymmetry and the efficiency of lift and thrust that are produced, pitch can be adjusted by bilaterally symmetrical changes in wingbeat kinematics that shift the net aerodynamic force vector either anterior or posterior to the CoM while changes in yaw and roll require bilateral asymmetries (Dudley, 2002). Furthermore, pitch modulation may also require less force than to produce rotational changes in yaw. The contribution of the wings to the total mass and to the moment of inertia can be considerable in bats (Kirkpatrick, 1990; Watts et al., 2001). For example, in a study of eight bat species, the mass of one wing accounted for about 8% of the total body mass and contributed to about 93% of the roll inertia (Thollesson and Norberg, 1991). In such case, yaw inertia is expected to be larger than pitch moment of inertia assuming that the pitch rotational axis passes through the wings. It is interesting to note that flapping fliers, even in straight, level flight at constant velocity show up and down pitching moments during upstroke and downstroke, respectively. However, comparison of the effect of these 'natural' pitching moments to

those observed on turning flight is not straightforward due to the banked orientation of the bat. Pitching moments are the result of both inertial and aerodynamic effects.

Although changes in pitch due to inertial forces are not expected to change when bats are in a bank compared to when they are in straight flight, we do expect changes in how aerodynamic forces would affect pitch due to the differences in orientation of the gravitational force with respect to the net aerodynamic force.

Mechanisms of heading rotation

Changes in heading are essential to the completion of the turn. However, we observed that heading rotation in the direction of the turn is limited to the upstroke. This portion of the wingbeat cycle, at least for slow flight, has been believed to be inactive aerodynamically (Norberg, 1990; Spedding et al., 2003). How, then, are bats able to change their heading orientation during the upstroke? One mechanism for producing changes in heading is to generate more thrust with the outside wing than with the inside wing, producing a torque in the direction of the turn. This could potentially be accomplished by a backward flick with the tip of the wing, which has been reported in some bats at the beginning of the upstroke, when flying at low speeds (Aldridge, 1986b; Norberg and Winter, 2006). Such a backward flick is observed in *C. brachyotis* at the wingtip (Fig. 16A) but not at the wrist (Fig. 16B) and it is unlikely to produce a global yaw moment because the backward velocities of the outside and the inside wing do not differ significantly during the upstroke (Fig. 16A).

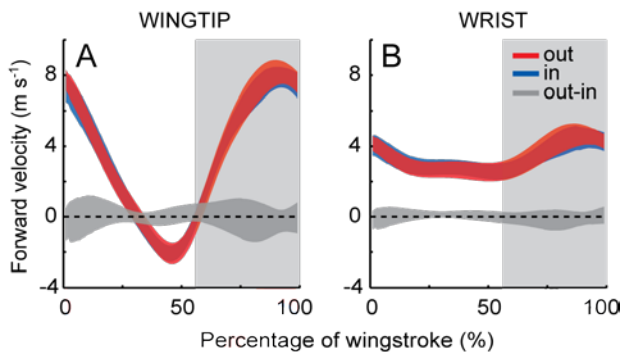


Fig. 16: Forward velocity profiles for the wingtip (A) and wrist markers (B) in a global coordinate system that has been rotated in the Z_g axis to align the X axis component to the bearing velocity vector and thus, the forward velocity represents the marker velocity in the direction of flight. This rotation maintains the elevation and bank orientation of the body. The width of the traces represents the $\text{mean} \pm 95\%$ CI. Shaded bars correspond to downstroke periods.

Differences in profile drag between the inside and outside wing could also potentially produce changes in heading by modulating the drag generated by each wing. The lateral projection of the wings suggest that differential drag between the inside and outside wing may act during upstroke, as the inside wing was more laterally projected than the outside wing during late upstroke. Differences in the lateral projection of the wings and the heading velocity reached at the upstroke-downstroke transition were significantly correlated, suggesting that differential drag due to differences in left vs. right wing area could explain the changes in the global yaw observed for *C. brachyotis*. To verify this, calculations of the profile drag generated by each wing will be necessary, which requires estimates of coefficient of drag during upstroke. Due to the three-dimensional complexity of the wing shape during upstroke, and the lack of empirical estimates of the drag coefficients of compliant airfoils, results from steady state calculations will likely be too unreliable to shed much light on the question.

An alternative means by which to produce changes in heading is the use of asymmetric movements of the wings during upstroke. Left-right asymmetry could generate inertial torques that differ between the inside and outside wing. Such a mechanism is an effective way to produce what is called a zero-angular-momentum

rotation, a maneuver used by self-righting cats (e.g., Arabyan and Tsai, 1998) and gymnasts (Yeadon, 1997). In a zero-angular-momentum rotation, body segments are rotated with respect to each other during the flight, hence the whole body will rotate as a consequence to conserve angular momentum. By this mechanism, changes in heading would arise from differences in the movement of the left and right wings in the horizontal X_g - Y_g plane. It is difficult to predict the effect of wing and body inertia on the body rotation without a modeling the time-varying contribution of a morphing wing and rotating body during the turn but considering that bats' wing masses are about 16% of body mass (Tholleson and Norberg, 1991) it could be expected that inertial reorientation of the body may be important. Inertial contributions to body rotations during turning have been estimated for birds, where asymmetries in the amplitude of the wingbeat were capable of transient changes in roll of only 6 degrees, with a net change of 1.6 degrees per wingbeat (Hedrick and Biewener, 2007). Bats are expected to have a smaller moment of inertia for roll than for yaw and pitch, hence the magnitude of changes due to inertial reorientation in yaw are not likely to be great enough to account for the average change of 20 degrees in yaw observed during upstroke. This issue cannot be resolved, however, without modeling the inertial effect of the observed wing kinematics.

Bat turning compared to other flying organisms

Experiments on maneuvering in birds show that pigeons and cockatiels use banked turns (Warrick and Dial, 1998; Hedrick et al., 2002). In pigeons, roll acceleration increases and decreases during a single wingbeat, and changes in acceleration are correlated with left-right asymmetry in downstroke wing velocity (Warrick and Dial, 1998). Cockatiels show a similar roll acceleration profile, with changes in roll orientation

within each wingbeat correlated with wing motion asymmetries (Hedrick and Biewener, 2007). This within-wingbeat variation, however, is likely the result of inertial forces produced by wing kinematic asymmetries and therefore tends to cancel out over a complete stroke cycle (Hedrick and Biewener, 2007). In fact, changes in cockatiel flight direction were best explained by changes in roll orientation between wingbeats, which are not correlated with changes in roll within each wingbeat, and that are likely the combined result of both inertial and aerodynamic effects (Hedrick and Biewener, 2007). When compared to birds performing similar turns, bats produced tighter maneuvers, allowing them to complete the turn in a smaller number of wingbeats than pigeons and cockatiels (Warrick and Dial, 1998; Hedrick and Biewener, 2007). These differences could be the result of differences in size. *C. brachyotis* are about 10 times smaller in mass than cockatiels, and it has been suggested that maneuverability is inversely related to body size (Aldridge, 1987; Stockwell, 2001). Whether these differences in turning performance are a consequence of differences in size or due to differences in turning mechanisms is not known.

Studies of 180-degree turns in microchiropteran bats have shown that bats initiate turns by flying upwards and decelerating (Rayner and Aldridge, 1985; Aldridge, 1987). We observed similar patterns in our experiments, although our bats maintained their net forward speed throughout the recorded portion of the turn. The curvatures of the turns observed in our experiment were 3 to 23 times smaller (i.e., greater turning radius) than those observed for other bat species performing 180-degree turns (Aldridge, 1987). Such variation is to be expected, considering the differences in task and body sizes.

The use of a combination of crabbed and banked mechanisms to produce a turn is likely to increase the maneuverability of bats compared to a mechanism that employs lift alone. The net influence of the crabbed component on turning is not readily quantified, but it is clearly important for insects (Dudley, 2002). For example, in dragonflies capable of both banked and crabbed turns, the latter strategy produces turns at much higher rates, with changes in direction of 180 degrees in less than 3 wingbeats (Alexander, 1986). This degree of maneuverability is similar to that observed in our bats, where 180-degree turns can be achieved in 3-4 wingbeats, although no information is available on whether the turn was banked, crabbed or a combination of both (Tian et al., 2006).

Our findings show that bats use a combination of crabbed and banked mechanisms to produce centripetal accelerations required to perform a turn. *C. brachyotis* changed its heading during upstroke and thus reorienting the body in such a way that the net aerodynamic force produced during downstroke is aligned with the direction of travel. Therefore, the reorientation of the body and the bank angle of the body will act synergistically to produce a centripetal force. Bats seemed to actively change their yaw and pitch, while changes in roll were compensatory to maintain a constant bank attitude. Reorientation during a wingbeat cycle is probably the result of the combination of aerodynamic and inertial forces and future research should include estimation of how asymmetries in wingbeat kinematics to estimate the magnitude of inertial reorientation.

Acknowledgments

We thank Lubee Bat Conservancy and Dr. Allyson Walsh for loaning us the bats; Andrew Biewener and the Harvard University Concord Field Station for allowing us the use of their facilities; Pedro Ramírez for caring for the bats; Kevin Middleton, Rachel Roemer, Allyce Sullivan, Ming-Ming Lee, Joe Wofford, Ann Atwood and Claudio Hetz for help with the experiments. We thank Ty Hedrick for his help during analysis and writing and David Willis for developing the mass model to estimate the CoM. Thanks to Daniel K. Riskin, Kenny Breuer, David Willis, Tatjana Hubel, Kristin Bishop and the Morphology group at Brown University for comments and discussions of the manuscript. This research was supported by the AFOSR, NSF-ITR, and the Bushnell Foundation.

List of symbols and abbreviations

\mathbf{A}_b	Acceleration vector of the body in the global coordinate system
$\mathbf{A}_{b,xy}$	Acceleration vector of the body in the horizontal plane X_g – Y_g of the global coordinate system
$\mathbf{A}_{c,bank}$	Estimated centripetal acceleration produced by the roll angle of the body
$\mathbf{A}_{c,total}$	Centripetal acceleration necessary to produce a turn with a radius $1/\kappa$
$\mathbf{A}_{COM,z}$	Vertical acceleration of the CoM in the global coordinate system
CoM	Center of mass
DLT	Direct linear transformation

\mathbf{g}	Acceleration of gravity
GLM	General lineal model
\mathbf{V}_b	Velocity vector of the body in the global coordinate system
$\mathbf{V}_{b,xy}$	Velocity vector of the body in the horizontal plane X_g - Y_g of the global coordinate system
$X_g Y_g Z_g$	Fixed, global coordinate system
$x_g y_g z_g$	Cartesian coordinates in the global coordinate system
$X_b Y_b Z_b$	Dynamic, body-based coordinate system (centered on the hip)
$x_b y_b z_b$	Cartesian coordinates in the body-based coordinate system
κ	Curvature in the horizontal plane X_g - Z_g
γ_v, γ_h	Vertical and horizontal stroke plane angle, respectively
φ	Bearing angle
ψ, θ, ϕ	Heading, elevation and bank angle, respectively, in the global coordinate system

References

- Aldridge, H.** (1986a). Manoeuvrability and ecological segregation in the little brown (*Myotis lucifugus*) and Yuma (*M. yumanensis*) bats (Chiroptera: Vespertilionidae). *Can. J. Zool.* **64**, 1878-1882.
- Aldridge, H. D. J. N.** (1986b). Kinematics and aerodynamics of the greater horseshoe bat, *Rhinolophus ferrumequinum*, in horizontal flight at various speeds. *J. Exp. Biol.* **126**, 479-497.
- Aldridge, H. D. J. N.** (1987). Turning flight of bats. *J. Exp. Biol.* **128**, 419-425.
- Alexander, D. E.** (1986). Wind tunnel studies of turns by flying dragonflies. *J. Exp. Biol.* **122**, 81-98.
- Arabyan, A. and Tsai, D.** (1998). A distributed control model for the air-righting reflex of a cat. *Biol. Cybern.* **79**, 393-401.
- Berger, S. and Kutsch, W.** (2003). Turning manoeuvres in free-flying locusts: high-speed video-monitoring. *J. Exp. Zool.* **299A**, 127-138.
- Bishop, K. L. and Brim-DeForest, W.** (2008). Kinematics of turning maneuvers in the Southern flying squirrel, *Glaucomys volans*. *J. Exp. Zool.* **309A**, 225-242.
- Card, G. and Dickinson, M.** (2008). Performance trade-offs in the flight initiation of *Drosophila*. *J. Exp. Biol.* **211**, 341-353.
- Dudley, R.** (2002). Mechanisms and implications of animal flight maneuverability. *Integ. Comp. Biol.* **42**, 135-140.
- Filippone, A.** (2006). Flight performance of fixed and rotary wing aircraft. Oxford: Butterworth-Heinemann.
- Fry, S. N., Sayaman, R. and Dickinson, M. H.** (2003). The aerodynamics of free-flight maneuvers in *Drosophila*. *Science* **300**, 495-498.
- Ghose, K., Horiuchi, T. K., Krishnaprasad, P. S. and Moss, C. F.** (2006). Echolocating Bats Use a Nearly Time-Optimal Strategy to Intercept Prey. *PLoS Biology* **4**, e108.
- Ghose, K. and Moss, C. F.** (2003). The sonar beam pattern of a flying bat as it tracks tethered insects. *J. Acoust. Soc. Amer.* **114**, 1120-1131.
- Ghose, K. and Moss, C. F.** (2006). Steering by hearing: a bat's acoustic gaze is linked to its flight motor output by a delayed, adaptive linear law. *J. Neurosci.* **26**, 1704-1710.

- Hatze, H.** (1988). High-precision three-dimensional photogrammetric calibration and object space reconstruction using a modified DLT-approach. *J. Biomech.* **21**, 533-538.
- Hedrick, T. L.** (2007). DLTDataviewer2 for Matlab. (<http://www.unc.edu/%7Eethedrick/software1.html>)
- Hedrick, T. L. and Biewener, A. A.** (2007). Low speed maneuvering flight of the rose-breasted cockatoo (*Eolophus roseicapillus*). I. Kinematic and neuromuscular control of turning. *J. Exp. Biol.* **210**, 1897-1911.
- Hedrick, T. L., Tobalske, B. W. and Biewener, A. A.** (2002). Estimates of circulation and gait change based on a three-dimensional kinematic analysis of flight in cockatiels (*Nymphicus hollandicus*) and ringed turtle-doves (*Streptopelia risotia*). *J. Exp. Biol.* **205**, 1389-1409.
- Hedrick, T. L., Usherwood, J. R. and Biewener, A. A.** (2007). Low speed maneuvering flight of the rose-breasted cockatoo (*Eolophus roseicapillus*). II. Inertial and aerodynamic reorientation. *J. Exp. Biol.* **210**, 1912-1924.
- Kalcounis, M. C. and Brigham, R. M.** (1995). Intraspecific variation in wing loading affects habitat use by little brown bats (*Myotis lucifugus*). *Can. J. Zool.* **73**, 89-95.
- Kirkpatrick, S. J.** (1990). The moment of inertia of bird wings. *J. Exp. Biol.* **151**, 489-494.
- McCay, M. G.** (2001). Aerodynamic stability and maneuverability of the gliding frog *Polypedates dennysi*. *J. Exp. Biol.* **204**, 2817-2826.
- Norberg, U. M.** (1976). Some advanced flight manoeuvres of bats. *J. Exp. Biol.* **64**, 489-495.
- Norberg, U. M.** (1990). Vertebrate flight. Berlin: Springer-Verlag.
- Norberg, U. M. and Rayner, J. M. V.** (1987). Ecological morphology and flight in bats (Mammalia; Chiroptera): wing adaptations, flight performance, foraging strategy and echolocation. *Philos. Trans. R. Soc. Lond. B* **316**, 335-427.
- Norberg, U. M. L. and Winter, Y.** (2006). Wing beat kinematics of a nectar-feeding bat, *Glossophaga soricina*, flying at different flight speeds and Strouhal numbers. *J. Exp. Biol.* **209**, 3887-3897.
- Phillips, W. F.** (2004). Mechanics of flight. Hoboken, NJ: Wiley.
- Rayner, J. M. V. and Aldridge, H. D. J. N.** (1985). Three-dimensional reconstruction of animal flight paths and the turning flight of microchiropteran bats. *J. Exp. Biol.* **118**, 247-265.

- Spedding, G. R., Rosén, M. and Hedenström, A.** (2003). A family of vortex wakes generated by a thrush nightingale in free flight in a wind tunnel over its entire natural range of flight speeds. *J. Exp. Biol.* **206**, 2313-2344.
- Stockwell, E. F.** (2001). Morphology and flight manoeuvrability in New World leaf-nosed bats (Chiroptera : Phyllostomidae). *J. Zool.* **254**, 505-514.
- Swartz, S. M., Groves, M. D., Kim, H. D. and Walsh, W. R.** (1996). Mechanical properties of bat wing membrane skin. *J. Zool.* **239**, 357-378.
- Thollessen, M. and Norberg, U. M.** (1991). Moments of inertia of bat wings and body. *J. Exp. Biol.* **158**, 19-35.
- Tian, X., Iriarte-Diaz, J., Middleton, K., Galvao, R., Israeli, E., Roemer, A., Sullivan, A., Song, A., Swartz, S. and Breuer, K.** (2006). Direct measurements of the kinematics and dynamics of bat flight. *Bioinspiration & Biomimetics* **1**, S10-S18.
- Walker, J. A.** (1998). Estimating velocities and accelerations of animal locomotion: a simulation experiment comparing numerical differentiation algorithms. *J. Exp. Biol.* **201**, 981-995.
- Warrick, D. R.** (1998). The turning- and linear-maneuvering performance of birds: the cost of efficiency for coursing insectivores. *Can. J. Zool.* **76**, 1063-1079.
- Warrick, D. R. and Dial, K. P.** (1998). Kinematic, aerodynamic and anatomical mechanisms in the slow, maneuvering flight of pigeons. *J. Exp. Biol.* **201**, 655-672.
- Warrick, D. R., Dial, K. P. and Biewener, A. A.** (1998). Asymmetrical force production in the maneuvering flight of pigeons. *Auk* **115**, 916-928.
- Watts, P., Mitchell, E. J. and Swartz, S. M.** (2001). A computational model for estimating the mechanics of horizontal flapping flight in bats: model description and validation. *J. Exp. Biol.* **204**, 2873-2898.
- Woltring, H. J.** (1986). A FORTRAN package for generalized, cross-validatorspline smoothing and differentiation. *Adv. Engng. Soft.* **8**, 104-113.
- Yeadon, M. R.** (1997). The biomechanics of the human in flight. *Am. J. Sports Med.* **25**, 575-580.

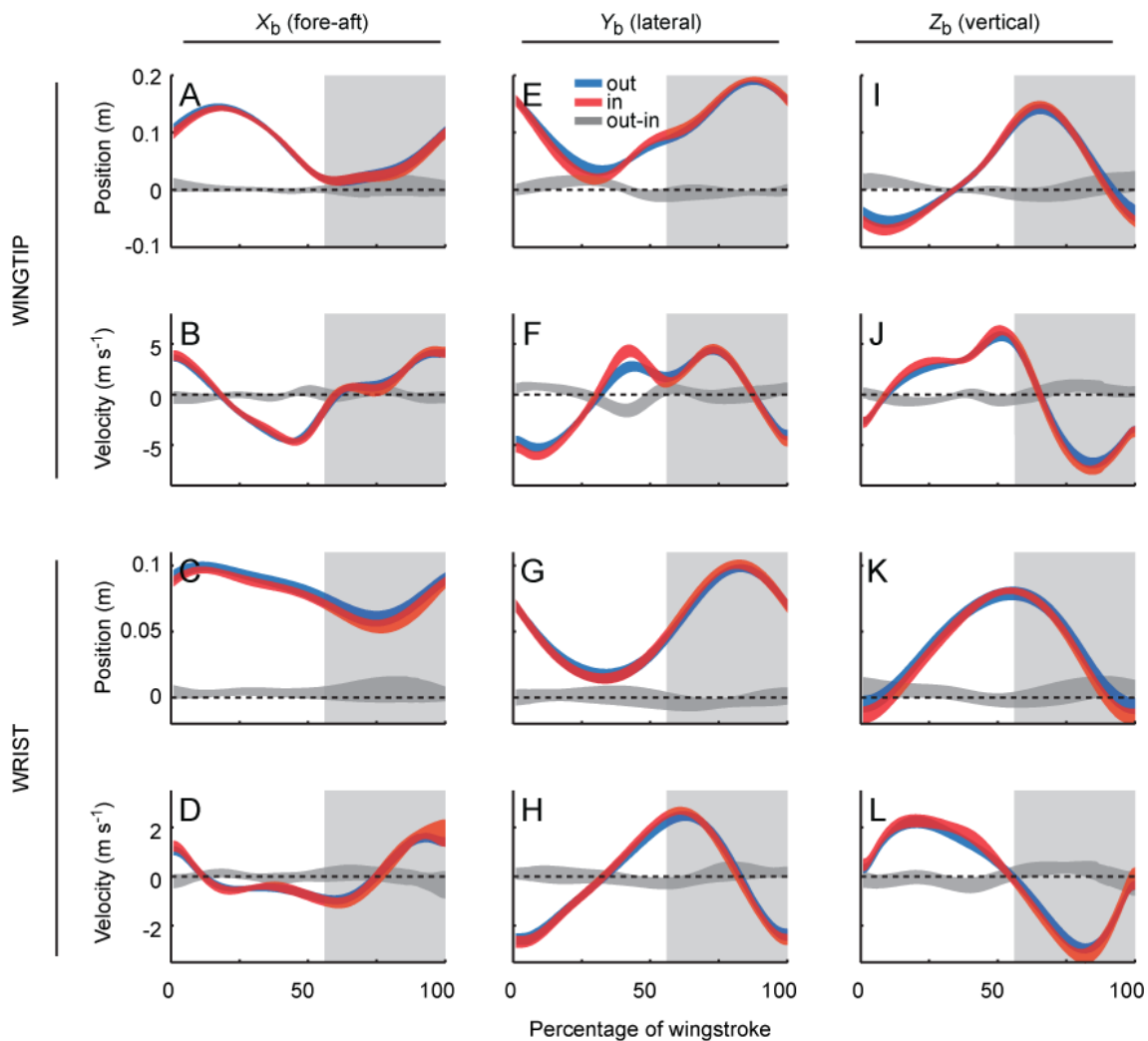


Fig. S1: Position and velocity for the wingtip (top six boxes) and wrist marker (bottom six boxes) in the body coordinate system. The left, middle and right columns correspond to values in the X_b (forward), Y_b (lateral) and Z_b (vertical) axes, respectively. Red, blue and grey traces represent the mean \pm 95% CI for the inside and outside wings and the difference between them, respectively. Shaded bars correspond to downstroke periods. Positive values in the right-side column represent that the position of the marker is on the ipsi-lateral side in I and K, and that the marker is moving laterally, away from the midline in J and L.

Chapter 2

Modulation of wingbeat kinematics with flight speed in the fruit bat *Cynopterus brachyotis*

José Iriarte-Díaz & Sharon M. Swartz

Department of Ecology and Evolutionary Biology, Brown University

Abstract

Powered, flapping flight has evolved at least three times in the extant animal groups: in insects, birds, and bats. In the last few years, research on the mechanics, energetics, and aerodynamics of insects and birds have greatly improved our understanding of the mechanism employed by flying animals. Although some aspects of flight mechanics are probably common to all flying lineages, each one represents a unique solution to the challenges of maneuverable, efficient flapping flight. This might be particularly true in bats, considering that bats possess wings with many independently controlled joints, and with flexible bones supporting a highly compliant and anisotropic membrane. Flight in bats, however, remains the least documented and understood among flying animals. In this study we investigated the flight kinematics of bats flying at a range of speeds. Four lesser dog-faced fruit bats (*Cynopterus brachyotis*) were trained to fly both in a flight corridor and a wind tunnel and were recorded with three phased-locked high-speed video cameras at 1000 Hz. Wingbeat kinematics changed gradually with speed indicating that there is no sudden gait change at any particular, critical speed. Changes in kinematics with speed, however, showed differences among individuals. These differences indicate that there are multiple strategies that can be used to modulate lift and thrust during flight. At speeds below 5 m s^{-1} , the observed kinematics suggest that bats' wings are affected by unsteady aerodynamic effects and therefore the use of steady-state flow analyses are likely to produce an inaccurate representation of the fluid dynamics around the wings.

Introduction

Bats, birds and insects are the only three extant animal groups that have evolved powered flight. Research in the last few years on the energetics, biomechanics, and aerodynamics of insects and birds has provided deep insight on the basic mechanisms of aerodynamic force generation and flight control, primarily due to advances in high-speed kinematic and wake visualization technologies (Dickinson et al., 2000; Sane, 2003; Tobalske, 2007; Lauder and Madden, 2008; Taylor et al., 2008). Bats, however, remain the least studied group of flying animals despite exhibiting remarkable flight capabilities that combine a high degree of maneuverability with energetic efficiency. For example, hovering flight in bats is 40% and 60% less metabolically costly than insects and birds of similar size, respectively (Winter, 1998; Voigt and Winter, 1999). To explain how bats achieve such a remarkable level of performance requires the identification of those aspects of the kinematics of flapping flight in bats that differ from birds and insects, and an understanding of how these aspects are modulated during normal flight.

In spite of previous work on the kinematics and mechanics of bat flight (Norberg, 1976; Aldridge, 1986, 1987; Watts et al., 2001; Norberg and Winter, 2006), the basic mechanisms by which bats generate aerodynamic force are still poorly understood, in part because of the absence of detailed three-dimensional descriptions of the motion of the body and wings of bats during flight. Such a description is essential when considering the inherent complexity of motion of bats that involves rapid three-dimensional folding, bending, and rotational wing movements to generate aerodynamic force which is evidenced by the highly complex wake structure to the air behind it (Swartz et al., 2005; Tian et al., 2006; Hedenström et al., 2007; Riskin et al., in press). In this study, we

describe the detailed three-dimensional kinematics of the body and wings of bats flying at a range of speeds, focusing on those aspects of wing structure that are most likely related to aerodynamic force generation and how these aspects are modulated with flight speed.

Material and methods

Animals and experimental procedures

Four female lesser short-nosed fruit bats, *Cynopterus brachyotis* (Muller) (Table 1), loaned by the Lube Bat Conservancy (Gainesville, FL) were used in this experiment. They were housed in the animal care facilities of the Harvard-Concord Field Station, where they were provided with food and water *ad libitum*. Before each experiment, bats were anesthetized with isoflurane gas, and key anatomical landmarks were marked with an array of high-contrast markers on the undersurface of one wing (Fig. 1A).

Table 1. Morphological measurements of the individuals used in this study.

Variable	Individual			
	Bat1	Bat2	Bat3	Bat4
Mass (kg)	0.0348	0.0371	0.0417	0.0331
Wing span (m)	0.361	0.386	0.411	0.355
Wing area (m ²)	0.0197	0.0212	0.0250	0.0188
Aspect ratio	6.6	7	6.8	6.7
Wing loading (N m ⁻²)	17.3	17.2	16.3	17.3

Bats were flown in two sets of experiments: (1) still air/flight corridor experiments, where bats were allowed to select their flight speed, and (2) wind tunnel experiments, where flight speed was experimentally controlled. Bats were flown in these

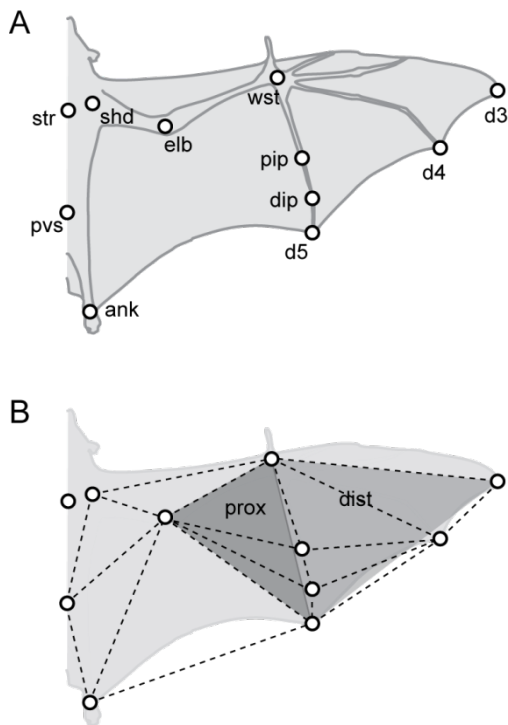


Fig. 1. Ventral view diagram of a bat indicating (A) the position of the wing and body markers and (B) the triangular segmentation used to calculate surface area, vertical force coefficient (C_{vf}), and the angles of attack. The dotted lines represent the vertices of the 11 segments used to calculate surface area and C_{vf} and the shaded triangles represent the segmentation used to calculate the proximal (prox) and distal (dist) angles of attack.

two setups to increase the range of speeds available for analysis, because they fly, on average, more slowly in the flight corridor than they would in the wind tunnel. In the flight corridor experiment, bats were trained to fly inside a 9 m long enclosure (1 m wide and 2 m high). Bats were hand-released on one end of the corridor, and allowed to select their flight speeds, which ranged from 1.8 to 3.3 m s⁻¹. Wind tunnel experiments were conducted at the Harvard Concord Field Station wind tunnel, an open-circuit tunnel with a closed jet in the flight chamber and a working section of 1.4 m length, 1.2 m width and 1.2 m height (Hedrick et al., 2002). In the wind tunnel, bats flew at speeds ranging from 3.1 up to 8 m s⁻¹.

All components of this study were approved by the Institutional Animal Care and Use Committees at Brown University, Harvard University, and the Lubee Bat Conservancy, and by the United States Air Force Office of the Surgeon General's Division of Biomedical Research and Regulatory Compliance.

Three-dimensional coordinate mapping

Flight corridor trials were recorded at 500 frames per second using three high-speed Redlake PCI 1000 digital cameras. The volume in which the bats were flown was calibrated using the Direct Linear Transformation (DLT) method, based on a 25-point (0.45x0.45x0.55 m) calibration cube, recorded at the beginning of each set of trials (Hatze, 1988). Wind tunnel flights were recorded at 1000 frames per second using three high-speed Photron 1024 PCI digital cameras and calibrated by using the DLT method with 40-point (0.35x0.35x0.30 m) calibration cube, recorded at the beginning of each set of trials.

For the flight corridor trials, six markers on the bats' body were digitized in each video frame (*str*, *pvs*, *shd*, *wst*, *d3* and *d5* in Fig. 1A), while for wind tunnel experiments, eleven markers were digitized (Fig. 1A). The three-dimensional position of each marker was resolved using the DLT coefficients obtained from the calibration cube (Hatze, 1988). A DLT root mean square (RMS) error was calculated for each point at every frame. The median RMS error was 0.5 cm for the flight corridor experimental setup and 0.1 cm for the wind tunnel setup. When a marker was not simultaneously visible in at least two cameras, gaps in the three-dimensional position of the markers occurred. These gaps were filled by over-constrained polynomial interpolation. For contiguous gaps in the data, with sufficiently rich data at the end points, a third order, over-constrained polynomial fit was used. For gaps that included sporadic intermediate points, a sixth order polynomial was used. After gap-filling, a 50 Hz digital Butterworth low-pass filter was used to remove high-frequency noise. This cut-off frequency was approximately 5 times higher than the wingbeat frequency recorded in our bats.

Calculation of kinematic parameters

A wingbeat cycle was defined by the vertical excursion of the wrist in a body coordinate system. Downstroke and upstroke phases were defined as the portions of the wingbeat cycle where wrist vertical velocities were negative and positive, respectively. Because markers along the wing reach their peak vertical position asynchronously, the wingbeat cycle would be slightly different if another marker were employed. The wingtip, for example, reaches its peak vertical position, between 6 and 8 ms after the wrist (Swartz et al., 2007). We chose the wrist because it is the most likely landmark to accurately reflect patterns of activation of the flight muscles.

Wingbeat frequency was defined as the inverse of the period between two consecutive downstrokes. The downstroke ratio was defined as the proportion of the wingbeat cycle occupied by the downstroke. Wingbeat amplitude was defined as the angle between the straight line connecting the wingtip (*d3*) and the shoulder (*shd*) markers at the beginning of the downstroke and the straight line connecting *d3* and *shd* markers at the end of the downstroke. To further explore the changes in the motion of the wing, we also calculated the velocity of the wingtip with respect to the body. These five variables were calculated from both flight corridor and wind tunnel experiments.

Body pitch was defined as the angle between the major axis of the body, defined by the line connecting the pelvis (*pvs*) and the sternum (*str*) marker, and the horizontal plane of the lab (Fig. 3A). Stroke plane angle was defined as the angle between the horizontal axis and the least-squares regression line through the lateral projection of the wingtip position during the downstroke (Fig. 2A). The vertical, forward, and lateral

excursion of the wingtip marker (D_{forw} , D_{lat} , and D_{vert} , respectively) was measured as the maximum distance, with respect to the pelvis marker, between two points within a wingbeat cycle, in the X , Y , and the Z axes, respectively (Fig. 2A,B).

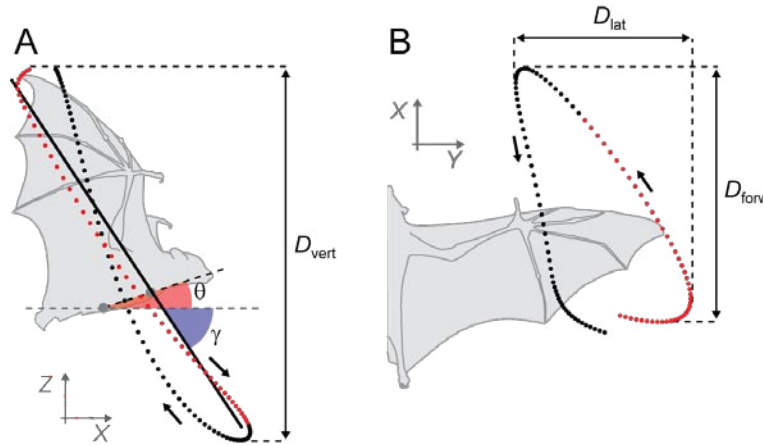


Fig. 2. Lateral (A) and ventral (B) view of a bat, indicating body pitch angle (θ), stroke angles (γ) and excursion of the wingtip. Stroke angle was estimated by the linear regression of lateral projection of the wingtip motion during the downstroke, with respect to the pelvis marker (red dotted line). Pitch angle was defined as the angle between the line connecting the pelvis and sternum marker and the X axis. The forward, lateral and vertical excursion of the wingtip with respect to the pelvis marker (D_{forw} , D_{lat} , and D_{vert} , respectively) was defined as the maximum distance between two points within a wingbeat cycle with respect to the X , Y , and Z axes, respectively.

The camber of the wing during downstroke was estimated by measuring the curvature of the digit V. We did so by fitting a parametric quadratic curve to the three-dimensional position of the four markers along that digit (*wst*, *pip*, *dip*, *d5* in Fig. 1A). The fitted quadratic curve was then divided into 50 segments and the curvature of each segment was calculated as the average rate of change in the tangent to the curve along its length (Crenshaw et al., 2000). Curvature has units of m^{-1} and in circle, for example, it represents the inverse of its radius.

We measured the elbow and wrist joint angles to estimate the change in folding of the wing at different speeds. Elbow joint angle was calculated as the three-dimensional

angle between the shoulder, elbow and wrist markers (*shd*, *elb*, and *wst* in Fig. 1A), while the wrist joint angle as the angle between the elbow, wrist and wingtip markers (*elb*, *wst*, and *d3* in Fig. 1A).

To estimate wing surface area, we divided the wing into 11 eleven segments (Fig. 1B) and calculated the area of each one. Total wing area was obtained by multiplying the obtained area for one wing by two. This value is necessarily smaller than the conventional value obtained from measurements of bats with completely extended wings over a flat surface because bats do not completely extend their wings during flight (Swartz et al., 2005) and because we do not include body area in this estimate.

We also divided the wing into a proximal and a distal triangular segment (Fig. 1B) and estimated angle of attack for each as the angle between the vector of the relative incident air velocity and a plane formed by the three vertices of each segment. The incident velocity vector was calculated as the first derivative of the position of the centroid of each segment.

Vertical force coefficient

The vertical force coefficient (C_{vf}) can be estimated from the measured vertical force produced to overcome gravity (F_v), air density (ρ), and the area (A) and velocity (V) of the wing (Usherwood and Ellington, 2002) with the equation

$$C_{vf} = \frac{F_v}{\frac{1}{2}\rho 2AV^2}, \quad (1)$$

where $2A$ represents the area of both wings and ρ is 1.2 kg m^{-3} . This coefficient is a dimensionless number that, among other factors, depends on the angle of attack and camber of the wing, and that indicates the capacity of the wing to produce vertical force. Therefore, C_{vf} is a useful measurement of the relative importance of changes of angle of attack and camber with respect to loading. For example, if the modulation of either wing velocity or wing area during downstroke is enough to produce the extra lift necessary to support extra weight, we expect to see no change in C_{vf} . In contrast, if modulation of angle of attack and/or camber is important to extra vertical force generation, C_{vf} will increase in bats flying with loads. The vertical force (F_v) was calculated by multiplying the body mass by the vector sum of the gravitational acceleration and instantaneous vertical acceleration of the center of mass (CoM) derived from a mass model (see below). Because of the flapping motion of the wings, more distal portions of the wings will move faster than proximal ones. Therefore, we divided the wing into 11 triangular segments (Fig. 1B), and for each of these segments we calculated surface area and velocity. We obtained the velocity of a segment by calculating the first derivative of the position vector of its centroid in the global coordinate system. The contribution of each of these segments was used to calculate C_{vf} as:

$$C_{vf} = \frac{F_v}{\frac{1}{2} \rho 2 \sum_{i=1}^{i=11} A_i V_i^2}, \quad (2)$$

where A_i and V_i are the area and velocity of the i -th segment.

Determination of the CoM

In a flapping animal, the motion of the wings changes the position of the CoM with respect of the body throughout the wingbeat cycle. To calculate F_v as above requires the true position of the CoM, which was estimated by building a dynamic mass model of the bat. This mass model is a time-varying, discrete mass approximation of the bat's mass distribution, based on the location of the markers. To develop the discrete mass system representing the bat, we partitioned total body mass into individual components or regions. The wing membrane, the wing bones and the trunk were treated as separate objects, each with its own position and mass, which were combined to form the total mass model.

To model the distribution of the wing membrane mass, we constructed a triangulation of the wing geometry at each time step. The large-scale, base triangulation was developed using the location of the marker positions at any given time, and a subsequent subdivision of those triangles was performed to give a mesh of fine-scale triangular elements. Each triangle element on the membrane was assigned a constant thickness (1×10^{-4} m) and density (1×10^3 kg m⁻³). A resulting discrete point mass (m_i) for each triangular membrane element was computed based on the volume of that triangular membrane and assigned a position at the centroid of the triangle element. To model the distribution of mass among and within each of the wing bones, we constructed a curve between the markers at the endpoints of the bones. The curve for each bone in the wing was defined from the location of the markers. Given the tapered shape of bat bones (Swartz, 1997), the cross-sectional radius of each bone element of the model was defined by a quadratic function with respect to the length of the bone. We assigned a constant

density to the bones ($2 \times 10^3 \text{ kg m}^{-3}$). Using the distribution of bone radii distribution and the location of the bone elements in space, the line was subdivided into smaller line-elements, from which discrete mass points were defined. The mass of the wings was scaled such that the constructed distribution represents the 16% of the total body mass, according to measurements of bats of similar size (Thollessen and Norberg, 1991). The mass and moment of inertia of the wing with respect to the shoulder was compared to measured values (Thollessen and Norberg, 1991) to ensure that the model represents the physical reality. Finally, the bat's body was defined as a 3-dimensional ellipsoid divided into discrete mass points.

The discrete mass representation of the membranes, bones and body was combined with detailed kinematic records of motion of each landmark to determine the center of mass of each one of the mass elements, m_i , using the equation

$$\vec{r}_{CoM} = \frac{\sum \vec{r}_i m_i}{m_T}, \quad (3)$$

where \vec{r}_{CoM} represents the position vector of the CoM, \vec{r}_i represents the position vector of the i -th discrete point mass and m_T represents the total mass of the bat.

Reduced frequency and Strouhal number

Reduced frequency (k) represents the ratio between flapping velocity and forward flight speed at the half chord, and it has been long used as a measure of the importance of unsteady effects during flight. Values of $k < 0.4$ are typically considered evidence of significant unsteadiness (Spedding, 1993). Similarly, Strouhal number (St) is a dimensionless frequency that also describes the relative importance of unsteady effects of

fluids. St represents a measure of the ratio between the inertial forces due to unsteadiness of the flow and the inertial forces due to changes in velocity from one point to another in the flow field (Norberg and Winter, 2006). Although k provides a better measure of unsteadiness than St by comparing spatial wavelength of the flow disturbance with the chord length, St is a better parameter for characterizing the dynamics of wake flow (Triantafyllou et al., 2000).

We calculated reduced frequency (k) as:

$$k = \frac{\pi fc}{V}, \quad (4)$$

where f is the wingbeat frequency, c is the wing cord, calculated as the mean distance between the wst and d5 markers during downstroke, and V is the flight speed. Strouhal number (St) was calculated as:

$$St = \frac{fD_{\text{vert}}}{V}, \quad (5)$$

where D_{vert} is the vertical excursion of the wingtip (Fig. 2A).

Statistical analyses

For each trial, a mean value was calculated from two to six wingbeats for each variable. For each bat, the linear relationship between a variable and speed was assessed by a multiple regression approach. For those variables in which a linear relationship was observed, the equality of slopes among individuals was determined by an analysis of covariance, with the interaction between the individual bat factor and the speed covariate. If inequality of variances was found, a multiple comparison was performed on the slopes by using a Tukey test (Zar, 1999). All analyses were performed in JMP (version 7; SAS

Institute, Cary, NC, USA) with a significance level, $\alpha=0.05$. Data are presented as mean \pm s.e.m.

Results

After combining flights from the flight corridor and the wind tunnel, bats flew at speeds ranging from 1.8 to 8 m s⁻¹. Kinematic parameters changed gradually with speed. Changes in kinematics with speed, however, varied among individuals.

The lateral projection of the reconstructed path of the wingtip with respect to still air showed that bats flying at slow speeds moved their wings upward and backward during upstroke, producing a so-called ‘tip-reversal upstroke’ (Fig. 3A). As speed increased, the backward movement of the wing gradually disappeared, becoming an upward and forward motion of the wingtip (Fig. 3A). The trajectory of the wingtip with respect to the body changed only subtly with speed, transitioning from a figure-eight shaped motion at low speed to an elliptical shape at higher speeds (Fig. 3B).

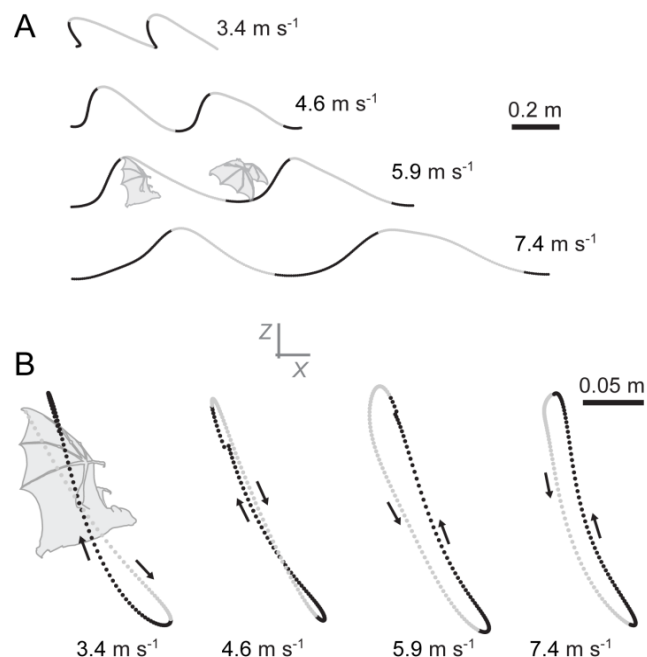


Fig. 3. Lateral projection of the wingtip with respect of still air (A) and with respect to the bat's body (B), for a representative bat flying at different speeds.

Table 2. Slopes of the linear relationships between kinematic variables and flight speed.

Variable	Slope, <i>b</i>				Slope comparison	
	Bat1	Bat2	Bat3	Bat4	<i>P</i> -value	Grouping
Frequency	-0.15 ± 0.06*	0.12 ± 0.04*	-0.17 ± 0.06*	-0.18 ± 0.04**	0.002	4-3-1 2
Amplitude	20.0 ± 1.4***	11.9 ± 1.8***	9.0 ± 1.1***	3.2 ± 1.9	<0.0001	4-3 3-2 1
Downstroke ratio	-0.004 ± 0.004	0.005 ± 0.002	0.003 ± 0.001*	0.005 ± 0.001*	0.12	
stroke plane	6.6 ± 1.0**	6.8 ± 0.8***	7.2 ± 0.6***	4.8 ± 0.7**	0.88	
Pitch angle	-3.77 ± 1.51	-4.48 ± 0.67***	-1.36 ± 0.41*	-0.91 ± 0.29**	0.004	1-2-3 3-4
Horizontal excursion wingtip	-0.010 ± 0.007	-0.027 ± 0.003***	-0.013 ± 0.006	-0.012 ± 0.004*	0.03	2 3-4-1
Vertical excursion wingtip	0.026 ± 0.005*	0.022 ± 0.003**	0.002 ± 0.013	0.003 ± 0.003	0.01	3-4 2-1
Lateral excursion wingtip	0.033 ± 0.012	0.014 ± 0.004*	-0.011 ± 0.005	0.002 ± 0.004	0.002	3-4-2-1
Proximal angle of attack	-4.53 ± 0.93*	-3.56 ± 0.48***	-3.32 ± 0.71**	-2.89 ± 0.54**	0.43	
Distal angle of attack	-4.57 ± 0.92*	-3.41 ± 0.50***	-3.34 ± 0.69**	-2.70 ± 0.51**	0.20	
Camber	-0.87 ± 0.17*	-0.92 ± 0.09***	-1.74 ± 0.25***	-1.02 ± 0.13***	0.01	3 4-1-2
Elbow extension (downstroke)	-0.88 ± 0.77	-0.68 ± 0.34	-3.30 ± 1.46	-1.56 ± 1.27	0.42	
Elbow extension (upstroke)	-4.65 ± 1.41*	-2.28 ± 0.27***	-0.85 ± 0.68	-1.02 ± 0.43	0.007	1-2 2-4-3
Wrist extension (downstroke)	0.80 ± 0.45	0.12 ± 0.49	-1.77 ± 0.87	-1.14 ± 0.72	0.11	
Wrist extension (upstroke)	-3.97 ± 0.79*	-4.27 ± 0.48***	-0.59 ± 0.80	-0.90 ± 0.57	0.0005	2-1 4-3

Slope from a least-square linear relationship (variable = *a* + *b* speed). Presented as mean ± s.e.m.

Slope significantly different than zero at * *P* < 0.05; ** *P* < 0.01; *** *P* < 0.001

Slope test corresponds to the interaction effect (individual x speed) of an ANCOVA analysis.

Grouping corresponds to significantly different slope groups based on Tukey test with $\alpha=0.05$. From low to high.

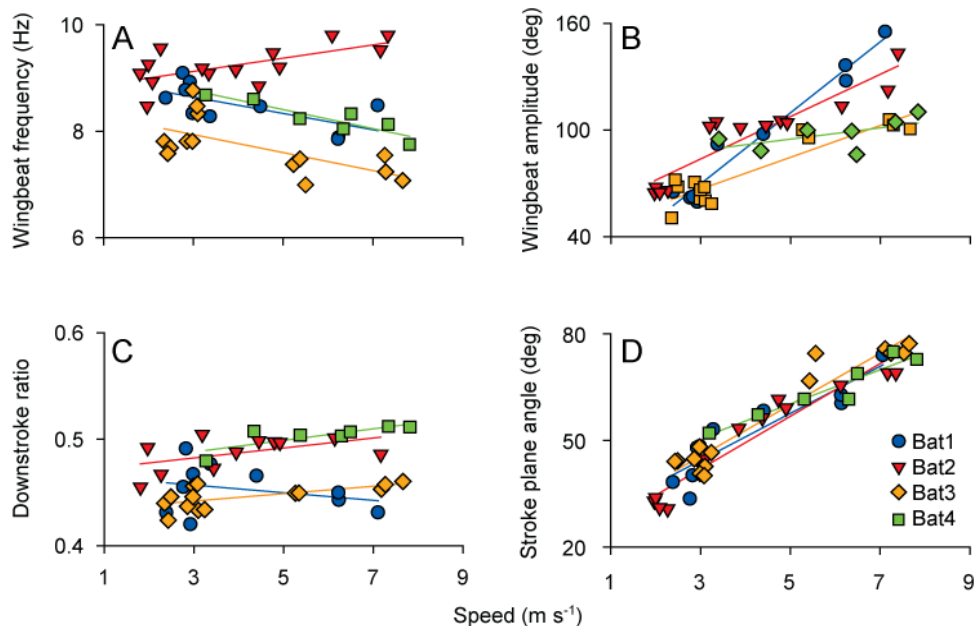


Fig. 4. Wingbeat frequency (A), wingbeat amplitude (B), downstroke ratio (C), and stroke plane angle (D) as a function of speed, for both flight corridor and wind tunnel flights.

Wingbeat frequency changed with speed differently among individuals (Table 2; Fig. 4A). In bat2, wingbeat frequency increased approximately 1 Hz over the observed range of speed, and other bats decreased their wingbeat frequency by a similar amount. Wingbeat amplitude increased in all individuals to varying degrees, but with only marginal significance for Bat4 (Table 2; $P=0.056$) (Fig. 4B). Downstroke ratio increased

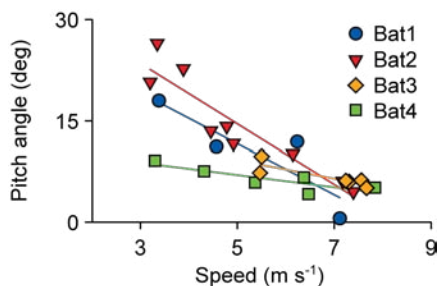


Fig. 5. Body pitch angle as a function of flight speed, for wind tunnel experiments only.

with speed in Bat3 and Bat4, although the magnitude of change was small. Overall, considering all four individuals, there was no significant increase with speed. Stroke plane angle increased with speed for all individuals (Fig. 4D), while pitch angle decreased with speed, although marginally significant in Bat1 (Table 2; Fig. 5).

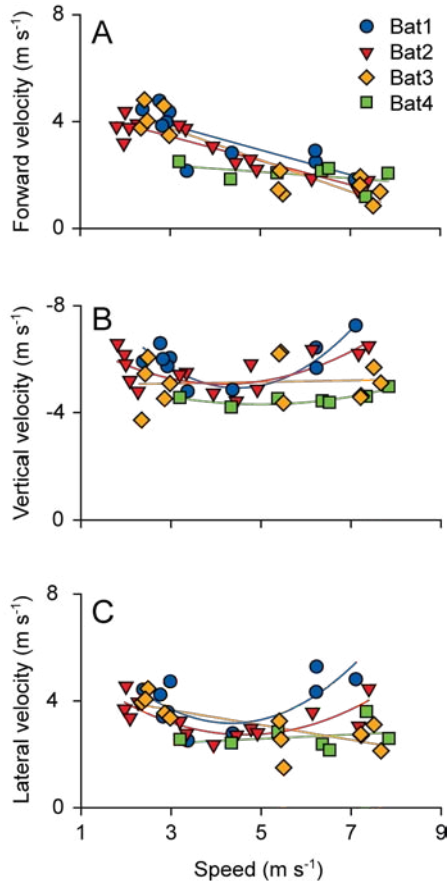


Fig. 6. Forward (A), vertical (B), and lateral (C) velocity of the wingtip with respect to the body, as a function of flight speed, for both flight corridor and wind tunnel trials. Forward velocity presents a linear relationship with speed ($P < 0.05$ for all individuals). Vertical velocity showed a quadratic relationship with speed for all individuals but Bat3, while lateral velocity showed a quadratic relationship with speed for Bat1 and Bat2.

The pattern of flight speed dependence of the velocity of the wingtip with respect to the body during downstroke is more complex. The average forward velocity of the wingtip during the downstroke decreased linearly with speed (ANCOVA, speed effect: $F_{1,35}=67.1$, $P < 0.0001$), along with an interaction individual \times speed effect ($F_{3,35}=3.22$, $P=0.03$) (Fig. 6A). This effect arises from the behavior of Bat4, whose forward wingtip showed a slight tendency to decrease ($P=0.27$).

In contrast, the average vertical wingtip velocity during downstroke changed in a curvilinear, U-shaped fashion (Fig. 6B). Bat1 and Bat2 showed a marked increase in vertical wingtip velocity at both low and high speed flights. Bat4 also showed a significant curvilinear response to

speed, but the increase during slow and fast flight was not as marked as those of the previous bats. For Bat3, vertical wingtip velocity did not change significantly with speed (slope = -0.03 ± 0.11 , $P=0.82$). The lateral velocity of the wingtip showed a similar pattern: Bat1 and Bat2 showed higher wingtip velocities at low and high speeds compared to those at intermediate speeds (Fig. 6C). Both Bat3 and Bat4 showed a linear change in

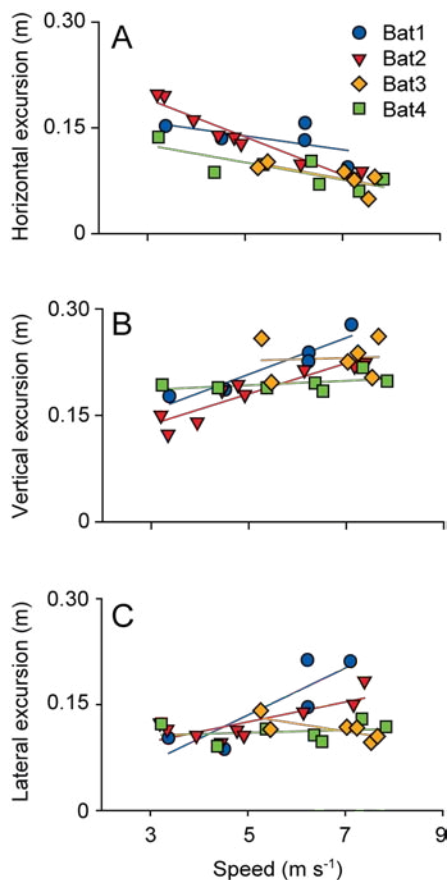


Fig. 7. Forward (A), vertical (B), and lateral (C) excursion of the wingtip with respect to the body, as a function of flight speed, for wind tunnel trials only.

wingtip velocity with speed, with a significant decrease in lateral velocity with speed in Bat4 (slope= 0.28 ± 0.08 , $P=0.007$).

The excursion of the wingtip during the wingbeat showed a consistent, complex pattern of change with speed, with clear differences among individuals (Fig. 7). In Bat1, vertical excursion increased significantly and there was a trend to decrease horizontal excursion. In Bat2, vertical and lateral excursion increased while horizontal motion of the wingtip decreased. In Bat3, the excursion of the wingtip in all directions remained similar across speeds. Finally, Bat4 only horizontal excursion decreased with speed.

Kinematic parameters that quantify 3D wing shape tended to change with speed in the same way among all individuals. Mean angle of attack of both proximal and distal portions of the wing during downstroke decreased with speed, consistently among individuals, from about 27 deg at 3 m s⁻¹ to 8 deg at 7.5 m s⁻¹ (Table 2; Fig. 8). Wing camber, measured as the curvature of the wing along the fifth digit, also decreased with speed in all bats (Table 2; Fig. 9). Individual bats, however, showed different amount of camber at any given speed; Bat3 and Bat2 possessed the highest and lowest amount of camber, respectively, and Bat1 and Bat4 showed an intermediate camber.

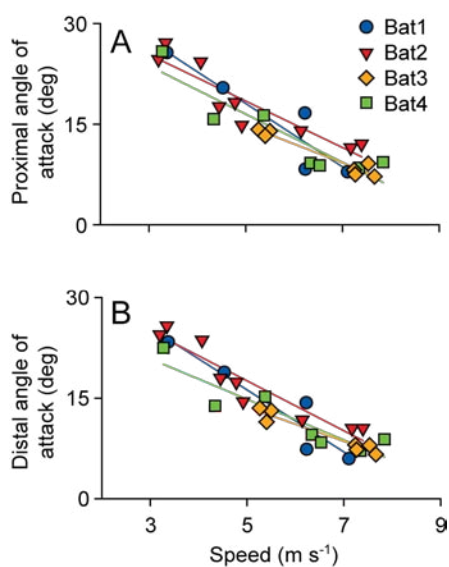


Fig. 8. Angle of attack as a function of flight speed, for the proximal (A) and distal (B) portion of the wing. Values from wind tunnel flights only.

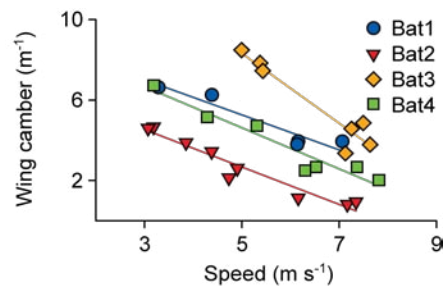


Fig. 9. Mean wing camber during downstroke as a function of flight speed. Values are from wind tunnel flights only.

Wing extension varied between the downstroke and the upstroke portion of the wingbeat cycle (Table 2; Fig. 10). The wing was more folded during the upstroke than during the downstroke, due to the extension of both elbow and wrist joints. As speed increased, there was a significant increase in the flexion of the elbow and wrist joints for Bat1 and Bat2.

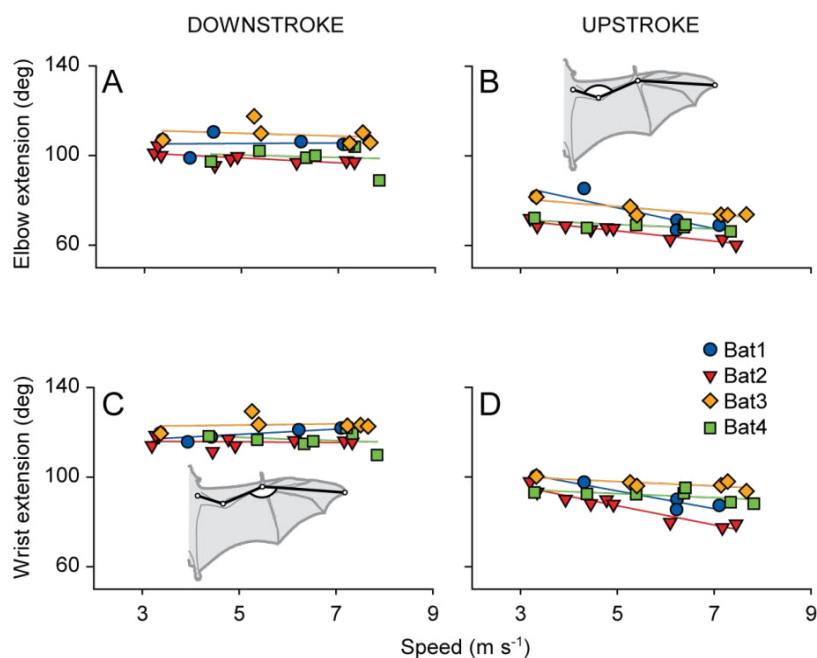
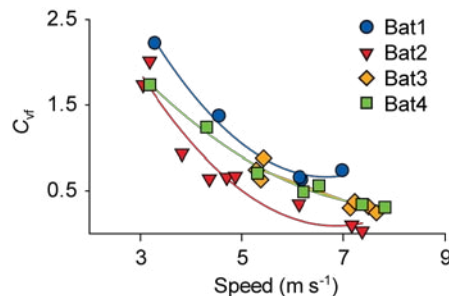


Fig. 10. Mean extension angle for the downstroke (A,C) and the upstroke (B,D) portions of the wingbeat cycle for the elbow (A-B) and wrist (C-D) joints, as a function of flight speed. Data are for wind tunnel flights only.

The vertical force coefficient (C_{vf}), computed from the kinematic parameters calculated above, decreased curvilinearly with flight speed (Fig. 11).

Fig. 11. Mean coefficient of lift during downstroke as a function of flight speed, for wind tunnel flights only.



Both reduced frequency (k) and Strouhal number (St) decreased non-linearly with speed (Fig. 12). k was similar for all bats at all speeds, although Bat2 showed a slightly higher k than the other bats (Fig. 12A). At slow speeds, k ranged between 0.6 and 0.7 and at higher speeds, k decreased to about 0.3. St was very similar among bats at low speeds ($St \approx 0.42$). As speed increased, however, St diverged among individuals, with Bat4 showing the lowest St , while Bat4 having the highest St , a result of the increased wingbeat frequency (Fig. 12B).

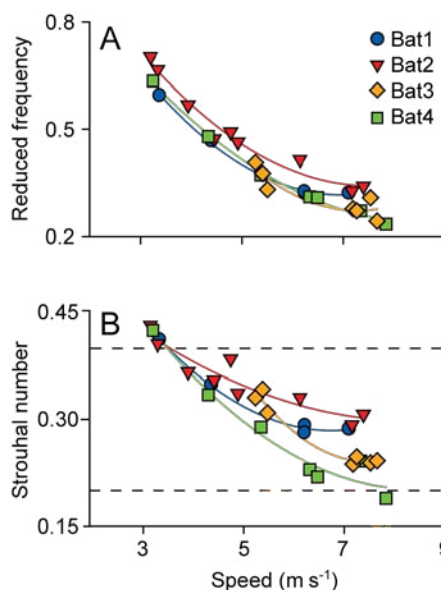


Fig. 12. Reduced frequency (A) and Strouhal number (B) as a function of flight speed, for wind tunnel flights only. In B, the dotted lines represent the range of St (0.2-0.4) that has been hypothesized to maximize propulsive efficiency.

Discussion

Virtually, all aspects of flight kinematics in the lesser dog-faced fruit bat changed gradually with speed. In all subjects, during slow flight, bats showed a marked tip-reversal upstroke that gradually disappeared as speed increased (the significance of this reversal upstroke will be discussed Chapter 3). As flight speed increased, bats oriented their bodies more horizontally and flapped their wings more vertically. It is likely that a primary function of this postural change is to reduce the parasite drag of the body. Wingbeat amplitude increased, and wing camber and angle of attack, both decreased with increasing speed.

Other kinematic parameters, however, changed in different ways among individuals. The most marked difference was the increase in wingbeat frequency with speed in Bat2, compared to a decrease in all other bats. More subtle differences were also observed in the excursion of the wings, where Bat2 showed a decrease in forward motion of the wingtip and an increase in the vertical and lateral motion, while the other individuals showed changes in one direction or no significant changes with changes in speed. Elbow and wrist joint extension during downstroke did not change with speed in any bat, but during upstroke wing extension decreased in the in Bat1 and Bat2 only.

As bats flew faster, the vertical force coefficient (C_{vf}) decreased gradually. Because wing area during downstroke, indicated by the wing joint angles, did not change with speed, the decrease in C_{vf} indicates that, at high flight speeds, the vertical force necessary to overcome gravity was provided primarily by the forward flight speed. In slow flights, however, forward flight speed becomes less important, and the increase in

forward velocity of the wingtip with respect to the body observed during downstroke probably helps to maintain a minimum flow velocity over the wings. Accordingly, wing shape parameters, such as angle of attack and wing camber became progressively more relevant as speed decreased. This was reflected in the higher values of C_{vf} , angle of attack, and camber during slow flights compared to fast flights.

Overall, the changes in the kinematic adjustments as speed increases were complex, with clear individual differences. These patterns suggest that there are multiple alternative that can be employed to fine-tune the generation of lift and thrust during flight. Physically, the generation of aerodynamic force by flapping wings can be modulated in multiple ways. Because aerodynamic force is proportional to V^2 (see eqn. 1), force can readily varied by changes in the flow velocity over the wings. Flapping fliers can control flow velocity by varying wingbeat frequency, wingbeat amplitude and/or downstroke ratio. Alternatively, changes in wing shape parameters such as wing area, camber, or angle of attack, thereby affecting aerodynamic force coefficients, could also be employed. These changes do not require changes of the activation patterns of the muscles that control the flapping movement of the wings, but instead require modulation of intrinsic muscles of the plagiotaigium and/or the muscles of the handwing proper. Finally, flapping organisms, especially bats, could use a combination of both strategies. Considering the array of alternatives to produce lift and thrust, it is perhaps not surprising to find differences among individual in the changes of kinematics with speed. It is difficult at present to compare our findings to individual variation in kinematic patterns in other flying animals. Individual variation has received little attention in studies of animal flight, although several researchers have stressed the importance of such variation in

physiological, ecological, and evolutionary studies (see Hayes and Jenkins, 1997 for a review).

Evidence of gait changes?

Pioneering studies of the wakes left by birds and bats flying through neutrally buoyant helium bubbles led to the view that flying vertebrates employ two basic, distinct wake structures: at low speeds, a series of discrete vortex rings or loops, each associated with a single downstroke; and at high speeds, a pair of continuous, undulating vortices (Spedding et al., 1984; Rayner et al., 1986; Spedding, 1986). As a consequence, it was hypothesized that flying bats and birds have two distinct gaits, where gait is defined as a pattern of locomotion described by one or more quantities that change discontinuously at transitions to other gaits (Alexander, 1989). Therefore, it was predicted that the detailed analysis of the kinematics and wake structure of flapping vertebrates flying at a range of speeds would provide evidence of a discontinuous change that would directly reflect the switch from one gait to another. To date, however, kinematic analyses of bat and bird flight at different speeds have failed to provide support for this hypothesis (e.g., Aldridge, 1986; Tobalske and Dial, 1996; Tobalske, 2000; Hedrick et al., 2002; Norberg and Winter, 2006). We too observed no discrete change in any kinematic parameters. Furthermore, more recent studies of the wake structure left by birds flying at a range of speeds showed that although wake patterns vary across speeds, the transition among wake patterns is not abrupt, as expected from the gait hypothesis, but continuous (Spedding et al., 2003; Rosen et al., 2004; Hedenstrom et al., 2006; Rosen et al., 2007). Similarly, a study of the wake structure of nectarivorous bats also showed a gradual change in the wake pattern as speed increased (Hedenström et al., 2007).

We note, however, that although our kinematic analyses show no evidence of the kind of discontinuity one would expect from a fundamental gait change, the individuals used in this study likely did not reach their maximum flight speed. Although, to our knowledge, no accurate measurements of peak natural flight speeds used by *C. brachyotis* have been made, it is probable that these bats are capable of faster flight. On the other hand, estimates based on our bats' wing morphology give values of 4.59 and 6.09 m s⁻¹ for minimal power speed and maximum range speed, respectively (eq. 4 and 5 from Norberg and Rayner, 1987). Thus, the range of speeds used in this study probably includes speeds that are ecologically relevant, although these estimates are derived from general equations for bats, without including differences in ecology and foraging behavior, so they should be employed with caution. It has been observed that natural populations of *C. brachyotis* are able to use both open and forest spaces (Campbell et al., 2007), which likely implies the use of different speeds in each environment.

Wingbeat kinematics compared to other bats

Numerous aspects of wingbeat kinematics of *C. brachyotis* measured in this study differ from those reported for other bat species. For example, wingbeat frequency decreased with speed for three of four subjects (mean slope=-0.167), a much lower decrease in frequency than reported for microbats: *Plecotus auritus* (9 g), decreases wingbeat frequency with flight speed from 13.5 Hz at 2 m s⁻¹ to about 10 Hz at 3 m s⁻¹ (slope=-3.0) (Norberg, 1976), *Rhinolophus ferrumequinum* (22 g) decreases wingbeat frequency from 14 Hz at 2 m s⁻¹ to about 10 Hz at 5 m s⁻¹ (slope=-0.71) (Aldridge, 1986), and *Glossophaga soricina* (10-13 g) decreases wingbeat frequency from 14.7 Hz at 2.4 m s⁻¹ to 7.5 Hz at 7.8 m s⁻¹ (slope=-1.2) (Norberg and Winter, 2006). The modulation of

wingbeat amplitude also differs among bats; amplitude increased with speed in *C. brachyotis*, but tended to decrease with speed in *R. ferrumequinum* (Aldridge, 1986). In contrast, stroke plane increased with speed in *P. auritus* and *R. ferrumequinum* (Norberg, 1976; Aldridge, 1986) and in a similar fashion as in *C. brachyotis*, although at any given speed, stroke plane angle was higher in the two microbats with respect to the bats in our study.

Observations of 23 species of free flying Australian bats, of six families including pteropodids, have shown that wingbeat frequency varied predictably with body mass and flight speed, and that wingbeat amplitude changed with wing area and flight speed (Bullen and McKenzie, 2002). These results suggested a simple empirical relationship between flight speed, and kinematic variables that reflects common themes underlying bat aerodynamics. Comparing our results to those predicted from the empirical model for Australian bats, we found only moderate agreement (Fig. 13). Wingbeat frequency was within the expected value for Bat1 and Bat3, but the published relationship underestimated frequency in Bat4 and even more substantially for Bat2, the subject that increased rather than decreased wingbeat frequency. Wingbeat amplitude, in contrast, was expected to increase with speed, a trend that was followed relatively well by Bat1 and Bat2, but that overestimated amplitude at low speeds in both individuals, and underestimated amplitude for Bat1 at fast flights. Bat3 and Bat4 flew with amplitudes consistently lower than those observed in Bullen and MacKenzie's dataset.

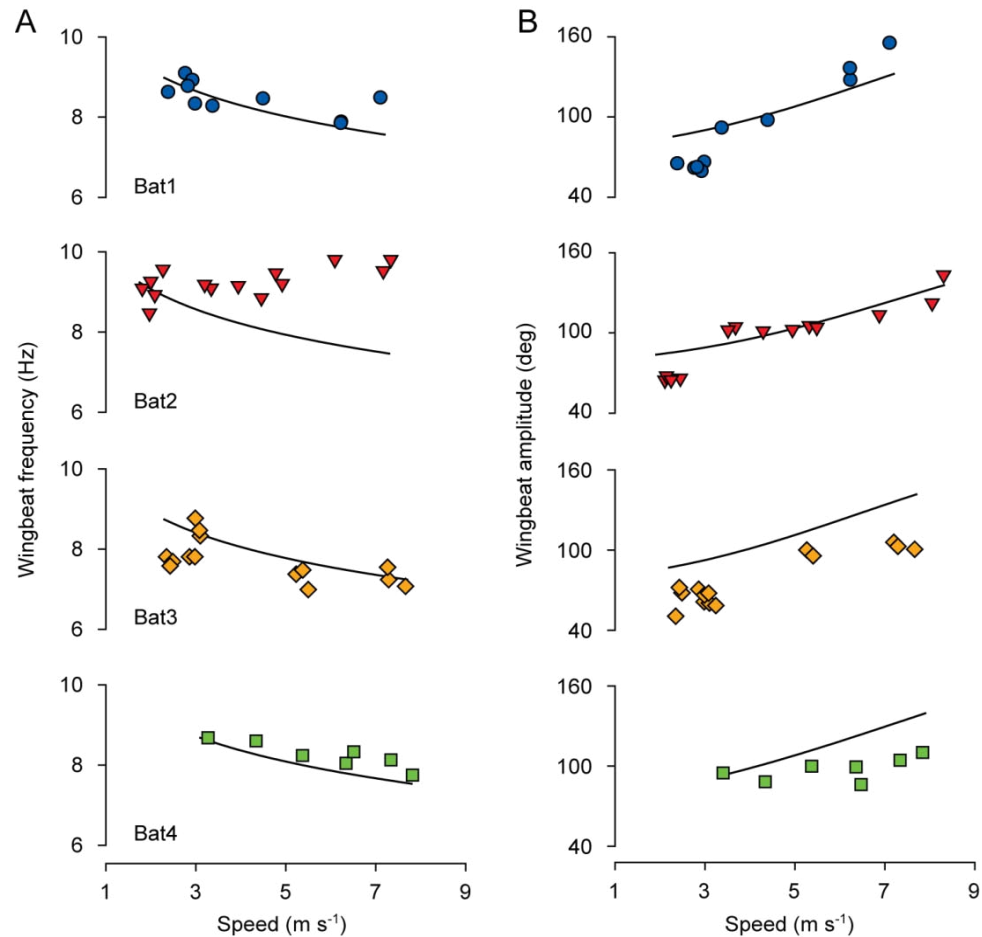


Fig. 13. Comparison between the measured wingbeat frequency (f) and amplitude (ϕ_v) and the predicted values derived from Bullen and McKenzie (2002) for all *C. brachyotis*. Measured values are represented by symbols and expected values by solid lines. Expected frequency was calculated as $f=5.54-3.068 \log_{10}(M_b) - 2.857 \log_{10}(V)$, where M_b is body mass and V is flight speed. Expected amplitude was calculated as $\phi_v=56.92+5.18V+16.06 \log_{10}(S)$, where ϕ_v is the vertical wingtip amplitude, V is flight speed, and S is wing area. θ_v was obtained by compensating our measurement of wingbeat amplitude for the effect of a tilted stroke plane angle.

Reduced frequency and Strouhal number

The dimensionless Strouhal number, St , has been used to describe oscillating mechanisms and unsteady flow, and it is useful to describe the propulsive efficiency of flapping airfoils. Controlled wind tunnel experiments with pitching, heaving and flapping airfoils have indicated that propulsive efficiency is maximized in the range $0.2 < St < 0.4$ (Triantafyllou et al., 2000; Taylor et al., 2003). It has been shown that flapping birds and

bats use flight cruise speeds within this range, although bats tend to use higher St than birds ($0.2 < St < 0.5$ and $0.2 < St < 0.4$ for bats and birds, respectively) (Taylor et al., 2003). In this study, flights at speeds between 3.5 and 8 m s^{-1} are characterized by St in the range of 0.2 and 0.4 . At speeds lower than 3.5 m s^{-1} , St increases above 0.4 , suggesting that the resulting vorticity will be insufficient to provide thrust to overcome the drag of the wings (Norberg and Winter, 2006). At low flight speeds, reduced frequency (k) is also high. In general, flight conditions of $k < 0.4$ support the assumption of steady flow (Spedding, 1993). Our data suggest that in bats flying at speeds below $5\text{-}6 \text{ m s}^{-1}$ k is higher than 0.4 , hence unsteady aerodynamics, such as rotational circulation, wake recapture or use of leading-edge vortices, mechanisms observed in insect flight at high reduced frequencies (e.g., Ellington, 1984; Ellington et al., 1996; Dickinson et al., 1999; Sane, 2003) might be important. Whether or not these bats are able to use similar unsteady aerodynamic mechanisms remains to be documented. However, a recent study found that a nectarivorous bat flying at 1 m s^{-1} ($St \approx 1.36$), develops a stable leading-edge vortex which enables it to increase lift by 40% (Muijres et al., 2008), suggesting that this might be a possibility for other bat species.

Concluding remarks and future studies

Wingbeat kinematics in bats changed gradually with speed, suggesting no abrupt changes consistent with the existence of distinct gaits during flight, at least over the range of speeds measured. Overall, kinematics of *C. brachyotis* differs from patterns previously reported from smaller microchiropteran, insectivorous bats, primarily due to a strong decrease in wingbeat frequency and an increase in amplitude. We also observed significant differences among individuals in kinematic changes with speed, indicating

that there are multiple strategies that can be used to modulate lift and thrust during flight. Finally, our kinematics suggest that speeds below 5 m s^{-1} are affected by unsteady aerodynamic effects and therefore the use of steady-state approaches (e.g., blade-element analysis) are likely to produce an inaccurate representation of the fluid dynamics around the wings. Wake visualization studies such as those that employ PIV are necessary to increase our understanding of the aerodynamics of bat flight, in particular at low speeds, where they may help evaluate the importance of unsteady effects. These studies should be coupled with detailed kinematic analyses that consider the degree of variability among species and among individuals.

List of symbols

CoM	center of mass
C_{vf}	vertical force coefficient
DLT	direct linear transformation
k	reduced frequency
St	Strouhal number

Acknowledgments

All experiments were conducted at the Concord Field Station (CFS) at Harvard University, and we express our thanks to the CFS staff, especially Andy Biewener for allowing us the use of the facilities, and Pedro Ramírez for taking care of the bats. Bats were provided through the generous support of Dr. Allyson Walsh and the Lube Bat Conservancy. We also thank everybody in the Bat Lab at Brown University, in particular Daniel Riskin, Kenny Breuer, Arnold Song, and Tatjana Hubel, for the help provided during the experiments and during the analysis of data. This work was supported by the Air Force Office of Scientific Research (AFOSR), the NSF-ITR program, and the Bushnell Foundation.

References

- Aldridge, H. D. J. N.** (1986). Kinematics and aerodynamics of the greater horseshoe bat, *Rhinolophus ferrumequinum*, in horizontal flight at various speeds. *J. Exp. Biol.* **126**, 479-497.
- Aldridge, H. D. J. N.** (1987). Body accelerations during the wingbeat in six bat species: the function of the upstroke in thrust generation. *J. Exp. Biol.* **130**, 275-293.
- Alexander, R. M.** (1989). Optimization and gaits in the locomotion of vertebrates. *Physiol. Rev.* **69**, 1199-1227.
- Bullen, R. D. and McKenzie, N. L.** (2002). Scaling bat wingbeat frequency and amplitude. *J. Exp. Biol.* **205**, 2615-2626.
- Campbell, P., Schneider, C. J., Zubaid, A., Adnan, A. M. and Kunz, T. H.** (2007). Morphological and ecological correlates of coexistence in Malaysian fruit bats (Chiroptera: Pteropodidae). *J. Mammal.* **88**, 105-118.
- Dickinson, M. H., Farley, C. T., Full, R. J., Koehl, M. A., Kram, R. and Lehman, S.** (2000). How animals move: an integrative view. *Science* **288**, 100-106.

- Dickinson, M. H., Lehmann, F. O. and Sane, S. P.** (1999). Wing rotation and the aerodynamic basis of insect flight. *Science* **284**, 1954-1960.
- Ellington, C. P.** (1984). The aerodynamics of hovering insect flight. IV. Aerodynamic mechanisms. *Philos. Trans. R. Soc. B* **305**, 1-15.
- Ellington, C. P., vandenBerg, C., Willmott, A. P. and Thomas, A. L. R.** (1996). Leading-edge vortices in insect flight. *Nature* **384**, 626-630.
- Hatze, H.** (1988). High-precision three-dimensional photogrammetric calibration and object space reconstruction using a modified DLT-approach. *J. Biomech.* **21**, 533-538.
- Hayes, J. P. and Jenkins, S. H.** (1997). Individual variation in mammals. *J. Mammal.* **78**, 274-293.
- Hedenström, A., Johansson, L. C., Wolf, M., von Busse, R., Winter, Y. and Spedding, G. R.** (2007). Bat flight generates complex aerodynamic tracks. *Science* **316**, 894-897.
- Hedenstrom, A., Rosen, M. and Spedding, G.** (2006). Vortex wakes generated by robins *Erithacus rubecula* during free flight in a wind tunnel. *J. R. Soc. Interface* **3**, 263-276.
- Hedrick, T. L., Tobalske, B. W. and Biewener, A. A.** (2002). Estimates of circulation and gait change based on a three-dimensional kinematic analysis of flight in cockatiels (*Nymphicus hollandicus*) and ringed turtle-doves (*Streptopelia risotia*). *J. Exp. Biol.* **205**, 1389-1409.
- Lauder, G. V. and Madden, P. G. A.** (2008). Advances in comparative physiology from high-speed imaging of animal and fluid motion. *Annu. Rev. Physiol.* **70**, 143-163.
- Muijres, F. T., Johansson, L. C., Barfield, R., Wolf, M., Spedding, G. R. and Hedenstrom, A.** (2008). Leading-edge vortex improves lift in slow-flying bats. *Science* **319**, 1250-1253.
- Norberg, U. M.** (1976). Aerodynamics, kinematics, and energetics of horizontal flapping flight in the long-eared bat *Plecotus auritus*. *J. Exp. Biol.* **65**, 179-212.
- Norberg, U. M. and Rayner, J. M. V.** (1987). Ecological morphology and flight in bats (Mammalia; Chiroptera): wing adaptations, flight performance, foraging strategy and echolocation. *Philos. Trans. R. Soc. B* **316**, 335-427.
- Norberg, U. M. L. and Winter, Y.** (2006). Wing beat kinematics of a nectar-feeding bat, *Glossophaga soricina*, flying at different flight speeds and Strouhal numbers. *J. Exp. Biol.* **209**, 3887-3897.

- Rayner, J. M. V., Jones, G. and Thomas, A.** (1986). Vortex flow visualizations reveal change in upstroke function with flight speed in bats. *Nature* **321**, 162-164.
- Riskin, D. K., Willis, D. J., Iriarte-Díaz, J., Hedrick, T. L., Kostandov, M., Chen, J., Laidlaw, D. H., Breuer, K. and Swartz, S. M.** (in press). Quantifying the complexity of bat wing kinematics. *J. Theor. Biol.*
- Rosen, M., Spedding, G. R. and Hedenstrom, A.** (2004). The relationship between wingbeat kinematics and vortex wake of a thrush nightingale. *J. Exp. Biol.* **207**, 4255-4268.
- Rosen, M., Spedding, G. R. and Hedenstrom, A.** (2007). Wake structure and wingbeat kinematics of a house-martin *Delichon urbica*. *J. R. Soc. Interface* **4**, 659-668.
- Sane, S. P.** (2003). The aerodynamics of insect flight. *J. Exp. Biol.* **206**, 4191-4208.
- Spedding, G. R.** (1986). The wake of a jackdaw (*Corvus monedula*) in slow flight. *J. Exp. Biol.* **125**, 287-307.
- Spedding, G. R.** (1993). On the significance of unsteady effects in the aerodynamic performance of flying animals. *Contemp. Math.* **141**, 401-419.
- Spedding, G. R., Rayner, J. M. V. and Pennycuick, C. J.** (1984). Momentum and energy in the wake of a pigeon (*Columba livia*) in slow flight. *J. Exp. Biol.* **111**, 81-102.
- Spedding, G. R., Rosén, M. and Hedenström, A.** (2003). A family of vortex wakes generated by a thrush nightingale in free flight in a wind tunnel over its entire natural range of flight speeds. *J. Exp. Biol.* **206**, 2313-2344.
- Swartz, S. M.** (1997). Allometric patterning in the limb skeleton of bats: implications for the mechanics and energetics of powered flight. *J. Morph.* **234**, 277-294.
- Swartz, S. M., Bishop, K. L. and Ismael-Aguirre, M.-F.** (2005). Dynamic complexity of wing form in bats: implications for flight performance. In *Functional and evolutionary ecology of bats* (eds. Z. Akbar G. McCracken and T. H. Kunz), pp. 110-130. Oxford: Oxford University Press.
- Swartz, S. M., Iriarte-Diaz, J., Riskin, D. K., Song, A., Tian, X., Willis, D. J. and Breuer, K. S.** (2007). Wing structure and the aerodynamic basis of flight in bats. In *AIAA Aerospace Science Meeting*. Reno, NV: AIAA.
- Taylor, G. K., Bacic, M., Bompfrey, R. J., Carruthers, A. C., Gillies, J., Walker, S. M. and Thomas, A. L. R.** (2008). New experimental approaches to the biology of flight control systems. *J. Exp. Biol.* **211**, 258-266.

- Taylor, G. K., Nudds, R. L. and Thomas, A. L. R.** (2003). Flying and swimming animals cruise at Strouhal number tuned for high power efficiency. *Nature* **425**, 707-711.
- Tholleson, M. and Norberg, U. M.** (1991). Moments of inertia of bat wings and body. *J. Exp. Biol.* **158**, 19-35.
- Tian, X., Iriarte-Diaz, J., Middleton, K., Galvao, R., Israeli, E., Roemer, A., Sullivan, A., Song, A., Swartz, S. and Breuer, K.** (2006). Direct measurements of the kinematics and dynamics of bat flight. *Bioinspiration & Biomimetics* **1**, S10-S18.
- Tobalske, B. W.** (2000). Biomechanics and physiology of gait selection in flying birds. *Physiol. Biochem. Zool.* **73**, 736-750.
- Tobalske, B. W.** (2007). Biomechanics of bird flight. *J. Exp. Biol.* **210**, 3135-3146.
- Tobalske, B. W. and Dial, K. P.** (1996). Flight kinematics of black-billed magpies and pigeons over a wide range of speeds. *J. Exp. Biol.* **199**, 263-280.
- Triantafyllou, M. S., Triantafyllou, G. S. and Yue, D. K. P.** (2000). Hydrodynamics of fishlike swimming. *Annu. Rev. Fluid Mech.* **32**, 33-53.
- Usherwood, J. R. and Ellington, C. P.** (2002). The aerodynamics of revolving wings I. Model hawkmoth wings. *J. Exp. Biol.* **205**, 1547-1564.
- Voigt, C. C. and Winter, Y.** (1999). Energetic cost of hovering flight in nectar-feeding bats (Phyllostomidae: Glossophaginae) and its scaling in moths, birds and bats. *J. Comp. Physiol. B* **169**, 38-48.
- Watts, P., Mitchell, E. J. and Swartz, S. M.** (2001). A computational model for estimating the mechanics of horizontal flapping flight in bats: model description and validation. *J. Exp. Biol.* **204**, 2873-2898.
- Winter, Y.** (1998). Energetic cost of hovering flight in a nectar-feeding bat measured with fast-response respirometry. *J. Comp. Physiol. B* **168**, 434-444.
- Zar, J. H.** (1999). Biostatistical analysis. Upper Saddle River, N.J.: Prentice Hall.

Chapter 3

No net thrust on the upstroke: whole-body kinematics of a fruit bat reveal the influence of wing inertia on body accelerations

José Iriarte-Díaz¹, Daniel K. Riskin¹,
David J. Willis², and Sharon M. Swartz¹

¹Department of Ecology and Evolutionary Biology, Brown University

²Department of Aeronautics and Astronautics, Massachusetts Institute of Technology

Abstract

During slow flight, some bats species produce a tip-reversal upstroke, where the distal portion of the wing is moved upward and backward with respect to still air. Tip-reversal upstroke has been widely hypothesized to produce thrust during upstroke, based on the observation that bats accelerate their body forward during upstroke in low speed flights. This forward acceleration, however, can be produced by inertial forces generated by the flapping motion of the wings with respect to the center of mass (CoM) rather than from thrust produced by the interaction of the wings with the airflow. To investigate the instantaneous aerodynamic force production during the upstroke and downstroke portions of the wingbeat cycle, we developed a model of the mass distribution of the wing and body of the lesser dog-faced fruit bat, *Cynopterus brachyotis* during flight, based on detailed high-speed, three-dimensional kinematics. The mass model allowed us to determine the position of the CoM and therefore to calculate the accelerations produced by aerodynamic forces. Our goal was to investigate the wingbeat kinematics and the variation in aerodynamic and inertial force generation throughout the wingbeat cycle across a range of speeds ($3-8 \text{ m s}^{-1}$) in order to answer whether or not thrust is produced when bats use wingtip-reversal upstrokes. We found that bats used wingtip-reversal upstroke only during slow flight and that bats accelerated their body forward during upstroke. This acceleration, however, was the results of the inertial force produced by the motion of the wings. Inertial forces affected both vertical and forward acceleration measurements at all speeds, but the horizontal inertial component decreased as speed increased while the vertical component remained constant across speeds. Our results

highlight the importance of the incorporation of inertial components to the study of acceleration in flapping organisms.

Introduction

The flapping flight of animals is complex, and many basic questions about how bats, birds, and insects fly have yet to be answered. For example, bats change their wing kinematics in subtle but predictable ways to fly at different speeds (Norberg, 1976; Aldridge, 1986, 1987; Norberg and Winter, 2006), but the precise aerodynamic mechanisms of how thrust and lift are produced are poorly understood. In particular, some bats and birds flying at low speeds use a distinctive, characteristic ‘tip-reversal’ upstroke, in which the distal portion of the wing is moved upwards and backwards with respect to still air (Brown, 1948; Norberg, 1976; Aldridge, 1986). These tip-reversals are believed to generate thrust, an aerodynamic force in the direction of flight, during the upstroke (Brown, 1953; Norberg, 1976; Aldridge, 1987; Norberg, 1990; Norberg and Winter, 2006). Because tip reversal is not performed at higher speeds, the upstroke is thought to generate thrust only at low speeds (Norberg, 1990). The objective of this study is to test the hypothesis that bats use tip-reversal upstroke to produce a forward-oriented force.

There are several ways to study the aerodynamic forces produced by a flying organism. One method is to evaluate the structure of the wake left behind by flow visualization. Some studies have used Particle Image Velocimetry (PIV), a laser-based technology, to quantify the patterns of motion of fluids produced during flight of birds

(e.g., Spedding et al., 2003) and bats (Tian et al., 2006; Hedenström et al., 2007; Muijres et al., 2008). This approach, however, requires high-energy, laser pulses that, unfortunately, can only be produced at relatively low sampling frequencies (f) with respect to natural wingbeat frequencies (PIV f : 5-10 Hz vs. animal f : 5-500 Hz). As a consequence, flow patterns over the course of a wingbeat cycle cannot be measured directly, and must instead be reconstructed based on snapshots from multiple portions of the wingbeat cycle (Lauder and Madden, 2008). Until laser technology improves, high-frequency, high-energy pulsed laser, real-time studies of aerodynamic force generation cannot be achieved. Another method is to use computational fluid dynamic (CFD) models, where the air flow around a flapping organism is modeled by solving the Navier-Stokes equation for a particular geometry. However, the Navier-Stokes equations are computationally intensive and difficult to solve for morphing wing geometries and for Reynolds number regimes such as that of bats (Shyy and Liu, 2007; Willis et al., in preparation).

Another way to estimate aerodynamic forces is by recording the instantaneous accelerations of the body of a flying organism. Indeed, this method has been applied to determine whether or not net thrust is produced during the upstroke by bats (Aldridge, 1987). The interpretation of accelerations of body landmarks, however, may not be straightforward. For any flapping organism, the motion of the relatively massive wings with respect to the body generates inertial forces that can accelerate fixed anatomical markers, without accelerating the center of mass (CoM) (Fig. 1). As a consequence, accelerations of body-fixed landmarks will reflect both the net effect of external (aerodynamic) forces produced by the interaction between the flying organism and the

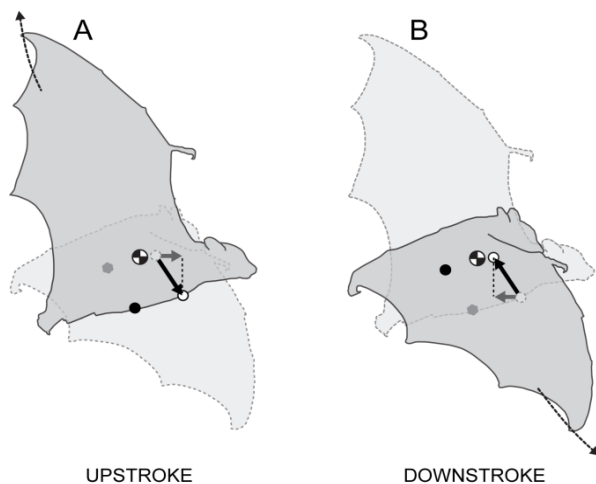


Fig. 1. Effect of the oscillation of the wings on the position of the CoM and accelerations of the body. When external forces, such as aerodynamic and gravitational forces, are absent, the position of the CoM will remain constant but the body moves in opposition to the flapping wings to conserve momentum. Closed and open symbols correspond to the pelvis and chest markers, and \odot corresponds to the CoM. (A) During upstroke (solid bat), the upward and backward motion of the wings will produce in response an inertial force (black arrow) that will move the body forward and downward with respect to the downstroke (dashed bat). This force will produce a forward-oriented component, or inertial thrust, during upstroke (grey arrow). (B) During downstroke (solid bat), the downward and forward motion of the wings will produce an inertial force (black arrow) that will move the body backward and upward while keeping the position of the CoM constant. The horizontal component of this inertial force will produce negative inertial thrust during downstroke (grey arrow).

surrounding fluid, and internal (inertial) forces produced by the motion of the wings. Inertial forces are likely to be significant in bats because the mass of the wings comprise a significant portion of total body mass, ranging from 11 to 20% (Thollesson and Norberg, 1991;

Watts et al., 2001). Indeed, in birds with relative wing mass comparable to that of bats, inertial forces contribute 25-33% of the total body accelerations in pigeons (Bilo et al., 1984) and 50% in cockatiels (Hedrick et al., 2004).

Horizontal accelerations of the CoM are not the result of thrust alone. The net horizontal force (net thrust) reflects the imbalance between thrust

produced by the wings and the drag produced by the whole body. Because drag is present throughout the wingbeat cycle, no net horizontal acceleration indicates that thrust equals drag, and positive accelerations that more thrust is produced than drag.

Here, we evaluate the hypothesis that wing-tip reversal in slow flight generates net horizontal force during upstroke. We employ a model of the dynamically changing mass distribution of the bat's body and wings, coupled with kinematic records of high

temporal and spatial resolution to independently estimate the inertial and aerodynamic components of body markers accelerations.

We predict that the wings contribute thrust during the upstroke at low speed, and that this upstroke contribution should decrease with increased speed. By applying analysis of the inertial contribution to the forces of flight, we hope to obtain new insight into the mechanics of bat flight.

Materials and methods

Animals and experimental procedures.

Four female lesser short-nosed fruit bats (*Cynopterus brachyotis*), on loan from the Lube Bat Conservancy (Gainesville, FL), were used in this experiment. They were housed in the animal care facilities of the Harvard-Concord Field Station, where they were provided with food and water *ad libitum*. Bats were anesthetized with isoflurane gas prior to each experimental session and key anatomical landmarks were marked with high-contrast markers on the undersurface of one wing (Fig. 2A). Bats were trained to fly in a wind tunnel over a range of speeds from 2 m s^{-1} to 8 m s^{-1} . The Harvard-Concord Field Station wind tunnel is an open-circuit tunnel with a closed jet in the flight chamber and a working section of 1.4 m length, 1.2 m width and 1.2 m height (Fig. 2B). Technical details and aerodynamic characteristics of the wind tunnel were described by Hedrick et al. (2002).

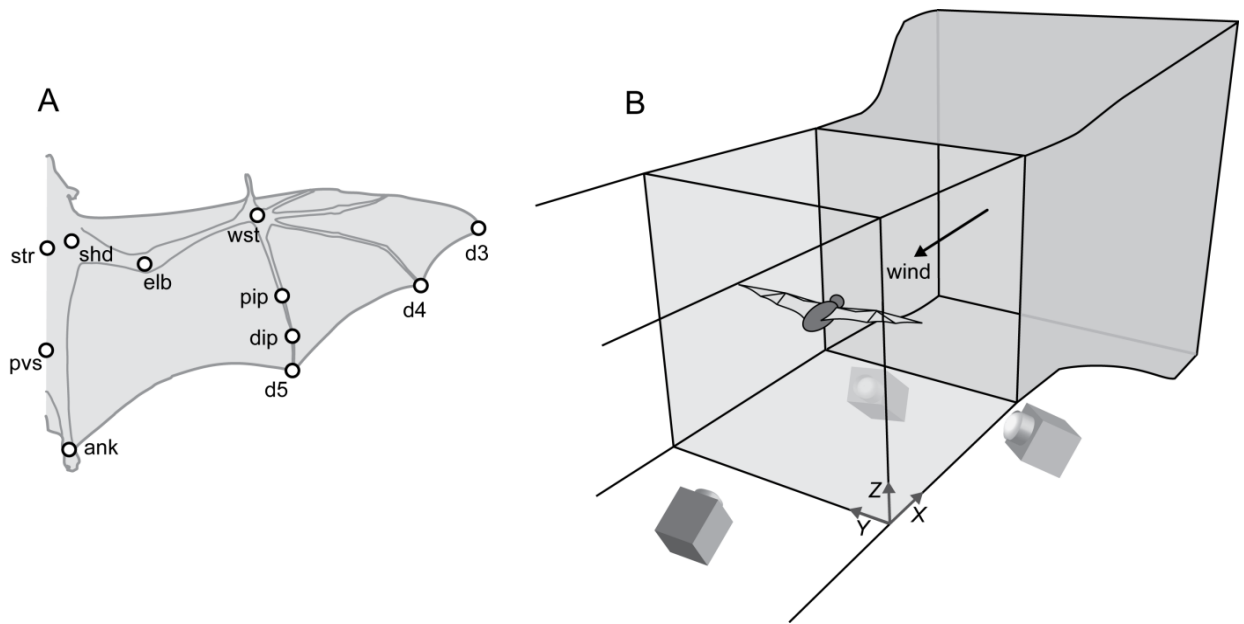


Fig. 2. Schematic of the experimental setup of the wind tunnel (A) and the dorsal view of a bat indicating the position of the body and wing markers used to calculate kinematic parameters (B). Three high-speed digital cameras were positioned outside of the working section of the wind tunnel as shown. Not to scale.

All components of this study were approved by the Institutional Animal Care and Use Committees at Brown University, Harvard University, and the Lubee Bat Conservancy, and by the Division of Biomedical Research and Regulatory Compliance of the Office of the Surgeon General, United States Air Force.

Three-dimensional coordinate mapping.

Flights were recorded using three phase-locked high-speed Photron 1024 PCI digital cameras (Photron, 1000 fps, 1024×1024 pixels). The volume of the wind tunnel in which the bat was flown was calibrated by using the Direct Linear Transformation (DLT) method, based on a 40-point calibration cube (0.35×0.35×0.29 m) recorded at the beginning of each set of trials (Hatze, 1988). From each video frame, 11 anatomical markers were digitized (Fig. 2A). The three-dimensional position of each marker was

resolved by the DLT coefficients obtained from the calibration cube (Hatze, 1988). Gaps in the three-dimensional position occurred when a marker was not visible in at least two cameras. These were filled by interpolation, using an over-constrained polynomial fitting algorithm. For contiguous gaps in the data, with sufficiently rich data at the end points, a third order, over-constrained polynomial fit was used. For gaps that included sporadic intermediate points, a sixth order polynomial was used. After gap-filling, a 50 Hz digital Butterworth low-pass filter was used to remove high-frequency noise. This cut-off frequency was approximately 5 times higher than the wingbeat frequency recorded in our bats.

Body Accelerations

Total body accelerations (i.e., aerodynamic + inertial accelerations) were calculated as the second derivatives of both the sternum and pelvis marker positions over time; both markers reflect the location of the relatively rigid axial skeleton, but provide slightly different information, depending on body pitch. To analytically uncouple aerodynamic from inertial accelerations, the true position of the CoM was estimated for each time step, using the mass model described below. The second derivative of the CoM true position with respect to time corresponds to the aerodynamic acceleration. Inertial acceleration of the body was calculated by subtracting the aerodynamic accelerations from the total acceleration. We defined downstroke and upstroke phases of the wingbeat cycle by the downward vs. upward movement of the wrist marker relative to the body, and calculated accelerations for the downstroke and upstroke separately.

Mass model

The mass model of dynamic change in location of the CoM is a time-varying, discrete mass approximation of the bat's mass distribution, based on the location of the markers. To develop the discrete mass system representing the bat, we partitioned total body mass into individual components or regions. The wing membrane, the wing bones, and the trunk were treated as separate objects, each with its own position and mass, which were combined to form the total mass model. To model the distribution of the wing membrane mass, we constructed a triangulation of the wing geometry at each time step. The large-scale, base triangulation was developed using the location of the marker positions at any given time, and a subsequent subdivision of those triangles was performed to give a mesh of fine-scale triangular elements (Fig. 3). Each triangle element (T_i) on the membrane was assigned a constant thickness (1×10^{-4} m) and density (1×10^3 kg

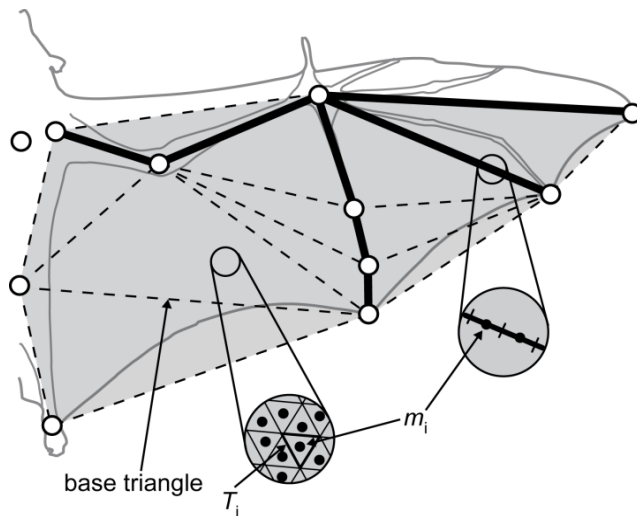


Fig. 3. Schematic of the mass distribution model used to calculate the CoM of the bat. The blue lines represent the wing bones, each of which is assigned a given mass based on dimensions and bone density. The colored triangle patches represent the base triangles of the skin mass model, and insets show detailed subdivisions of bone and skin masses (m_i) and individual triangular elements (T_i) of the model.

m^{-3}), based on measured characteristics of bat wing membrane skin (Swartz et al., 1996). A resulting discrete point mass (m_i) for each triangular membrane element was computed based on the volume of that triangular membrane and assigned a position at the centroid of the triangle element. To model the distribution of mass among and

within each of the wing bones, we constructed a curve between the markers at the endpoints of the bones. The curve for each bone in the wing was defined from the location of the markers. Given the tapered shape of bat bones (Swartz, 1997), the cross-sectional radius of each bone element of the model was defined by a quadratic function with respect to the length of the bone. We assigned a constant density to the bones ($2 \times 10^3 \text{ kg m}^{-3}$). Using the distribution of bone radii distribution and the location of the bone elements in space, the line was subdivided into smaller line-elements, from which discrete mass points were defined. The mass of the wings was scaled such that the constructed distribution represents the 16% of the total body mass, according to measurements of bats of similar size (Thollessen and Norberg, 1991). The mass and moment of inertia of the wing with respect to the shoulder was compared to measured values (Thollessen and Norberg, 1991) to ensure that the model represents the physical reality. Finally, the bat's body was defined as a 3-dimensional ellipsoid divided into discrete mass points.

The discrete mass representation of the membranes, bones and body was combined with detailed kinematic records of motion of each landmark to determine the center of mass of each one of the mass elements, m_i , using the equation

$$\vec{r}_{CoM} = \frac{\sum \vec{r}_i m_i}{m_T}, \quad (1)$$

where \vec{r}_{CoM} represents the position vector of the CoM, \vec{r}_i represents the position vector of the i -th discrete point mass and m_T represents the total mass of the bat.

Results

The lateral and horizontal projection of the reconstructed path of the wingtip with respect to still air showed that the bats flying at slow speeds moved their wings upward and backward during upstroke, producing a tip-reversal upstroke (Fig. 4A). As speed increased, the backward movement of the wing gradually disappeared, becoming an upward and forward motion of the wingtip (Fig. 4A). The tip-reversal upstroke diminishes with increasing speed, even though the trajectory of the wing tip with respect to the body does not change considerably with speed (Fig. 4B).

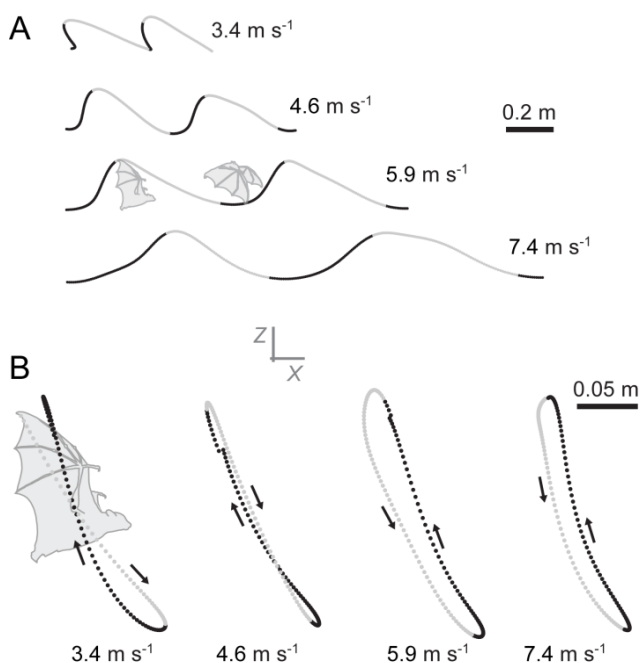


Fig. 4. Lateral projection of the trace of the wingtip over two wingbeats for a bat flying at different speeds, with respect to still air (A) and with respect to its own body (B). Grey traces correspond to the downstroke portion of the wingbeat. Note in (A) that at the slowest speed (3.4 m s^{-1}), the wingtip moves posteriorly during part of the upstroke, but this pattern diminishes with increases in speed.

Horizontal and vertical accelerations of both body markers and the CoM changed cyclically through the wingbeat cycle. Body markers decelerated in the horizontal plane mostly during the downstroke and then accelerated during upstroke (Fig. 5). In contrast, the CoM, at the slowest speed, accelerated during the late downstroke and part of the upstroke, and decelerated during mid-upstroke and part of downstroke (Fig. 5). As speed

increased, the CoM accelerated during downstroke and decelerated during upstroke, and reaching a maximum earlier in the wingbeat cycle (Fig. 5). The magnitude of markers' horizontal accelerations decreased with increased speed for both upstroke and downstroke, while the CoM did not show such a decrease (Fig. 5 and 6A,B).

Both body marker and CoM vertical accelerations reached a maximum during downstroke and a minimum during upstroke, but the magnitude of the CoM accelerations were again consistently smaller than body marker accelerations. The pelvis marker experienced higher peak vertical accelerations than the sternum marker, particularly during slow flight (Fig. 5). This difference in accelerations reflects the body pitching down around the CoM during downstroke.

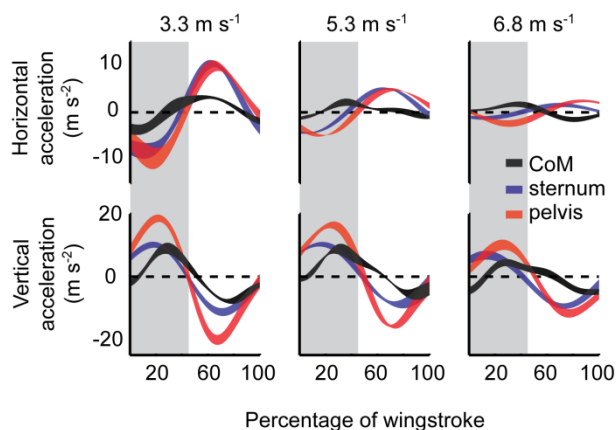


Fig. 5. Acceleration profiles over a standardized wingbeat cycle for the CoM (black trace), estimated from the mass-model, and for the body-fixed sternum and pelvis markers (blue and red traces, respectively) at three speeds representing slow, intermediate and fast flights for a representative individual. The width of the traces represent the mean ± 1 S.D. ($n = 3, 3$ and 4 wingbeats for each speed, respectively). The vertical shadow bar represents the downstroke portion of the wingbeat.

These temporal and magnitude differences in accelerations were reflected in the average accelerations at each speed. Horizontal accelerations calculated from body markers (i.e., with no correction for inertial effects) suggest that negative net horizontal acceleration was produced during downstroke and positive net horizontal acceleration during upstroke (Fig. 6A,B). Net horizontal accelerations derived from the motion of the CoM indicate the opposite: positive acceleration was produced during downstroke and

negative during upstroke (Fig. 6A,B). Vertical accelerations of the body markers and the CoM were similar, with positive accelerations during downstroke and negative accelerations during upstroke, and the magnitude of those accelerations smaller for the CoM than for the body markers (Fig. 6C,D).

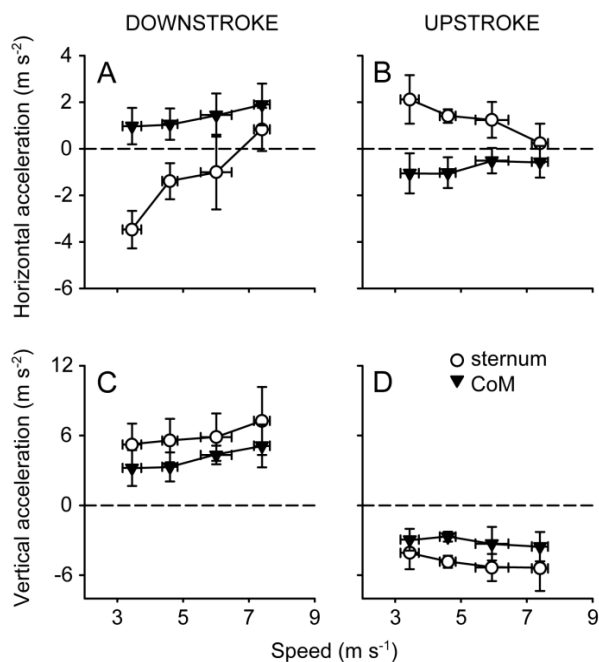


Fig. 6. Horizontal and vertical accelerations during downstroke and upstroke for the sternum marker (open symbol) and the CoM (closed symbol). Each point corresponds to the mean value of the four individuals used in this study. At each speed, the individual values were calculated as the mean of all wingbeats (3-7 wingbeats) for a particular trial. Error bars correspond to ± 1 S.D.

Discussion

Our results demonstrate that *C. brachyotis* do not produce net thrust during the upstroke, and that the positive horizontal accelerations of the body markers that occur during the upstroke result from the inertial forces produced by the backward motion of the wings. We conclude, therefore, that horizontal accelerations calculated from the motion of body markers lead to the incorrect conclusion that positive net thrust is produced during the upstroke at almost every speed. When accelerations of the CoM are calculated, accounting for the contribution from inertial forces, positive net horizontal

acceleration is observed exclusively during downstroke, and net negative horizontal accelerations are observed during upstroke.

Our observation that net thrust does not occur during the upstroke is supported by previous studies on the wake patterns behind flying bats. It has been hypothesized that the structure of the wake behind a bat flying slowly, based on the idea that thrust is generated during the upstroke, should be a series of linked vortex rings but of opposite circulation (Norberg, 1976; Aldridge, 1986, 1987). However, flow visualizations suggested that slow-flying *Plecotus auritus* produce discrete vortex rings, wake structures found in organisms where lift and thrust generation are restricted to the downstroke phase (Rayner et al., 1986). This result contrasts with the prediction for an active force-generating upstroke. The basis of this discrepancy has eluded researchers. Some have hypothesized that the observed wake structure might be explained by variations in flight style, or that the circulation produced during upstroke might have been too small to detect among the larger circulation patterns that resulted from the downstroke (Rayner et al., 1986; Aldridge, 1987). In light of our results, we suggest a different alternative: we propose that the tip-reversal upstroke observed in *P. auritus* produces little or no thrust, but instead, the observed forward acceleration of the body during upstroke at slow flights was the result of inertial effects of forward movement of the wings, and therefore, the discrete vortex wake structure reflects the fact that most of thrust and lift were produced during downstroke.

The vertical accelerations of body markers and the CoM are qualitatively similar, but during downstroke, the downward movement of the wing moved the CoM upwards and during upstroke, the opposite motion of the wing translated the CoM downwards

(Fig. 1). The net result is that body markers exaggerate the magnitude of vertical accelerations compared to that of the CoM. Moreover, the inertial contribution to vertical body acceleration does not depend strongly on speed, in contrast to the substantial speed effect on the inertial contribution of horizontal accelerations (Fig. 6). The smaller inertial contribution to horizontal body accelerations at higher speeds vs. low speeds probably reflects the decrease in horizontal excursion of the wingtip as speed increased (ANCOVA, speed effect: slope = -0.015, $F_{1,19} = 37.6$, $P < 0.0001$). Although the vertical excursion of the wingtip also varied with speed (ANCOVA, speed effect: slope = 0.013, $F_{1,19} = 20.0$, $P < 0.001$), the lack of noticeable change in the inertial contribution to the vertical acceleration component, could be explained by the magnitude of the vertical excursion compared to the horizontal excursion. Vertical excursion is almost twice as large as the horizontal excursion, so the changes observed in excursion of the wingtip will have a smaller effect on the vertical component of the inertial forces than for the horizontal component.

For almost thirty years, studies of bat kinematics have led to the common conclusion that net thrust is generated on the upstroke. For example, Norberg's (1976) classic study of the kinematics of the bat *Plecotus auritus* in forward flight estimated the coefficients of lift and drag of the wings using steady-state aerodynamic theory, and estimated that 86% of thrust is provided during upstroke while most of weight support is provided during downstroke. In other studies, accelerations of body-fixed markers were taken to directly reflect the pattern of acceleration of the CoM, assuming that the inertial component was negligible compared with aerodynamic forces (e.g., Thomas et al., 1990).

Were we to base our analyses based on body markers, we would reach similar conclusions.

Our study is not the first of bat flight to acknowledge the potential effect of inertial forces produced by the motion of the wings. Aldridge (1987) studied the wing kinematics and body accelerations of six species of bats, and also concluded that net thrust occurs during tip-reversal upstrokes. In this case, wing inertia was computed from the angular acceleration of the wingtip and the wing length. During upstroke, however, the three-dimensional configuration of the wing differs substantially from the downstroke condition, as the wings are brought close to the body by significant flexion of the elbow and wrist (Norberg, 1976; Aldridge, 1986; Norberg and Winter, 2006; Tian et al., 2006; Riskin et al., in press). If the wings are folded during upstroke, estimates of the wing moment of inertia with respect to the body that are based on the angular acceleration of the wingtip will be highly unreliable. To adequately assess upstroke function, a more detailed model that combines accurate kinematics and morphological description is required.

One potential source of error in our study is inaccurate reconstruction of the mass distribution in the head, thorax and abdomen. We estimated the body's mass as uniformly distributed throughout an ellipsoid, the position of which was based on the position of the pelvis, sternum and shoulder markers. Due to the smaller horizontal than vertical excursion of the wing, errors in body mass distribution estimates will have a larger effect on the estimated horizontal position of the CoM. Thus, pitching moments of the body might have an important effect on horizontal accelerations. However, pitching effects are more clearly visible for vertical accelerations, as noted in the differences between the

accelerations of the sternum and pelvis markers (Fig. 5). We also estimated the body mass as the point-mass located between the sternum and the pelvis marker; this alternative model did not significantly change the results presented here (data not shown). Thus, although there is potential for error in the estimations of horizontal accelerations, our data is consistent with the idea that no positive net horizontal acceleration is present during upstroke at any speed.

We conclude that the forward accelerations of body markers observed during the upstroke of slow flights by *C. brachyotis* are the result of inertial accelerations generated by the forward movement of the wings, and not the aerodynamic forces produced during flight. Wing kinematics and body accelerations of these fruit bats are similar to those reported for other species, hence it is likely that the upstroke of most bats is similar to that reported here, and generates no or little thrust. However, there may be exceptions, especially among bats that hover, such as *Glossophaga soricina*. Indeed, a recent study on the wake structure of that species found evidence of active upstroke function (Hedenström et al., 2007). We hypothesize that this is likely the result of kinematic and perhaps morphological characteristics of hovering species that allow them to strongly supinate the distal portion of the wing and to produce a stroke reversal, similar to that used by hummingbirds during hovering. Hovering species, however, do not characterize the full diversity present among the >1,200 species of bats found worldwide. The species used in this study is less specialized, and thus likely to represent a trend common to larger numbers of species. We predict that when the inertial effects are accounted for in a manner analogous to the methods we used in this study, measurements of accelerations of

the CoM of bats generally will fail to show net positive horizontal acceleration during upstroke.

List of symbols

ANCOVA	analysis of covariance
CoM	center of mass
DLT	direct linear transformation
PIV	particle image velocimetry

Acknowledgments

All experiments were conducted at the Concord Field Station (CFS) at Harvard University, and we express our thanks to the CFS staff, especially Andy Biewener for allowing us the use of the facilities, and Pedro Ramírez for taking care of the bats. Bats were provided through the generous support of Dr. Allyson Walsh and the Lube Bat Conservancy. We also thank everybody in the Bat Lab for the help provided during the experiments and during the analysis of data. This manuscript was greatly improved by conversations with Kenny Breuer, Tatjana Hubel, and the Morphology discussion group at Brown University. This work was supported by the Air Force Office of Scientific Research (AFOSR), the NSF-ITR program, and the Bushnell Foundation.

References

- Aldridge, H. D. J. N.** (1986). Kinematics and aerodynamics of the greater horseshoe bat, *Rhinolophus ferrumequinum*, in horizontal flight at various speeds. *J. Exp. Biol.* **126**, 479-497.
- Aldridge, H. D. J. N.** (1987). Body accelerations during the wingbeat in six bat species: the function of the upstroke in thrust generation. *J. Exp. Biol.* **130**, 275-293.
- Bilo, D., Lauck, A. and Nachtigall, W.** (1984). Measurement of linear body accelerations and calculation of the instantaneous aerodynamic lift and thrust in a pigeon flying in a wind tunnel. In *Biona - Report 3* (ed. W. Nachtigall). Stuttgart: Gustav Fischer.
- Brown, R. H. J.** (1948). The flight of birds: the flapping cycle of the pigeon. *J. Exp. Biol.* **25**, 322-333.
- Brown, R. H. J.** (1953). The flight of birds: II. wing function in relation to flight speed. *J. Exp. Biol.* **30**, 90-103.
- Hatze, H.** (1988). High-precision three-dimensional photogrammetric calibration and object space reconstruction using a modified DLT-approach. *J. Biomech.* **21**, 533-538.
- Hedenström, A., Johansson, L. C., Wolf, M., von Busse, R., Winter, Y. and Spedding, G. R.** (2007). Bat flight generates complex aerodynamic tracks. *Science* **316**, 894-897.
- Hedrick, T. L., Tobalske, B. W. and Biewener, A. A.** (2002). Estimates of circulation and gait change based on a three-dimensional kinematic analysis of flight in cockatiels (*Nymphicus hollandicus*) and ringed turtle-doves (*Streptopelia risotia*). *J. Exp. Biol.* **205**, 1389-1409.
- Hedrick, T. L., Usherwood, J. R. and Biewener, A. A.** (2004). Wing inertia and whole-body acceleration: an analysis of instantaneous aerodynamic force production in cockatiels (*Nymphicus hollandicus*) flying across a range of speeds. *J. Exp. Biol.* **207**, 1689-1702.
- Lauder, G. V. and Madden, P. G. A.** (2008). Advances in comparative physiology from high-speed imaging of animal and fluid motion. *Annu. Rev. Physiol.* **70**, 143-163.
- Muijres, F. T., Johansson, L. C., Barfield, R., Wolf, M., Spedding, G. R. and Hedenstrom, A.** (2008). Leading-edge vortex improves lift in slow-flying bats. *Science* **319**, 1250-1253.
- Norberg, U. M.** (1976). Aerodynamics, kinematics, and energetics of horizontal flapping flight in the long-eared bat *Plecotus auritus*. *J. Exp. Biol.* **65**, 179-212.

- Norberg, U. M.** (1990). Vertebrate flight. Berlin: Springer-Verlag.
- Norberg, U. M. L. and Winter, Y.** (2006). Wing beat kinematics of a nectar-feeding bat, *Glossophaga soricina*, flying at different flight speeds and Strouhal numbers. *J. Exp. Biol.* **209**, 3887-3897.
- Rayner, J. M. V., Jones, G. and Thomas, A.** (1986). Vortex flow visualizations reveal change in upstroke function with flight speed in bats. *Nature* **321**, 162-164.
- Riskin, D. K., Willis, D. J., Iriarte-Díaz, J., Hedrick, T. L., Kostandov, M., Chen, J., Laidlaw, D. H., Breuer, K. and Swartz, S. M.** (in press). Quantifying the complexity of bat wing kinematics. *J. Theor. Biol.*
- Shyy, W. and Liu, H.** (2007). Flapping wings and aerodynamic lift: the role of leading-edge vortices. *AIAA Journal* **45**, 2817-2819.
- Spedding, G. R., Rosén, M. and Hedenström, A.** (2003). A family of vortex wakes generated by a thrush nightingale in free flight in a wind tunnel over its entire natural range of flight speeds. *J. Exp. Biol.* **206**, 2313-2344.
- Swartz, S. M.** (1997). Allometric patterning in the limb skeleton of bats: implications for the mechanics and energetics of powered flight. *J. Morph.* **234**, 277-294.
- Swartz, S. M., Groves, M. D., Kim, H. D. and Walsh, W. R.** (1996). Mechanical properties of bat wing membrane skin. *J. Zool.* **239**, 357-378.
- Thollesson, M. and Norberg, U. M.** (1991). Moments of inertia of bat wings and body. *J. Exp. Biol.* **158**, 19-35.
- Thomas, A. L. R., Jones, G., Rayner, J. M. V. and Hughes, P. M.** (1990). Intermittent gliding flight in the pipistrelle bat (*Pipistrellus pipistrelus*) (Chiroptera: Vespertilionidae). *J. Exp. Biol.* **149**, 407-416.
- Tian, X., Iriarte-Díaz, J., Middleton, K., Galvao, R., Israeli, E., Roemer, A., Sullivan, A., Song, A., Swartz, S. and Breuer, K.** (2006). Direct measurements of the kinematics and dynamics of bat flight. *Bioinspiration & Biomimetics* **1**, S10-S18.
- Watts, P., Mitchell, E. J. and Swartz, S. M.** (2001). A computational model for estimating the mechanics of horizontal flapping flight in bats: model description and validation. *J. Exp. Biol.* **204**, 2873-2898.
- Willis, D. J., Riskin, D. K., Breuer, K. S., Swartz, S. M. and Peraire, J.** (in preparation). Computational modeling of the aeromechanics of a bat, *Cynopterus brachyotis*, based on high resolution, experimentally recorded kinematics: I. description of the computational models.

Chapter 4

The effect of loading on the flight kinematics of a fruit bat

Jose Iriarte-Diaz¹, Daniel K. Riskin¹,
Kenneth S. Breuer² & Sharon M. Swartz¹

¹Department of Ecology and Evolutionary Biology, Brown University

²Division of Engineering, Brown University

Abstract

All bats experience daily and seasonal fluctuation in body mass. Presumably, an increase in mass requires changes in flight kinematics to produce the extra lift necessary to compensate for the increased weight. How bats modify their kinematics to increase lift, however, is not well understood. In this study we investigated the effect of added mass on flight kinematics for bats flying between 1.8 and 8.0 m s⁻¹. Three lesser dog-faced fruit bats (*Cynopterus brachyotis*) were trained to fly both in a flight corridor and in a wind tunnel, with and without a load of ca. 20% of original body mass. Reflective markers were placed on the body and wings and flights were recorded with three synchronized, high-speed digital video cameras. Data from the three cameras were combined to reconstruct the 3D motion of each marker, from which we calculated wing shape and motion parameters. Bats showed a marked change in wingbeat kinematics in response to loading, but changes were non-uniform among individuals. Each bat adjusted a different combination of kinematic parameters to increase lift, indicating that aerodynamic force generation can be modulated in multiple ways. Two main kinematic strategies were distinguished: bats either changed the motion of the wings by increasing primarily wingbeat frequency, or changed the shape of the wings by increasing wing area and wing camber. Interestingly, wingbeat amplitude tended to decrease with loading, in contrast to kinematic responses observed in other flying vertebrates. The complex, individual-dependent response to increased loading suggests that caution should be applied when using aerodynamic models to predict flight characteristics of bats. Where possible, we recommend that variation among individuals should be measured when analyzing complex locomotion, such as the flight of bats.

Introduction

Bats, like most mammals, experience both seasonal and daily changes in body mass. For example, during pregnancy, a female bat's body mass can be normally 20-30% up to 40% higher than during non-reproductive periods (Funakoshi and Uchida, 1981; Kurta and Kunz, 1987), and even higher during lactation (Speakman and Racey, 1987). Similarly, both males and females of hibernating species experience changes in body mass as large as those observed in pregnant females (Beasley et al., 1984; Kunz et al., 1998; Barclay and Harder, 2003). On a daily scale, significant variation in mass is associated with foraging, with changes of mass as large as 20-30% for insectivorous bats, 15-30% for nectarivorous bats (Winter and von Helversen, 1998; Winter, 1999), and just over 50% for sanguivorous bats (Wimsatt, 1969). Also frugivorous bats often carry fruits as large as 40.5% of body mass to feeding roosts (Jones, 1972). How these large changes in body mass affect flight performance, however, is still poorly understood.

Over a wingbeat of level flight at constant speed, a flying animal produces enough lift to counteract body weight and enough thrust to overcome drag. Thus, any increase in body mass requires a proportional increase in lift to maintain level flight. Since the increased mass comes without increased surface area of the wings, classic aerodynamic theory suggests that weighted flying organisms, with increased wing loading, should increase their flight speed to produce enough lift (e.g., Norberg and Rayner, 1987). It has also been predicted that flying organisms will increase wingbeat frequency to increase mechanical power output of the wings (Hughes and Rayner, 1991).

Experimental studies where body mass has been manipulated show no clear, consistent pattern. For example, kestrels carrying loads of up to 30% body mass (Videler et al., 1988a; Videler et al., 1988b) and insectivorous bats carrying loads up to 46% body mass (Hughes and Rayner, 1991) decrease flight speed and increase wingbeat frequency. In contrast, nectarivorous bats increase flight speeds in response to loading (Winter, 1999). In other cases, response can be complex, and animals may adopt different strategies depending on the amount of load. With loads smaller than 15% body mass, cockatiels decrease their flight speed with no changes in wingbeat frequency, but at higher loads (i.e., 20% body mass), they increase both flight speed and wingbeat frequency (Hambly et al., 2004). These results suggest that the kinematic response to loading may not be straightforward, and that an individual may be able to select among multiple strategies for accommodating increased loading, depending on the magnitude of load and other factors, such as flight speed.

One challenge inherent in interpreting the results of studies carried out to date is that the effect of changes in flight speed cannot be decoupled from other changes in wingbeat kinematics, as kinematics change with speed as well as with loading (e.g., Norberg, 1976; Aldridge, 1986). For example, it has been noted that wingbeat frequency tends to increase as speed decreases (Bullen and McKenzie, 2002). Thus, if a weighted bat decreases flight speed and increases frequency, the frequency increase could be the result of the increase in loading, the decrease in speed, or both. Furthermore, bats are also able to modulate their aerodynamic force generation by relatively subtle changes of their morphology and kinematics such as angle of attack, camber, wing area, among others (Swartz et al., 2005). As a consequence, the three-dimensional kinematics of the body

and wings are necessary to get a complete view of how changes in mass affect flight in bats.

The aim of this study is to evaluate the effect of a substantial, transient increase in body mass on the three-dimensional kinematics of the lesser dog-faced fruit bat, *Cynopterus brachyotis* (Muller) across a range of speeds. We assessed detailed kinematics by employing animals trained to fly both in a wind tunnel, where speed was controlled, and in a flight corridor, where bats were free to select their flight speeds. Increased aerodynamic force can be achieved by changing the force coefficient of the wings, which is a function of wing shape; by changing the wing surface area, a function of wing folding; or by increasing the flow velocity over the wing surface, a function of flight speed, wingbeat frequency and wingbeat amplitude. We measured several wing shape and motion parameters, and predict that bats will employ some repeatable combination of these alternatives to increase aerodynamic forces in response to loading.

Material and methods

Animals and loading protocol

Three female lesser dog-faced fruit bats (*Cynopterus brachyotis*) (Table 1), loaned by the Lube Bat Conservancy (Gainesville, FL) were subjects in this experiment. They were housed in the animal care facilities of the Harvard-Concord Field Station (Bedford, MA), where they were provided with food and water *ad libitum*.

Table 1. Morphological measurements of the three individuals used in this study. Measurements were performed following Norberg and Rayner (1987).

Variable	Individual		
	Bat1	Bat2	Bat3
Mass (kg)	0.0348	0.0371	0.0417
Wing span (m)	0.361	0.386	0.411
Wing area (m ²)	0.0197	0.0212	0.0250
Aspect ratio	6.6	7.0	6.8
Wing loading (N m ⁻²)	17.3	17.2	16.3

Table 2. Body mass of experimental subjects for wind tunnel and flight corridor experiments, prior to the experiment, immediately injection and approximately one hour subsequent to the experiment.

	Body mass (g)		
	Bat1	Bat2	Bat3
Flight corridor			
original	35.53	36.62	42.36
after injection	42.49 (19.6%)	44.12 (20.4%)	51.06 (20.5%)
after experiment	42.01 (18.2%)	43.73 (19.4%)	50.67 (19.6%)
Wind tunnel			
original	34.87	37.42	41.10
after injection	41.82 (19.9%)	45.00 (20.2%)	49.29 (19.9%)
after experiment	41.65 (19.4%)	44.37 (18.6%)	48.96 (19.1%)

Percentage of increase with respect to original mass appears in parenthesis

Before experiments, bats were anesthetized with isoflurane gas and key anatomical landmarks were marked with an array of high-contrast markers on the undersurface of one wing (Fig. 1A). All individuals experienced two treatments: *control*, in which there was no body mass modification, and *loaded*, in which body mass was increased by 20% (Table 2). Body mass was modified by injecting 0.9% saline solution into the peritoneal cavity, a technique that has been previously used to increase body mass in birds (Jones, 1986) and small terrestrial mammals (Iriarte-Díaz et al., 2006). We chose this method for three reasons. First, it allows us to precisely control the amount of

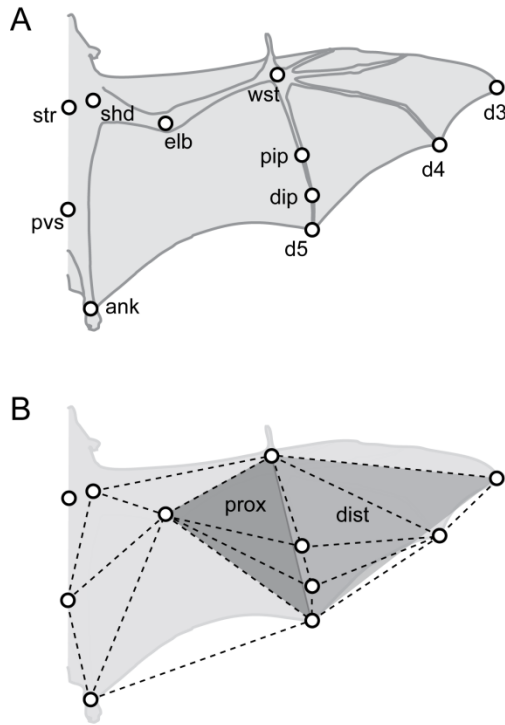


Fig. 1. Ventral view diagram of a bat indicating (A) the position of the wing and body markers and (B) the triangular segmentation used to calculate surface area, vertical force coefficient (C_{vf}), and the angles of attack. The dotted lines indicate the 11 segments used to calculate surface area and C_{vf} and the grey-shaded triangles represent the segmentation used to calculate the proximal (prox) and distal (dist) angles of attack.

added weight. Second, the injection of saline solution has a very transient effect, with the bats returning to their original body mass in 4-5 hours. Third, intraperitoneal injection more closely reflects the mass distribution of a bat during pregnancy or after a meal than does other loading methods such as external backpacks, which shift the center of mass in an artificial and potentially anomalous manner.

Saline injection was performed while the bats were anesthetized, with no apparent discomfort. Subjects began to urinate immediately after awaking from anesthesia, so we provided fruit juice between trials to

maintain body mass. Bats were weighed before and after every experimental session, which lasted <1 hr, to ensure that no substantial changes in mass had occurred.

Flight experimental setups: flight corridor and wind tunnel

The flight response of bats to increased loading was tested in two sets of experiments: one in still air (a flight enclosure), where bats were allowed to select their flight speed, and one in a wind tunnel, where flight speed could be experimentally controlled. In the flight corridor experiment, bats were trained to fly inside a enclosure (9

m long \times 1 m wide \times 2 m high). Bats were hand-released to fly from one side of the corridor to the opposite end and allowed to select their flight speeds, which ranged from 1.8 to 3.3 m s⁻¹. They also flew in the Harvard-Concord Field Station wind tunnel, an open-circuit tunnel with a closed jet in the flight chamber and a working section 1.4 m long \times 1.2 m wide \times 1.2 m high (for technical details and aerodynamic characteristics see Hedrick et al., 2002). In the wind tunnel, bats flew at speeds ranging from 3.1 to 8 m s⁻¹.

All components of this study were approved by the Institutional Animal Care and Use Committees at Brown University, Harvard University, and the Lube Bat Conservancy, and by the United States Air Force Office of the Surgeon General's Division of Biomedical Research and Regulatory Compliance.

Three-dimensional coordinate mapping

Flight corridor trials were recorded at 500 frames per second using three high-speed Redlake PCI 1000 digital video cameras. The volume in which the bats were flown was calibrated using the Direct Linear Transformation (DLT) method, based on a 25-point (0.45 \times 0.45 \times 0.55 m) calibration cube recorded at the beginning of each set of trials (Hatze, 1988). Wind tunnel flights were recorded at 1000 frames per second using three high-speed Photron 1024 PCI digital cameras and calibrated by using the DLT method with a 40-point (0.35 \times 0.35 \times 0.30 m) calibration cube, recorded at the beginning of each set of trials.

For the flight corridor trials, six markers on the bats' bodies and wings were digitized from each video frame (*str*, *pvs*, *shd*, *wst*, *d3* and *d5* in Fig. 1A); for wind tunnel experiments, eleven markers were digitized (Fig. 1A). The three-dimensional position of

each marker was resolved using the DLT coefficients obtained from the calibration cube (Hatze, 1988). When a marker was not simultaneously visible in at least two cameras, gaps in the three-dimensional position of the markers occurred. These gaps were filled by over-constrained polynomial interpolation. For contiguous gaps in the data with sufficiently rich data at the end points, a third order, over-constrained polynomial fit was used. For gaps that included sporadic intermediate points, a sixth order polynomial was used. After gap-filling, a 50 Hz digital Butterworth low-pass filter was used to remove high-frequency noise. This cut-off frequency was approximately 5 times higher than the wingbeat frequency recorded in our bats.

Kinematic variables

A wingbeat cycle was defined by the vertical excursion of the wrist in a body coordinate system. Downstroke and upstroke phases were defined as the portions of the wingbeat cycle where wrist vertical velocities were negative and positive, respectively.

Wing motion descriptors

Wingbeat frequency was defined as the inverse of the period between two consecutive downstrokes. The downstroke ratio was defined as the proportion of the wingbeat cycle occupied by the downstroke. Wingbeat amplitude was defined as the angle between the straight line connecting the wingtip (*d3*) and the shoulder (*shd*) markers at the beginning of the downstroke and the straight line connecting *d3* and *shd* markers at the end of the downstroke. We note that the amplitude values reported depend on this definition, and somewhat different values are obtained when other anatomical landmarks define this parameter. Overall results do not, however, depend strongly on the

definition of amplitude employed. Stroke plane angle was defined as the angle between the horizontal axis and the least-squares regression line to the lateral projection of the wingtip during the downstroke. Again, a somewhat different stroke plane is defined by the wrist or other landmarks on the wing, but results are qualitatively similar.

To further explore the changes in the motion of the wing, we also calculated the average velocity of the wingtip with respect to the body during downstroke. Wingbeat frequency, downstroke ratio, wingbeat amplitude, stroke plane angle, and wingtip velocity were calculated from both flight corridor and wind tunnel experiments.

Wing shape descriptors

Wing shape descriptors were calculated only for the wind tunnel experiments. The camber of the wing during downstroke was estimated by measuring the curvature of the digit V, by fitting a parametric quadratic curve to the three-dimensional position of the four markers along that digit (*wst*, *pip*, *dip*, *d5* in Fig. 1A). The fitted quadratic curve was then divided into 50 segments and the curvature of each segment was calculated as the average rate of change in the tangent to the curve along its length (Crenshaw et al., 2000).

We measured the elbow and wrist joint angles to estimate the change in folding of the wing at different speeds. Elbow joint angle was calculated as the three-dimensional angle between the shoulder, elbow and wrist markers (*shd*, *elb*, and *wst* in Fig. 1A), and the wrist joint angle as the three-dimensional angle between the elbow, wrist and wingtip markers (*elb*, *wst*, and *d3* in Fig. 1A).

To estimate wing surface area, we divided the wing into 11 eleven triangular elements (Fig. 1B) and calculated the area of each. Total wing area was obtained by

multiplying the obtained area for one wing by two. This value is necessarily smaller than the conventional value obtained from measurements of bats with wings completely extended over a flat surface because bats do not completely extend their wings during flight (Swartz et al., 2005) and because we do not include body area in this estimate.

We also divided the wing into a proximal and a distal triangular element (Fig. 1B) and estimated angle of attack was independently for each; a single angle of attack is not appropriate for the complex three-dimensional geometry of the bat wing. Angle of attack was calculated as the angle between the vector of the relative incident air velocity and a plane formed by the three vertices of each segment. The incident velocity vector was calculated as the first derivative of the position of the centroid of each segment.

Vertical force coefficient

The vertical force coefficient (C_{vf}) can be estimated from the measured vertical force produced to overcome gravity plus the area and velocity of the wing. This coefficient is a dimensionless number that depends, among other factors, on the angle of attack and camber of the wing, and that indicates the shape and surface characteristic-related capacity of the wing to produce vertical force. Therefore, C_{vf} is a useful measurement of the relative importance of changes of angle of attack and camber with respect to loading. For example, if the modulation of wing velocity during downstroke is enough to produce the extra lift necessary to support extra weight, we expect to see no change in C_{vf} with external loading. In contrast, if modulation of angle of attack and/or camber is important to extra vertical force generation, C_{vf} will increase with respect to the control condition in bats flying with loads. Vertical force (F_v) was calculated by

multiplying the body mass by the vector sum of the gravitational acceleration and instantaneous vertical acceleration of the center of mass (CoM) derived from a mass model (see below). C_{vf} was then calculated from a modification of an standard formula as:

$$C_{vf} = \frac{F_v}{\frac{1}{2} \rho 2AV^2}, \quad (1)$$

where ρ is the air density, taken to be 1.2 kg m^{-3} ; $2A$ is the area of both wings and V is the velocity of the wing (Usherwood and Ellington, 2002). Because of the flapping motion of the wings, more distal portions will move faster than proximal ones. Therefore, we divided one wing into 11 triangular elements (Fig. 1B), and for each of these segments we calculated surface area and velocity. We obtained the velocity of a segment by calculating the first derivative of the position vector of its centroid in the global coordinate system. The contribution of each of these segments was used to calculate C_{vf} as:

$$C_{vf} = \frac{F_v}{\frac{1}{2} \rho 2 \sum_{i=1}^{i=11} A_i V_i^2}, \quad (2)$$

where A_i and V_i are the area and velocity of the i -th segment.

Determination of the CoM

In a flapping organism, the motion of the wings changes the position of the CoM with respect to the body over the wingbeat cycle. To calculate F_v as described above requires the actual position of the CoM. We therefore computed the cyclically changing

location of the CoM by building a dynamic mass distribution model of the bat. This mass model is a time-varying, discrete mass approximation of the bat's mass distribution, computed from the changing spatial locations of the anatomical markers. To develop the discrete mass system representing the bat, we partitioned total body mass into individual components or regions. The wing membrane, the wing bones and the trunk were treated as separate objects, each with its own position and mass, which were combined to form the total mass model.

To model the distribution of the wing membrane mass, we constructed a triangulation of the wing geometry at each time step. The large-scale base triangulation was developed using the location of the marker positions at any given time, and a subsequent subdivision of those triangles was performed to give a mesh of finer-scale triangular elements. Each triangle element on the membrane was assigned a constant thickness (1×10^{-4} m) and density (1×10^3 kg m⁻³). A resulting discrete point mass (m_i) for each triangular membrane element was computed based on the volume of that triangular membrane and assigned a position at the centroid of the triangle element. To model the distribution of mass among and within each of the wing bones, we constructed a curve between the markers at the endpoints of the bones. The curve for each bone in the wing was defined from the location of the markers. Given the tapered shape of bat bones (Swartz, 1997), the cross-sectional radius of each bone element of the model was defined by a quadratic function with respect to the length of the bone. We assigned a constant density to the bones (2×10^3 kg m⁻³). Using the distribution of bone radii distribution and the location of the bone elements in space, the line was subdivided into smaller line-elements, from which discrete mass points were defined. The mass of the wings was

scaled such that the constructed distribution represents the 16% of the total body mass, consistent with the measurements of bats of similar size (Thollesson and Norberg, 1991). The mass and moment of inertia of the wing with respect to the shoulder was compared to measured values (Thollesson and Norberg, 1991) to ensure that the model represents the physical reality. Finally, the bat's body was defined as a 3-dimensional ellipsoid divided into discrete mass points.

The discrete mass representation of the membranes, bones and body was combined with detailed kinematic records of motion of each landmark to determine the center of mass of each one of the mass elements, m_i , using the equation

$$\vec{r}_{CoM} = \frac{\sum \vec{r}_i m_i}{m_T}, \quad (3)$$

where \vec{r}_{CoM} represents the position vector of the CoM, \vec{r}_i represents the position vector of the i -th discrete point mass and m_T represents the total mass of the bat.

Statistical analysis

The effect of loading on wingbeat kinematics was estimated using analysis of covariance (ANCOVA), with loading as treatment and speed as a covariate. The linearity of the relationship with speed was estimated using a multiple regression approach with a quadratic component of speed. If a variable did not change linearly with speed or if the slope significantly differed between the unloaded and loaded treatments, the effect of loading was estimated by Tsutakawa's Quick test (Tsutakawa and Hewett, 1977). All analyses were performed with JMP v.7, with a significance level of 0.05.

Results

Wingbeat kinematics changed significantly in response to loading (Table 3). However, each individual responded by modulating a different combination kinematic parameters. With increased loading, Bat1 increased wingbeat frequency (Fig. 2A), slightly decreased wingbeat amplitude (Fig. 2D), and increased downstroke ratio, but only at high flight speeds (Fig. 2G). Similarly, Bat3 increased wingbeat frequency (Fig. 2C) and downstroke ratio (Fig. 2I), but also decreased stroke plane angle (Fig. 2L). In contrast, Bat2 decreased both wingbeat frequency and wingbeat amplitude, in particular at high speeds (Fig. 2B,E).

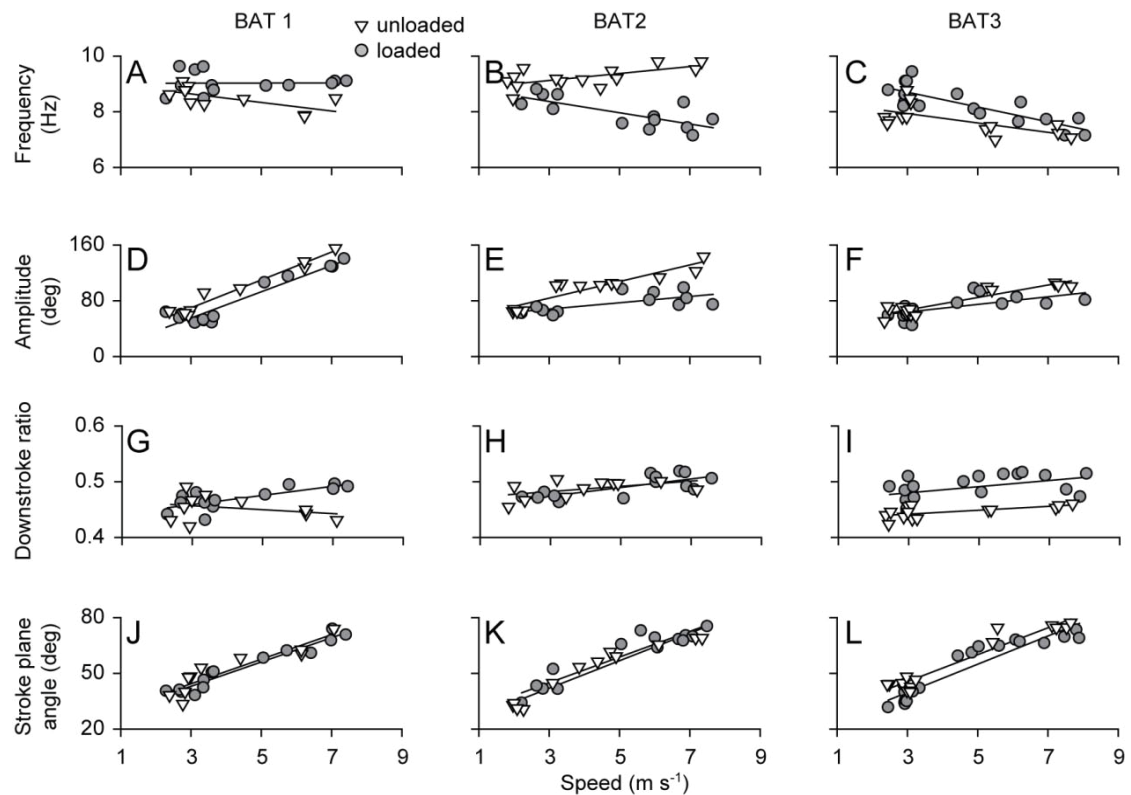


Fig. 2. Wing motion parameters of bats in unloaded (closed triangles) and loaded (open circles) treatments. Relationship between wingbeat frequency (A-C), wingbeat amplitude (D-F), downstroke ratio (G-I) and stroke plane angle (J-L) with flight speed. Each point represents the mean value for a particular trial, using both wind tunnel and flight corridor flights.

Table 3. Summary of ANCOVA analyses of kinematic variables in response to loading and speed as a covariate.

Variable	BAT1			BAT2			BAT3		
	effect ¹	slope ²	elevation ³	effect	slope	elevation	effect	slope	elevation
Frequency (Hz)	↑	$F_{1,19}=3.07$	$F_{1,19}=14.17^{**}$	↓	$F_{1,23}=22.4^{***}$	TQT ^{***}	↑	$F_{1,28}=1.81$	$F_{1,28}=19.8^{***}$
Amplitude (deg)	↓	$F_{1,19}=0.21$	$F_{1,19}=14.1^{**}$	↓	$F_{1,21}=11.4^{**}$	TQT*		$F_{1,26}=2.80$	$F_{1,26}=3.55$
Downstroke ratio		$F_{1,19}=8.87^*$	TQT		$F_{1,21}=0.85$	$F_{1,21}=0.31$	↑	$F_{1,27}=0.93$	$F_{1,27}=44.4^{***}$
Stroke plane angle (deg)		$F_{1,20}=0.005$	$F_{1,20}=0.70$		$F_{1,23}=0.009$	$F_{1,23}=0.49$	↓	$F_{1,31}=0.31$	$F_{1,31}=10.8^{**}$
Camber (m ⁻¹)	↑	$F_{1,7}=2.14$	$F_{1,7}=11.7^*$	↑	$F_{1,11}=2.92$	$F_{1,11}=90.3^{***}$		$F_{1,13}=0.53$	$F_{1,13}=0.14$
Proximal AoA (deg)		$F_{1,6}=4.2$	$F_{1,6}=0.82$		$F_{1,14}=0.0007$	$F_{1,14}=4.10$		$F_{1,13}=1.60$	$F_{1,13}=3.61$
Proximal AoA (deg)		$F_{1,6}=5.06$	$F_{1,6}=0.21$		$F_{1,14}=0.004$	$F_{1,14}=0.64$		$F_{1,13}=0.37$	$F_{1,13}=3.44$
Elbow extension (deg)	↑	$F_{1,6}=0.37$	$F_{1,6}=222.4^{***}$	↑	$F_{1,12}=2.42$	$F_{1,12}=115.5^{***}$	↑	$F_{1,12}=0.04$	$F_{1,12}=15.8^{**}$
Wrist extension (deg)	↑	$F_{1,6}=0.69$	$F_{1,6}=26.1^{**}$	↑	$F_{1,12}=5.70^*$	TQT*	↑	$F_{1,12}=0.36$	$F_{1,12}=24.0^{***}$
Wing area (m ²)		$F_{1,7}=2.66$	$F_{1,7}=3.08$	↑	$F_{1,12}=0.63$	$F_{1,12}=294.6^{***}$		$F_{1,13}=0.72$	$F_{1,13}=4.04$

¹Effect represents the positive (↑) or negative (↓) change of a variable in response to loading.

²The equality of slope was determined by the interaction effect of 'loading' and 'speed' effects in an ANCOVA analysis.

³The elevation effect reflects the effect of the loading treatment over a variable and it was determined by ANCOVA analysis. If the slopes were different between unloaded and loaded treatments, significance was tested by a Tsutakawa's Quick test (TQT).

Statistical significance: * $P < 0.05$, ** $P < 0.01$, *** $P < 0.001$

Changes in wingtip velocity with respect to the body in response to speed and loading also differed among individuals. Forward velocity of the wingbeat decreased linearly with speed for all individuals (Fig. 3A-C). Also, forward velocity significantly increased with loading only in Bat1 (ANCOVA, slope effect: $F_{1,19}=34.3$, $P<0.00001$; loading effect, TQT: $P=0.0006$) and Bat3 (ANCOVA, slope effect: $F_{1,23}=2.38$, $P=0.14$; loading effect: $F_{1,23}=6.89$, $P=0.02$). The vertical velocity of the wingtip presented a more complex response. For Bat1 and Bat2, wingtip vertical velocity showed a quadratic response to speed with low vertical wingtip velocity at intermediate flight speeds (Fig. 3D,E), while for Bat3 did not change with speed (Fig. 3F). In loading flight, the vertical velocity decreased slightly in all individuals (all $P<0.04$). Lateral wingtip velocity tended also to be higher at slow speeds, due to the non-linear relationship with speed (Fig. 3G-I).

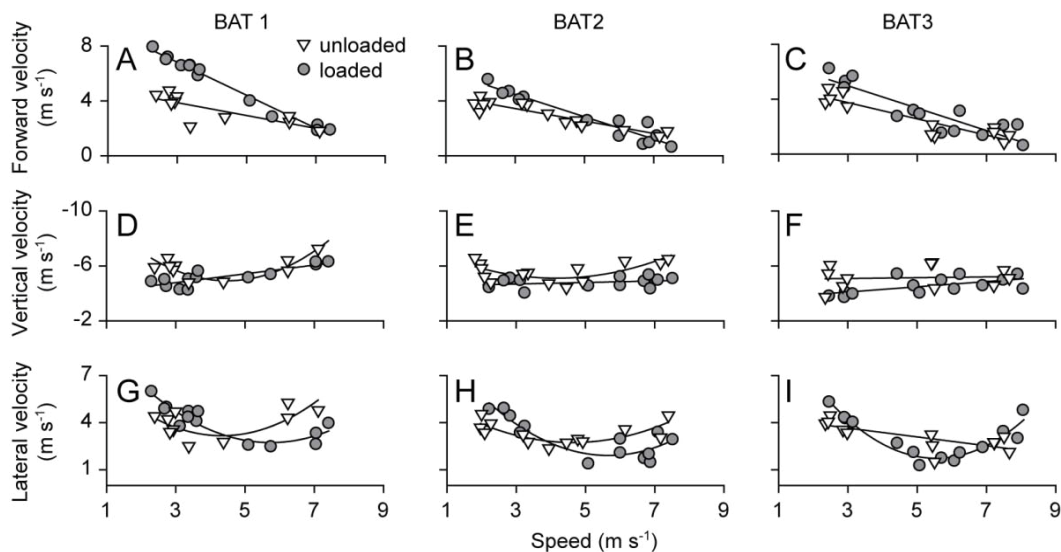


Fig. 3. Relationship between forward (A-C), vertical (D-F), and lateral (G-I) wingtip velocity with respect to the body with flight speed for unloaded (closed triangles) and loaded (open circles) flights. Each point represents the mean value for a particular trial, using both wind tunnel and flight corridor flights.

Individual bats varied in their manner of wing shape modulation in response to loading. Bat1 showed a small increase in camber, and elbow and wrist extension (Fig. 4A,J,M). Bat3 also slightly increased elbow and wrist extension (Fig. 4L,O) but showed no significant change in wing area (Fig. 4R). Bat2, however, showed a very substantial increase in camber (Fig. 4B), elbow and wrist extension (Fig. 4J,N), and wing area (Fig. 4Q).

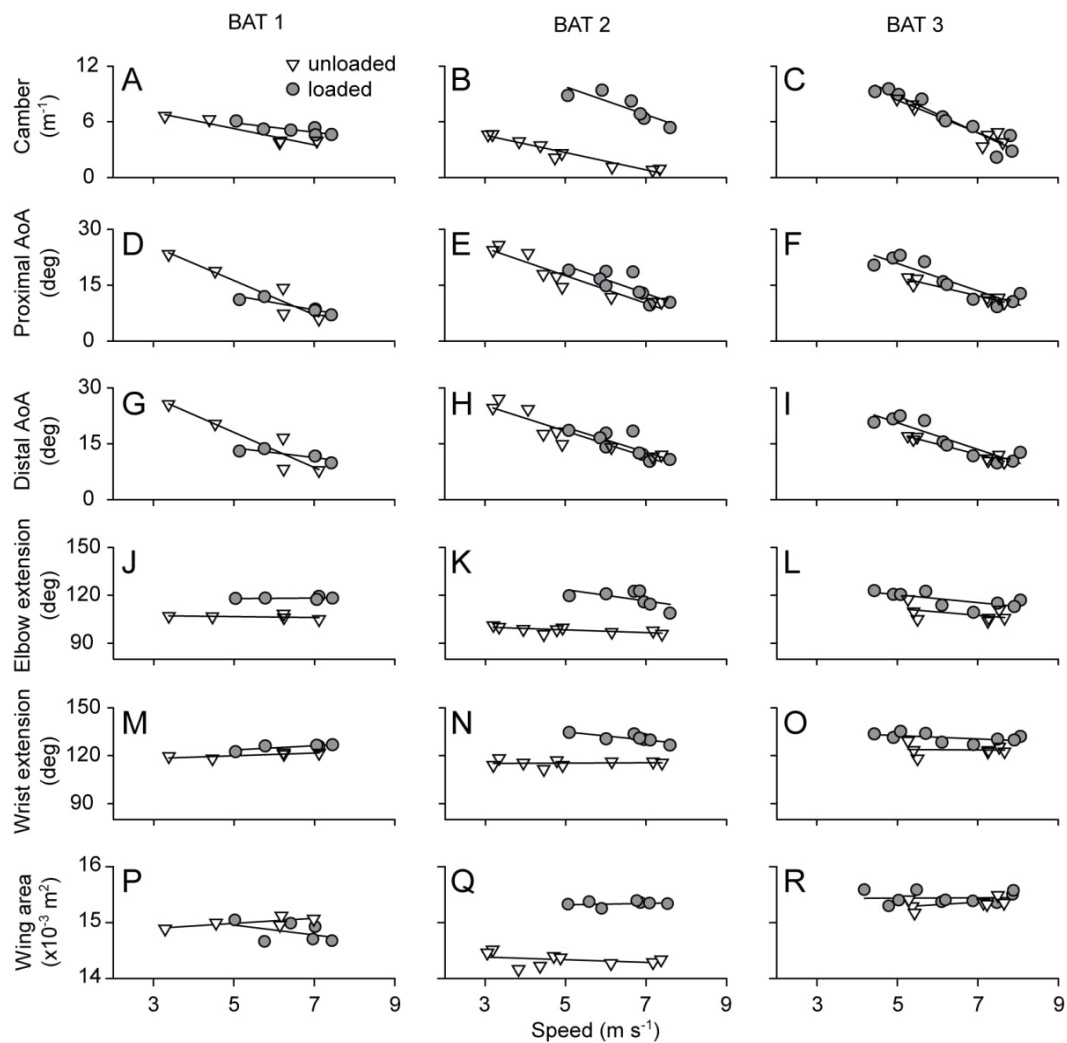


Fig. 4. Wing shape parameters of bats in unloaded (closed triangles) and loaded (open circles) treatments. Relationship between camber (A-C), proximal (D-F) and distal (G-I) angle of attack, elbow (J-L) and wrist (M-O) extension, and wing area (P-R) with flight speed. Each point represents the mean value for a particular trial, using only wind tunnel flights.

Vertical force coefficient (C_{vf}) decreased curvilinearly with speed (Fig. 5), and increased with loading only for Bat2 (TQT, $P=0.041$; Fig. 5B).

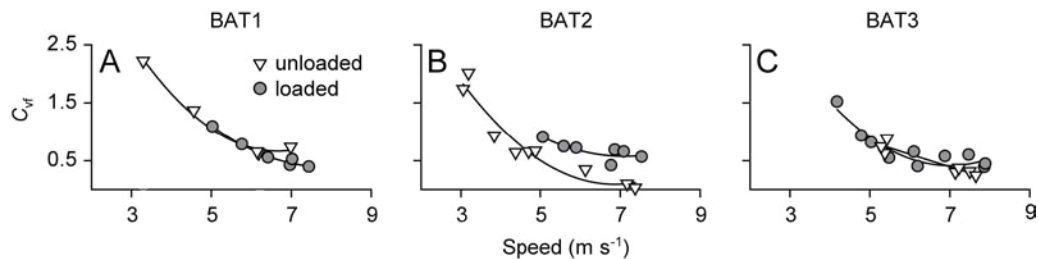


Fig. 5. Relationship between the vertical force coefficient, C_{vf} , and flight speed for unloaded (closed triangles) and loaded (open circles) flights. Each point represents the mean value for a particular trial, using only wind tunnel flights.

Discussion

Cynopterus brachyotis showed a marked change in wingbeat kinematics in response to a 20% increase in body mass. The response, however, was non-uniform among individuals; each bat used a different kinematic strategy, modulating different combinations of kinematic parameters to increase vertical force generation.

Individual strategies in response to loading

Although marginally significant for Bat3, wingbeat amplitude decreased with increased load in all bats. Similarly, major joints in the wing were more extended in the loaded flights in all bats. Outside of these consistent patterns, no two individuals responded to loading in exactly the same way. The variation we observed, however, can be summarized as two main strategies to increase vertical force generation. Both Bat1 and Bat3 increased the flow over the wings by increasing wing speed, without significant changes in C_{vf} . In contrast, Bat2 modulated the shape aspect of the wing, primarily

camber and wing area, and accordingly employed an increase in C_{vf} to increase vertical force. The first strategy, henceforth called the ‘motion’ strategy, requires that the wingbeat kinematics changes in a manner that results in greater airflow per unit time over the wings. In bats that used this strategy, we observed an increased forward velocity of the wingtip during downstroke, due to an increase in wingbeat frequency and an increased downstroke ratio.

The second strategy, henceforth called the ‘shape’ strategy, involved the modulation of shape aspects of the wing. Bat2 showed strong modulation of camber and wing area, and a marginally significant increase in the angle of attack of proximal portion of the wing. The combined effect of the modulation of angle of attack and camber was reflected in the higher C_{vf} when loaded (Fig. 5B). Bat2 also modulated the motion of the wing, but did so in the opposite direction of predictions and of the behavior of the other subjects, by decreasing both wingbeat frequency and amplitude (Fig. 2B,E, respectively).

Why might a flying animal adopt a reduced ‘motion’/increased ‘shape’ response to generating larger aerodynamic forces? One possibility is that this strategy could minimize mechanical power and metabolic costs. Muscle metabolism and mechanical power tend to increase with frequency of contraction (Hill, 1950; Harrison and Roberts, 2000) and aerodynamic models predict that the mechanical power output the flight muscles must generate to support the weight of a flying organism increases with body mass (Pennycuick, 1989; Norberg, 1995). Therefore, a reduction in wingbeat frequency and/or amplitude might be an appropriate response to increase force generation without unnecessary increases in mechanical power or metabolic cost. This may be particularly critical if an animal’s flight repertoire requires a substantial power margin, the relative

excess power available for flight tasks other than straight flight at constant speed (Hughes and Rayner, 1991).

If reducing wingbeat frequency to decrease metabolic costs and mechanical power output is important for bats, why do Bat1 and Bat3 increase their wingbeat frequency? One possibility is that when a flier increases wing area, camber or angle of attack, profile drag also increases, and this component of the energetic cost of flight can be particularly high in fast flight (Norberg, 1990). Another possibility is that increased wingbeat frequency does not entail increased metabolic cost in a simple fashion, and may not, therefore, be as metabolically expensive as one might predict. The mechanical power and metabolic costs associated with load carrying in birds increases less than predicted, due to behavioral modifications of kinematics and increased muscle efficiency (Dial and Biewener, 1993; Biewener and Dial, 1995; Kvist et al., 2001; Nudds and Bryant, 2002; Altshuler et al., 2004; Hambly et al., 2004). Alternatively, mechanical power output might not constrain flight kinematics at all. If that is the case, changes in frequency might be a more effective way to maintain enough vertical force. Aerodynamic force generation in steady-state flow is proportional to wing area, to the force coefficient (i.e, angle of attack and camber), and to the flow velocity squared. Thus, any increase in wing velocity (e.g, wingbeat frequency) would produce a larger increase in aerodynamic force than would changes in wing area or the force coefficient.

Comparison with other flying vertebrates

The responses to increased load that we observed in bats were complex, involving the modulation of both wing shape and wing motion. Wingbeat amplitude changed in a

very similar fashion among all individuals, tending to decrease with loading. This stands in direct contrast to observation for other flying vertebrates. For example, loading experiments in hummingbirds have shown that wingbeat amplitude increases with loading, along with minor changes in wingbeat frequency (Chai et al., 1997; Altshuler and Dudley, 2003; Altshuler, 2006). Similarly, when hummingbirds are flown in low air density, a task that is functionally and mechanically similar to flying while carrying loads, they increase wingbeat amplitude to increase their lift generation, thereby effectively counteracting the effect of diminished air density (Chai and Dudley, 1996; Dudley and Chai, 1996; Chai and Millard, 1997; Chai and Dudley, 1999; Altshuler and Dudley, 2003; Altshuler et al., 2004). Interestingly, bats hovering in low-density conditions show a similar response, with an increase in wingbeat amplitude, but no significant changes in wingbeat frequency (Dudley and Winter, 2002). This trend suggests that the modulation of the wingbeat frequency in hovering vertebrates is somehow constrained and therefore, changes in amplitude must supply the necessary extra mechanical power.

Implications for the use of aerodynamic theory

A primary thrust in the study of animal flight has been to develop aerodynamic models based on the aerodynamics of human-engineered aircraft, and to use these models to predict the relationship between morphology and flight performances in flying organisms (e.g., Norberg, 1995). However, experimental support for these predictions has been limited, and several studies have suggested that flying animals may respond to changes in morphology or other flight parameters in a complex manner (e.g., Hambly et al., 2004). This might be particularly true for bats because of the unique features of the

complex structural design of their wings, such as more than two dozen joints which can be controlled independently to some degree, a highly anisotropic, non-linearly elastic wing membrane with adjustable stiffness (Swartz et al., 1996; Swartz, 1998), and with an array of sensory organs believed to provide local flow information during flight (Zook and Fowler, 1986; Zook, 2007). Because there are multiple mechanisms a flapping flier can use to modulate the generation of aerodynamic forces, deviations from predictions derived from aerodynamic theory could be explained by recourse to this redundancy. To date, many studies have assumed that flying organisms will modulate a few specific variables, usually flight speed, wingbeat frequency and/or wingbeat amplitude. However, even under assumptions of purely steady-state aerodynamics, many more aspects of wing form or kinematics can influence flight performance, beginning with such logical candidates as stroke angle, wing surface area, angle of attack and camber. How these kinematic variables are modulated to generate aerodynamic forces under different conditions is still poorly studied, and the manipulation of unsteady effects for flight control has rarely been considered.

This study, combined with others that have experimentally manipulated body mass and flight performance, suggests that predicting the effect of loading on a flying animal using models derived from fixed-wing aerodynamics requires considerable caution. Different taxa vary considerably in their responses to increased loads (Videler et al., 1988a; Hughes and Rayner, 1991; Winter, 1999; Hambly et al., 2004). Moreover, to add a layer of complexity, our results point to individual differences within a species in the kinematic strategies used to respond to loading. Although few studies have been specifically designed to measure individual differences flight mechanics, the use of

different strategies among individuals of a species, as shown in this study, is not a phenomenon restricted to bats. Measurement of mechanical power output of pigeons carrying loads have shown large variations in the mechanical forces recorded for individual birds, indicating that response strategies to loading may differ among individuals (Biewener and Dial, 1995). Evidence of individual-specific flight strategies can also be found outside of experimental manipulation of loads. For example, there are individual differences in the control of body stabilization in sugar gliders (Bishop, 2007) and also in the mechanisms of turning in Southern flying squirrels (Bishop and Brim-DeForest, 2008). Although biologists have acknowledged the importance of individual variation on physiological, ecological, and evolutionary studies (see Hayes and Jenkins, 1997 for a review), it remains largely neglected in the study of flight biomechanics.

The use of individual strategies by bats in our study resembles the concept of functionally equivalent systems (Koehl, 1996). Functionally equivalent systems are, in essence, redundant systems that exhibit a pattern in which multiple combinations of underlying parts can give rise to emergent traits with similar mechanical, physiological, or performance values. Redundancy is widespread in biological systems. For example, almost any genotype-phenotype relationship implies a redundant (or many-to-one) mapping of genotype to phenotype (Stadler et al., 2001). Such redundancy has been described in biomechanical systems as well. At the muscle level, similar performance can be produced by diverse muscle architectures, with different combinations of muscle fiber lengths, fiber orientations, and specific tensions (Powell et al., 1984). At the whole-organism level, morphologically different species can produce similar levels of biomechanical performance (e.g., Toro et al., 2004; Alfaro et al., 2005; Wainwright et al.,

2005; Collar and Wainwright, 2006; Wainwright, 2007). Similarly, our results suggest that the mechanisms of generation of aerodynamic force can also be considered redundant and therefore subject to many-to-one-mapping. Such redundancy allows structural changes to be functionally neutral and therefore can potentially generate a non-linear response between a functional response and the underlying structural changes (Alfaro et al., 2005). If individual differences in kinematic strategies, such as those we observed in bats experiencing naturalistic loading, were found to be widespread in flying animals, studies of individual variability and how differences in kinematics map onto a kinematic-performance relationship might shed light on the underlying mechanisms and level of control involved in aerodynamic force generation and control of flight performance.

List of symbols

ANCOVA	analysis of covariance
CoM	center of mass
C_{vf}	vertical force coefficient
DLT	direct linear transformation
F_v	vertical component of aerodynamic force
TQT	Tsutakawa's quick test

Acknowledgments

All experiments were conducted at the Concord Field Station (CFS) at Harvard University, and we express our thanks to the CFS staff, especially Andy Biewener for allowing us the use of the facilities, and Pedro Ramírez for taking care of the bats. Bats were provided through the generous support of Dr. Allyson Walsh and the Lube Bat Conservancy. We also thank everybody in the Bat Lab for the help provided during the experiments and during the analysis of data. This work was supported by the Air Force Office of Scientific Research (AFOSR), the NSF-ITR program, and the Bushnell Foundation.

References

- Aldridge, H. D. J. N.** (1986). Kinematics and aerodynamics of the greater horseshoe bat, *Rhinolophus ferrumequinum*, in horizontal flight at various speeds. *J. Exp. Biol.* **126**, 479-497.
- Alfaro, M. E., Bolnick, D. I. and Wainwright, P. C.** (2005). Evolutionary consequences of many-to-one mapping of jaw morphology to mechanics in labrid fishes. *Am. Nat.* **165**, E140-E154.
- Altshuler, D. L.** (2006). Flight performance and competitive displacement of hummingbirds across elevational gradients. *Am. Nat.* **167**, 216-229.
- Altshuler, D. L. and Dudley, R.** (2003). Kinematics of hovering hummingbird flight along simulated and natural elevational gradients. *J. Exp. Biol.* **206**, 3139-3147.
- Altshuler, D. L., Dudley, R. and McGuire, J. A.** (2004). Resolution of a paradox: Hummingbird flight at high elevation does not come without a cost. *Proc. Natl. Acad. Sci. USA* **101**, 17731-17736.
- Barclay, R. M. R. and Harder, L. D.** (2003). Life histories of bats: life in the slow lane. In *Bat ecology* (eds. T. H. Kunz and M. B. Fenton), pp. 209-253. Chicago: The University of Chicago Press.

- Beasley, L. J., Pelz, K. M. and Zucker, I.** (1984). Circannual rhythms of body weight in pallid bats. *Am. J. Physiol.* **246**, R955-R958.
- Biewener, A. A. and Dial, K. P.** (1995). *In vivo* strain in the humerus of pigeons (*Columba livia*) during flight. *J. Morph.* **225**, 61-75.
- Bishop, K. L.** (2007). Aerodynamic force generation, performance and control of body orientation during gliding in sugar gliders (*Petaurus breviceps*). *J. Exp. Biol.* **210**, 2593-2606.
- Bishop, K. L. and Brim-DeForest, W.** (2008). Kinematics of turning maneuvers in the Southern flying squirrel, *Glaucomys volans*. *J. Exp. Zool.* **309A**, 225-242.
- Bullen, R. D. and McKenzie, N. L.** (2002). Scaling bat wingbeat frequency and amplitude. *J. Exp. Biol.* **205**, 2615-2626.
- Chai, P., Chen, J. S. C. and Dudley, R.** (1997). Transient hovering performance of hummingbirds under conditions of maximal loading. *J. Exp. Biol.* **200**, 921-929.
- Chai, P. and Dudley, R.** (1996). Limits to flight energetics of hummingbirds hovering in hypodense and hypoxic gas mixtures. *J. Exp. Biol.* **199**, 2285-2295.
- Chai, P. and Dudley, R.** (1999). Maximum flight performance of hummingbirds: Capacities, constraints, and trade-offs. *Am. Nat.* **153**, 398-411.
- Chai, P. and Millard, P.** (1997). Flight and size constraints: hovering performance of large hummingbirds under maximal loading. *J. Exp. Biol.* **200**, 2757-2763.
- Collar, D. C. and Wainwright, P. C.** (2006). Discordance between morphological and mechanical diversity in the feeding mechanism of centrarchid fishes. *Evolution* **60**, 2575-2584.
- Crenshaw, H. C., Ciampaglio, C. N. and McHenry, M.** (2000). Analysis of the three-dimensional trajectories of organisms: estimates of velocity, curvature and torsion from positional information. *J. Exp. Biol.* **203**, 961-982.
- Dial, K. P. and Biewener, A. A.** (1993). Pectoralis muscle force and power output during different modes of flight in pigeons (*Columba livia*). *J. Exp. Biol.* **176**, 31-54.
- Dudley, R. and Chai, P.** (1996). Animal flight mechanics in physically variable gas mixtures. *J. Exp. Biol.* **199**, 1881-1885.
- Dudley, R. and Winter, Y.** (2002). Hovering flight mechanics of neotropical flower bats (Phyllostomidae: Glossophaginae) in normodense and hypodense gas mixtures. *J. Exp. Biol.* **205**, 3669-3677.

- Funakoshi, K. and Uchida, T. A.** (1981). Feeding activity during breeding season and postnatal growth in the Namie's Frosted bat *Vespertilio superans superans*. *Jap. J. Ecol.* **31**, 67-77.
- Hambly, C., Harper, E. J. and Speakman, J. R.** (2004). The energy cost of loaded flight is substantially lower than expected due to alterations in flight kinematics. *J. Exp. Biol.* **207**, 3969-3976.
- Harrison, J. F. and Roberts, S. P.** (2000). Flight respiration and energetics. *Annu. Rev. Physiol.* **62**, 179-205.
- Hatze, H.** (1988). High-precision three-dimensional photogrammetric calibration and object space reconstruction using a modified DLT-approach. *J. Biomech.* **21**, 533-538.
- Hayes, J. P. and Jenkins, S. H.** (1997). Individual variation in mammals. *J. Mammal.* **78**, 274-293.
- Hedrick, T. L., Tobalske, B. W. and Biewener, A. A.** (2002). Estimates of circulation and gait change based on a three-dimensional kinematic analysis of flight in cockatiels (*Nymphicus hollandicus*) and ringed turtle-doves (*Streptopelia risotia*). *J. Exp. Biol.* **205**, 1389-1409.
- Hill, A. V.** (1950). The dimensions of animals and their muscular dynamics. *Sci. Prog.* **38**, 209-230.
- Hughes, P. M. and Rayner, J. M. V.** (1991). Addition of artificial loads to brown long-eared bats *Plecotus auritus* (Chiroptera: Vespertilionidae): handicapping flight performance. *J. Exp. Biol.* **161**, 285-298.
- Iriarte-Díaz, J., Bozinovic, F. and Vásquez, R. A.** (2006). What explains the trot-gallop transition in small mammals? *J. Exp. Biol.* **209**, 4061-4066.
- Jones, C.** (1972). Comparative ecology of three pteropodid bats in Rio Muni, West Africa. *J. Zool.* **167**, 353-370.
- Jones, G.** (1986). Sexual chases in sand martins (*Riparia riparia*): cues for males to increase their reproductive success. *Behav. Ecol. Sociobiol.* **19**, 179-185.
- Koehl, M. A. R.** (1996). When does morphology matter? *Annu. Rev. Ecol. Syst.* **27**, 501-542.
- Kunz, T. H., Wrazen, J. A. and Burnett, C. D.** (1998). Changes in body mass and fat reserves in pre-hibernating little brown bats (*Myotis lucifugus*). *Ecoscience* **5**, 8-17.
- Kurta, A. and Kunz, T. H.** (1987). Size of bats at birth and maternal investment during pregnancy. *Symp. Zool. Soc. Lond.* **57**, 79-106.

- Kvist, A., Lindström, Å., Green, M., Piersma, T. and Visser, G. H.** (2001). Carrying large fuel loads during sustained bird flight is cheaper than expected. *Nature* **413**, 730-732.
- Norberg, U. M.** (1976). Aerodynamics, kinematics, and energetics of horizontal flapping flight in the long-eared bat *Plecotus auritus*. *J. Exp. Biol.* **65**, 179-212.
- Norberg, U. M.** (1990). Vertebrate flight. Berlin: Springer-Verlag.
- Norberg, U. M.** (1995). How a long tail and changes in mass and wing shape affect the cost for flight in animals. *Funct. Ecol.* **9**, 48-54.
- Norberg, U. M. and Rayner, J. M. V.** (1987). Ecological morphology and flight in bats (Mammalia; Chiroptera): wing adaptations, flight performance, foraging strategy and echolocation. *Philos. Trans. R. Soc. B* **316**, 335-427.
- Nudds, R. L. and Bryant, D. M.** (2002). Consequences of load carrying by birds during short flights are found to be behavioral and not energetic. *Am. J. Physiol.* **283**, R249-R256.
- Pennycuik, C. J.** (1989). Bird flight performance: a practical calculation manual: Oxford University Press.
- Powell, P. L., Roy, R. R., Kanim, P., Bello, M. A. and Edgerton, V. R.** (1984). Predictability of skeletal muscle tension from architectural determinations in guinea pig hindlimbs. *J. Appl. Physiol.* **57**, 1715-1721.
- Speakman, J. R. and Racey, P. A.** (1987). The energetics of pregnancy and lactation in brown long-eared bats (*Plecotus auritus*). In *Recent advances in the study of bats* (eds. M. B. Fenton P. A. Racey and J. M. V. Rayner), pp. 367-393. Cambridge: Cambridge University Press.
- Stadler, B. M. R., Stadler, P. F., Wagner, G. P. and Fontana, W.** (2001). The topology of the possible: formal spaces underlying patterns of evolutionary change. *J. Theor. Biol.* **213**, 241-274.
- Swartz, S. M.** (1997). Allometric patterning in the limb skeleton of bats: implications for the mechanics and energetics of powered flight. *J. Morph.* **234**, 277-294.
- Swartz, S. M.** (1998). Skin and bones: functional, architectural, and mechanical differentiation in the bat wing. In *Bat: biology and conservation* (eds. T. H. Kunz and P. A. Racey), pp. 109-126. Washington: Smithsonian Institution Press.
- Swartz, S. M., Bishop, K. L. and Ismael-Aguirre, M.-F.** (2005). Dynamic complexity of wing form in bats: implications for flight performance. In *Functional and evolutionary ecology of bats* (eds. Z. Akbar G. McCracken and T. H. Kunz), pp. 110-130. Oxford: Oxford University Press.

- Swartz, S. M., Groves, M. D., Kim, H. D. and Walsh, W. R.** (1996). Mechanical properties of bat wing membrane skin. *J. Zool.* **239**, 357-378.
- Thollessen, M. and Norberg, U. M.** (1991). Moments of inertia of bat wings and body. *J. Exp. Biol.* **158**, 19-35.
- Toro, E., Herrel, A. and Irschick, D.** (2004). The evolution of jumping performance in Caribbean *Anolis* lizards: solutions to biomechanical trade-offs. *Am. Nat.* **163**, 844-856.
- Tsutakawa, R. K. and Hewett, J. E.** (1977). Quick test for comparing two populations with bivariate data. *Biometrics* **33**, 215-219.
- Usherwood, J. R. and Ellington, C. P.** (2002). The aerodynamics of revolving wings II. Propeller force coefficients from mayfly to quail. *J. Exp. Biol.* **205**, 1565-1576.
- Videler, J. J., Groenewegen, A., Gnodde, M. and Vossebelt, G.** (1988a). Indoor flight experiments with trained kestrels: II. the effect of added weight on flapping flight kinematics. *J. Exp. Biol.* **134**, 185-199.
- Videler, J. J., Vossebelt, G., Gnodde, M. and Groenewegen, A.** (1988b). Indoor flight experiments with trained kestrels: I. flight strategies in still air with and without added weight. *J. Exp. Biol.* **134**, 173-183.
- Wainwright, P. C.** (2007). Functional versus morphological diversity in macroevolution. *Annu. Rev. Ecol. Evol. Syst.* **38**, 381-401.
- Wainwright, P. C., Alfaro, M. E., Bolnick, D. I. and Hulsey, C. D.** (2005). Many-to-one mapping of form to function: a general principle in organismal design? *Int. Comp. Biol.* **45**, 256-262.
- Wimsatt, W. A.** (1969). Transient behavior, nocturnal activity patterns, and feeding efficiency of vampire bats (*Desmodus rotundus*) under natural conditions. *J. Mammal.* **50**, 233-244.
- Winter, Y.** (1999). Flight speed and body mass of nectar-feeding bats (Glossophaginae) during foraging. *J. Exp. Biol.* **202**, 1917-1930.
- Winter, Y. and von Helversen, O.** (1998). The energy cost of flight: do small bats fly more cheaply than birds? *J. Comp. Physiol. B* **168**, 105-111.
- Zook, J.** (2007). Somatosensory adaptations of flying mammals. In *Evolution of nervous systems: a comprehensive reference. Volume 3: Mammals* (eds. J. H. Kaas and L. Krubitzer), pp. 215-226. Boston: Elsevier Academic Press.
- Zook, J. M. and Fowler, B. C.** (1986). A specialized mechanoreceptor array of the bat wing. *Myotis* **23-24**, 31-36.

Chapter 5

Ecomorphological approach to the study of flight in bats

José Iriarte-Díaz & Sharon M. Swartz

Department of Ecology and Evolutionary Biology, Brown University

Introduction

The relationship between form and function is one of the oldest and most thoroughly investigated areas in biology. In the last 20 years, research in morphology, physiology, and behavior of organisms has produced a significant change in the way we understand organismal design, in terms of its influence on the relationship of an organism and its environment and in the processes that originated such a design. The inherent complexity of this topic has led to an integration of biological disciplines such as biomechanics, physiology, genetics, and ecology that were viewed for a long time as completely independent (Reilly and Wainwright, 1994). In the last few years, a new integration has emerged between biology and engineering, generating an incredibly productive field related to modeling aspects that sometimes are too difficult to measure and/or estimate on real organisms.

The aim of this work is to examine recent advances in the study of the relationship between morphology, behavior, performance, and ecology of bats, focusing on the morphology of the wing with relation to flight performance. We give a general view of ecomorphology as a discipline, and we focus on how researchers have approached the study of bat flight and its relation to bat ecology. In particular, we emphasize topics such as the effect of size on aerodynamics and ecological characteristics; we review some recent advances in compliant wing aerodynamics and their effect on the study of flight in bats; the importance of variation in body mass on flight performance, and in general a call of caution in assuming wing morphology-flight performance connections, recognizing the effect of behavior in modulating this relationship.

What is ecomorphology?

Ecomorphology studies the relationship between functional design of an organism and its environment (Wainwright, 1991, 1994). In particular, it investigates how functional morphology shapes ecological attributes of organisms. Several studies have documented correlations between morphological and ecological patterns (e.g., Karr and James, 1973; Gatz, 1979; Findley and Black, 1983; Miles et al., 1987; Crome and Richards, 1988) but no causal connection of how functional morphology determines aspects of an organism's ecology was made. In the early 80s, Arnold (1983) proposed a method to study the effect of morphology on fitness. A similar approach can be used to study the link between morphology and aspects of an individual's ecology. The main idea is that morphology influences patterns of resource use by setting limits to the performance of key tasks relevant to obtaining resources from the environment. Thus, the process of relating morphology and ecology can be separated in two steps. The first step is the determination of the effect of morphological variation on performance of an ecologically relevant task. This is usually performed through laboratory studies, under controlled conditions, where biomechanical analysis can lead to testable predictions on the performance of a system. As pointed out by Wainwright (1991, p. 681), “the strength of the functional approach lies in the ability to assign causation to otherwise correlative relationships between specific design features and observed performance, based on independent functional analyses”.

The second step is to determine what has been called ‘ecological performance’ (Irschick and Garland, 2001), which is the actual performance employed by organisms in natural conditions from field studies on natural populations. Several studies have

emphasized the importance of measuring ecological performance when inferring the ecological consequences of morphological variability (Garland and Carter, 1994; Garland and Losos, 1994; Reilly and Wainwright, 1994; Irschick and Garland, 2001; Irschick, 2002; Irschick et al., 2005; Irschick et al., 2006; Irschick et al., 2007; Irschick et al., 2008) but there has been remarkably little work done on this topic nonetheless. In part, this is due to the common assumption that behavior is not a substantial confounding factor when relating morphology and performance (Irschick, 2002). A growing body of evidence, however, suggests that behavioral modification of the morphology-performance axis may be substantial, with many organisms exhibiting behaviors in natural conditions that are not observed in the laboratory, and therefore giving different levels of performance (see Irschick and Garland, 2001 for a review).

Ecomorphology of the flight of bats:

wing shape, flight performance and ecology

Powered flight and echolocation are the most characteristic features of bats and they have been considered major drivers of the ecological success of this group. As of 2005, with 1116 species in 202 genera, bats are the most taxonomically diverse mammal group after rodents comprising more than 20% of extant mammals, and with worldwide distribution, covering all continents except Antarctica (Simmons, 2005b, a).

The first studies that focused on the relationship between morphology and ecological aspects of bats were comparisons of the diversity of external morphological characters of bat species among communities (e.g., McNab, 1971; Fenton, 1972; Findley, 1976; Findley and Black, 1983; McKenzie and Rolfe, 1986). These studies were

correlational in essence, looking for patterns of interrelationship between morphology and ecology. The idea behind these studies was that morphological diversity would define the use of resources and therefore would be reflected in their ecological diversity. Thus, the link between these aspects corresponds to the performance of a particular morphology in a particular environment. Several performance aspects have been evaluated, in particular foraging and flight abilities. Here, we will focus on the relationship between external morphology, in particular, wing morphology of bats, and flight abilities.

Many early authors have studied wing morphology of bat species with intention to find a relation with their flight characteristics (e.g., Poole, 1936; Struhsaker, 1961; Hayward and Davis, 1964; Vaughan, 1966; Fenton, 1972; Findley et al., 1972; Lawlor, 1973; Strickler, 1978; Norberg, 1981; Norberg and Rayner, 1987). The development of mathematical and aerodynamic models of animal flight that explored the relationship between wing shape, aerodynamics, and flight patterns (Pennycuick, 1968, 1971a, 1975; Rayner, 1979a, b, c) gave the study of the relationship of wing morphology and ecology a strong starting point by providing a mechanistic relationship between wing morphology and flight performance. These articles highlighted the importance of the shape, measured by the aspect ratio (AR) and relative size of the wing, measure by the wing loading (WL), on flight performance. AR is defined as the ratio between half wingspan and mean cord of the wing and describes the slenderness of the wing. Thus, low AR wings correspond to broad wings. In aircraft engineering, AR is usually considered a measure of flight efficiency. During flight, circulation is produced around the wing producing lift. At the wingtip, this circulation is shed as a wingtip vortex that generates induced drag. An

efficient wing (i.e., high AR), is capable of producing high amount of lift with respect to the amount of induced drag generated by the wingtip vortex. Wing loading, defined as the ratio between the surface area of the wing and the weight of the organism, is a measure of the relative size of the wing and represents the amount of weight that an airfoil has to support in air. During flight, aerodynamic pressure over the wing must equal WL , and because aerodynamic pressure varies as V^2 , then V is proportional to $WL^{-0.5}$. Therefore, low WL would allow slower flights than wings with higher WL . This provided researchers with a tool to make testable predictions about flight behavior and its effect on habitat use and foraging behavior.

During the 80's, a series of articles defined the growing discipline of ecomorphological studies of bats by summarizing the results derived from aerodynamic models and the observed differences in habitat use and foraging behavior in bats (Norberg, 1981; Norberg, 1986; Norberg and Rayner, 1987). In a seminal paper, Norberg and Rayner (1987) employed a principal component analysis approach to investigate wing shapes of 215 bat species from 16 families to obtain mass-independent indices for wing loading (second component) and aspect ratio (third component) to clarify the functional basis of the ecomorphological correlations in bats. Based on the idea that flight is an energetically expensive mode of locomotion (e.g., Norberg, 1990), Norberg and Rayner assume that there must be a strong selection for minimizing these costs. Therefore, natural selection would favor wing designs that minimize the work needed for flight in the manner and at the speeds optimal for the animal's ecology (Norberg and Rayner, 1987; Norberg, 1994). A bat occupying a certain ecological 'space' is expected to have a wing design adapted for that particular role. Thus, the variation in wings

morphology is expected to be correlated with different flight modes and speeds (Norberg, 1994). In the analysis, species for which flight and/or behavior patterns had been documented were placed into four quadrants that characterized wing shape whose aerodynamic properties could be predicted based on fixed-wing aerodynamic theory (Fig. 1). For example, species in the low wing loading/low aspect ratio quadrant would be characterized as species with slow, maneuverable flight able to navigate within clutter, while species inside the high wing loading/high aspect ratio quadrant would be

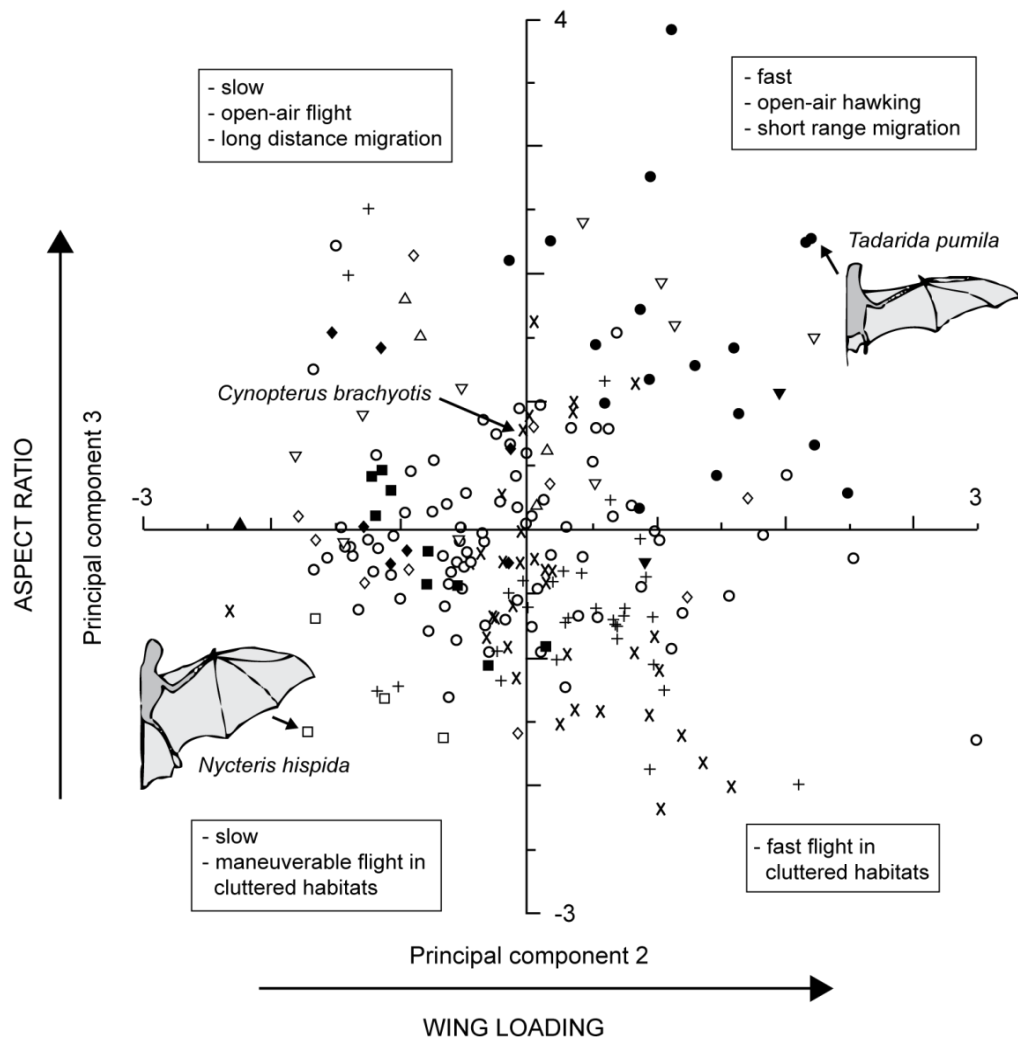


Fig. 1. Scatter plot of the second and third principal components of the wing morphology in bats, identified as measures of wing loading and aspect ratio, respectively. Symbols correspond to different bat families. Modified from Norberg and Rayner (1987).

characterized as fast fliers in open areas (Norberg and Rayner, 1987). This study (Norberg and Rayner, 1987), in concert with similar studies (Norberg, 1987, 1990, 1994), provided bat researchers with an ecomorphological framework, based on predictions from fixed-wing aerodynamic analyses, in which to analyze and interpret differences in wing morphology and behavior among bats species observed in the field. “From this analysis, flight style hypotheses have been generated assuming that if only wing parameters are known for a bat (i.e., body mass, wing span, and wing area), the predominant flight performance can usually be predicted” (Norberg, 1994, p. 216).

We believe it is important to highlight some critical points with respect the use of ecomorphological predictions on the ecology of bats, in particular related to use of space and species distribution in natural communities.

The effect of body size

The second and third component used to describe species’ wing shape and size in Norberg and Rayner’s (1987) analysis explained 1.8 and 0.8% of the overall variation, respectively. The authors argued that even though the wing loading and aspect ratio component were statistically unimportant, they reflect morphological deviations from the average bat wing shape that will be subjected to strong selective pressures. The first component, interpreted as a measure of overall body size, accounted for 97.4% of the total variation indicating that wing morphology has a very strong dependence on body mass. Thus, any analysis based on size-corrected wing shape parameters is going to ignore a huge portion of the variability present in bat communities.

Size is probably the most important factor that determines the morphology and physiology of organisms, and therefore, it will likely have a strong influence in the way organisms interact with their environment. Although the original correlations reported wing morphology and ecological characteristics in bats were conducted on mass-corrected wing shape parameters, several studies have studied the effect of wing morphology using uncorrected measurements (Crome and Richards, 1988; Hodgkison et al., 2004; Moreno et al., 2006; Thabah et al., 2007; Zhang et al., 2007). Therefore, differences in community structuring found in these studies cannot be explained solely by differences in wing morphology but in combination with differences in overall body size. The relative importance of body size and wing shape in determining flight performance and in shaping bats' ecological niches is still poorly understood.

Aerodynamic of compliant membranes

The functional relationship between wing morphology and flight abilities described above relies heavily on aerodynamic models of fixed wings (e.g., Norberg, 1990). For example, quoting from an introductory chapter about the history of ecomorphology and methodological approaches: "Thus, our belief that long, slender wings of some bats species cause their relatively poor hovering performance is rooted in our confidence in the aerodynamic theory that underlies the interpretation of wing design." (Wainwright, 1994, p. 45). Although aerodynamic models are at the core of the ecomorphological approach to bat flight, providing the functional link between wing morphology and flight abilities, little work has been done to test how well fixed-wing aerodynamics describes the aerodynamic of bats during flight.

The aerodynamics and mechanics of flight of bats has received far less attention than they have for insects and birds. Advances in bird and insect aerodynamics, however, cannot necessarily be extrapolated to bats, as bats present unique morphological and flight characteristics that most likely will influence the way that wing shape will affect their aerodynamic performance. For example, recent studies investigating the wake left by flying bats have found that they produce complex wake structures, different from birds (Tian et al., 2006; Hedenström et al., 2007), and that some species employ leading-edge vortex mechanisms to increase lift generation, producing up to 40% of the necessary lift during slow flight (Muijres et al., 2008). Bats fly at Reynolds numbers (Re) ranging approximately from 8×10^3 for small bats to 10^5 in large bats. Re is a measure of the ratio of inertial forces to viscous forces, and the Re employed by bats is considered to be a transitional physics range, between the viscous-dominated, low Re (typical of insects) and the inertia-dominated, high Re , typical of large birds and airplanes (Shyy et al., 1999). At this range of Re , flow over the wings is characterized by laminar boundary layer separation, transition, and low lift-to-drag ratio, and basic parameters such as wing loading, aspect ratio, camber, and angle of attack can influence aerodynamic force production in dramatically different ways than in high Re flows (Shyy et al., 1999; Lian et al., 2003). Despite this, bats show energetically efficient flight performance with respect to insects and birds of similar size (Winter et al., 1993; Winter, 1998; Voigt and Winter, 1999) and high levels of maneuverability (Aldridge, 1987; Tian et al., 2006; Iriarte-Díaz and Swartz, in review). The successful flight performance of bats in such challenging flight regime is partly due to significant structural differences to insects and birds, such as more than a dozen partially independently controlled joints in the wing,

bones that deform adaptively during different portions of the wingbeat cycle (Swartz et al., 2005; Swartz et al., 2007), a compliant wing membrane which is highly anisotropic with adjustable stiffness (Swartz et al., 1996; Swartz, 1998), and sensory organs distributed along the wing believed to provide information about flow over the wing membrane surface (Zook and Fowler, 1986; Zook, 2007).

The membranous nature of the wings of bats is a feature likely to have major effect on the aerodynamic performance. Although virtually unexplored in the animal flight literature (but see Swartz et al., 2007), there has been a growing interest in engineering and fluid dynamics circles on the aerodynamic properties of compliant membranes at the range of Re at which bats perform (e.g., Shyy et al., 1999; Ho et al., 2003; Lian et al., 2003; Song et al., in press). Both experimental and theoretical approaches indicate that flexible airfoils, such as those observed in bat wings, facilitate passive shape adaptation to flow unsteadiness, which results in delayed stall, higher lift coefficients, and less severe decrease in lift at the onset of stall with respect to rigid airfoils (Shyy et al., 1999; Ho et al., 2003; Song et al., in press). However, the improved aerodynamic properties of compliant wings in comparison to rigid ones will depend on the flow characteristics. The deformation of a wing, and consequently, its aerodynamic performance will depend on time-varying variables such as dynamic pressure and local airflow velocities. An experimental study of the aerodynamic properties of airfoils with different levels of flexibility at different flow conditions suggests that modulation of the flexibility could improve the aeroelastic characteristics of the wing and ultimately flight performance (Shyy et al., 1997). Bat wings structural design may be ideally suited in this respect. Wing membrane tension can be controlled by the flexion/extension of the elbow

and wrist joints and the abduction/adduction of the digits. In addition, bats have intrinsic chordwise wing muscles, the *plagiopatagiales mm.*, which have long been assumed to have a role in the regulating the stiffness of the membrane (Strickler, 1978; Norberg, 1990; Swartz et al., 2005; Swartz et al., 2007). The relative importance of wing bone configuration and the intrinsic muscles in the control of the mechanical properties of the wing membrane during flight is still poorly understood and remain challenges for future investigations.

The effect of behavior on flight performance

Traditional ecomorphological analyses of bat flight do not address the fact that flight performance is, per se, a behavioral trait. In the original definition of the ecomorphological approach, performance represents the mechanistic link between organismal design and the ecological and evolutionary consequences of design. Performance can be divided in two levels: ‘potential’ and ‘realized’ performance (Reilly and Wainwright, 1994). Potential performance represents the maximum measured range of performance of an organisms and it can be used to predict potential limitations of the organisms in a particular environment. Alternatively, realized performance corresponds to the ecological performance previously mentioned, i.e., the performance that an organism actually uses in natural conditions, which at the end determines the interaction of an organism with its environment. As a consequence, our ability to link the structural design and the ecological characteristics of an organism will depend of how well potential and realized performance reflect each other. While potential performance is determined by the structural design of an organism, realized or ecological performance is

a behavioral function and it will vary depending of ecological circumstances such as presence of predators, prey availability, environment structural complexity among others. The effect of the behavioral factors can significantly influence the relationship between morphology and performance (Lauder and Reilly, 1996), and may also determine levels of performance used by animals (Losos et al., 2002). For example, studies of locomotor performance in lizards have demonstrated ‘locomotor compensation’, where species with low intrinsic performance capacities compensate in nature by moving close to their maximal capacities, while species with high performing capacities use consistently sub-maximal speeds (Irschick et al., 2005). Assuming that aerodynamic theory can accurately predict the aerodynamics of the flight of bats, the predictions derived from these models can be considered as bats’ potential performance. To date, no information exists on the how much of this potential performance bats actually use in nature, or the effect of differences across species (or individuals) in behavioral performance when comparing flight abilities. It has been well documented, however, that bats are often opportunistic in their feeding behavior and habitat use (e.g., Fenton, 1982; Norberg and Rayner, 1987; Altringham, 1996; Campbell et al., 2007), suggesting a degree of flexibility in their ecological performance.

Case studies

Maneuverability and turning abilities

For any flying animal, turns are produced by the generation of a centripetal force that will move the body through the turn. From physical principles, the centripetal force (F_c) produced by a body in motion of mass M_b in a turn of radius r is

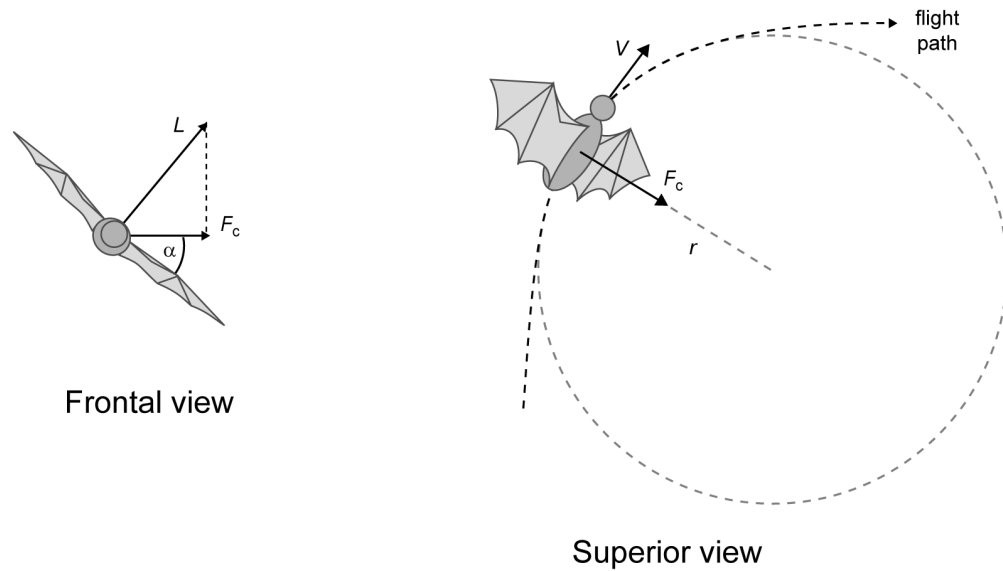


Fig. 2. Schematic of a typical banked turn. By rolling the body into a bank, the lift vector (L) is oriented toward to the turn generating a centripetal force, $F_c = L \sin(\alpha)$, that, for a given flight speed V , will produce a turn of radius r .

$$F_c = \frac{M_b V^2}{r} \quad (1)$$

where V is forward speed (Fig. 2). Therefore, the turning radius of an organism will be

$$r = \frac{M_b V^2}{F_c}. \quad (2)$$

Thus, the more maneuverable bats would have smaller r values that can be produced by reducing speed, having low body mass, or increasing the centripetal force. The theory of turning flight has been extensively discussed in the literature (e.g., Pennycuick, 1971b; Norberg, 1990; Thollesson and Norberg, 1991; Norberg, 1994) based on the assumption that organisms turn by rolling their bodies into a bank, which is similar to what airplanes do. By banking through an angle α , a bat reorients its lift (L) toward the center of the turn, so that now the centripetal force is given by $L \sin(\alpha)$ (Fig. 2). The turning radius (r) is

$$r = \left(\frac{M_b \mathbf{g}}{A_w} \right) \left(\frac{2}{\mathbf{g} \rho C_L \sin \alpha} \right) = WL \left(\frac{2}{\mathbf{g} \rho C_L \sin \alpha} \right) \quad (3)$$

where A_w is the wing area, \mathbf{g} is the acceleration of gravity, ρ is the air density, and C_L is the lift coefficient. Thus, at any given lift coefficient and bank angle, the turning radius will be smaller in animals with lower wing loading. This equation predicts the performance during gliding turns but that might be not the standard way of turning. For example, among six species of British bats, all but one species employed powered turns (Aldridge, 1987). Furthermore, one species, *Rhinolophus ferrumequinum* employed a different method of turning, achieving much tighter turns than predicted based on morphology alone (Aldridge, 1987). Recent findings have shown that predictions might not be completely accurate even during gliding flight as well. Swifts can morph their wings during different task to improve performance by effectively modifying wing area and lift coefficient (Lentink et al., 2007). It is increasingly evident that both wing morphology and flight kinematics are important determinants of maneuverability, although, to date, we have little information of their relative importance. The only study that evaluated wing kinematics and body rotations during turns in bats suggests, however, that turning performance is highly dependent on flight kinematics (Chapter 1, this thesis). Fruit bats performing 90-degree turns in laboratory conditions showed yaw, pitch, and roll rotations during upstroke that orient the body towards the turn in such a way that during downstroke, the centripetal have both lift and thrust components, allowing bats to perform tighter turns than predicted by morphology alone (Chapter 1, this thesis). In fact, based on morphological characteristics, *C. brachyotis* would be considered to have poor maneuvering abilities (Norberg and Rayner, 1987), but they can actually perform a 180-degree turn on the spot in just three wingbeats (Tian et al., 2006).

Turning performance and maneuvering abilities should be studied experimentally by designing measurable tasks. Flight performance through an obstacle course is one useful experimental metric of maneuverability that can be performed in the laboratory or in enclosures in the field, and that does not require sophisticated of equipment such as high speed cameras. Among several species of insectivorous British bats, those able to negotiate the most tightly arranged array of obstacles also foraged in the most cluttered areas (Aldridge, 1986b). Similarly, in several species of African microchiropterans, wing loading and body mass were negatively correlated with maneuverability measured in an obstacle course, and foraging in densely cluttered patches of vegetation was positively related to maneuverability (Aldridge and Rautenbach, 1987). Additionally, Neotropical phyllostomids showed that morphological variables associated to body size, such as mass, forearm length, and wing span, were negatively correlated with obstacle course maneuverability, while variables associated to the ability to camber the wings were positively correlated with maneuverability (Stockwell, 2001).

An alternative setup to measure maneuvering performance is to train bats to fly through a flight corridor and to suddenly place a barrier to make them perform a 180-degree turn (e.g., Aldridge, 1987). This kind of setup allows the investigator to control the place where the maneuver will occur and permits to zoom in with cameras and to measure wing and body kinematic parameters.

In these experimental designs, however, motivation can be a significant factor, and may profoundly influence level of performance. Food rewards can be used to elicit better performance. For example, in a study of echolocation behavior in three-dimensionally complex environments, the microbat *Eptesicus fuscus*, was trained to

capture a mealworm tethered at a variable distance from background vegetation (Moss et al., 2006). High speed video cameras synchronized with echolocation call recordings allowed evaluation of changes in echolocation parameters with respect to distance to prey and to clutter. A simple modification of this experimental setup could be employed to assess, in laboratory or semi-natural conditions, flight maneuvers employed by bats while capturing prey under controlled levels of clutter. Similar designs, such as an array of strings that bats must traverse to reach food, have been used in field experiments to estimate the effect of different amount of clutter on bat flight activity (Mackey and Barclay, 1989; Brigham et al., 1997; Sleep and Brigham, 2003).

Natural and experimental variation in body mass

A fruitful way to probe the limits of flight performance is to evaluate the effect of variation in body mass, and hence wing loading, on the flight kinematics and performance capabilities of bats. Body mass changes substantially on a daily and seasonal basis due to fluctuations in stomach contents, transport of food and young, and percentage of body fat due to hibernation or lactation. The magnitude of the changes in mass observed in nature suggests that bats have a great capacity to carry loads. For example, the maximum amount of loads that bats can carry while taking off from the ground varies from 9.5% of body mass in *Tadarida brasiliensis* to 73% of body mass in *Plecotus townsendi* (Davis and Cockrum, 1964). For a any flapping flier, during level flight at constant speed, any increase in body mass will require some change in wing kinematics to generate lift to compensate for the added weight. In classic aerodynamic

theory, lift, L , produced by a wing is going to be a function of wing area, A_w , coefficient of lift, C_L , and the speed of airflow over the wing, V :

$$L = \frac{1}{2} \rho A_w C_L V^2. \quad (4)$$

To increase lift in response to added load, a bat can adopt one or more of several strategies. It can increase A_w by extending the elbow and/or wrist joints, increase C_L by changing wing shape parameters such as angle of attack or wing camber, or increase the airflow speed over the wing by either flying faster or by flapping the wings faster, or a combination of these strategies. Even though lift can be modulated in multiple ways in response to loading, predictions based on aerodynamic theory have focused solely on changes in wingbeat frequency and flight speed (e.g., Norberg and Rayner, 1987; Norberg, 1995).

The strength of this hypothesis has been tested in several microchiropteran bat species. In both *Plecotus auritus* carrying artificial loads of up 46% of body mass, and *Pipistrellus pipistrellus* during pregnancy and lactation, in agreement with aerodynamic theory predictions, wingbeat frequency increased with respect to the unloaded condition, but contrary to expectations, flight speed also decreased (Hughes and Rayner, 1991, 1993). In contrast, several species of nectarivorous glossophagine bats flying in large flight corridors, have shown an increase in flight speed with an increase in body mass, although wingbeat frequency was not measured (Winter, 1999). These bats also showed great variability among individuals in preferred flight speeds, and in their response to loading (Winter, 1999), suggesting a degree of flexibility in flight kinematics and modulation of aerodynamic force.

Flying in conditions of reduced air density is similar to flying carrying loads. In an experiment in which air density was gradually reduced while maintaining oxygen availability, Dudley and Winter (2002) investigated hovering kinematics of the glossophagine phyllostomid *Leptonycteris curasoae*. In contrast to observations from loading experiments in other species, wingbeat frequency changed little, but wingbeat amplitude increased significantly as air density decreased (Dudley and Winter, 2002). This response is similar to that observed in hovering birds during both load carrying and reduced air density experiments (Chai and Dudley, 1995, 1996; Chai et al., 1996; Dudley and Chai, 1996; Chai et al., 1997; Chai and Dudley, 1999; Altshuler and Dudley, 2003; Altshuler et al., 2004). Constancy in wingbeat frequency in hovering vertebrates might indicate some kind of physiological constraints, or might indicate that flight muscles are tuned to perform at or near a frequency that provides maximum efficiency.

In contrast to results from microchiropteran bats in previous studies, fruit bats flying at a range of speeds respond to increase loading in a complex manner with clear variation in kinematic strategies among individuals (Chapter 4, this thesis). For example, some bats increased lift by increasing wingbeat frequency and the length of the downstroke, with minor changes of the shape of the wings. In contrast, another bat showed a very different response, decreasing wingbeat frequency but increasing wing area and the camber of the wing (Chapter 4, this thesis). This variability in response to loading indicates that there is redundancy in kinematic and aerodynamic mechanisms of aerodynamic force generation, and as a consequence, demonstrates that individual bats employ different mechanisms to produce the same aerodynamic results. Kinematic flexibility was also observed in the kinematic modulation in response to speed, where lift

remains constant to balance weight, but thrust varies as a function of speed (Chapter 3, this thesis). In this case, individual bats also employed different combination of kinematic changes as speed increased but the individual differences were not as marked as during load carrying.

Birds also modulate wing kinematics in response to loading, and show some patterns in variation among species and individuals that are reminiscent of the patterns found in bats. Some studies have found that an increase in body mass produced detectable changes in flight performance during escape (Witter et al., 1994; Metcalfe and Ure, 1995; Kullberg et al., 1996; Lee et al., 1996) but in others, no changes have been observed (Kullberg, 1998; Kullberg et al., 1998; Veasey et al., 1998; van der Veen and Lindström, 2000; Macleod, 2006). Interestingly, changes in kinematic strategies with different amount of loading have been described in cockatiels, in which at low levels of loading birds flew slowly without changing wingbeat frequency, but at higher loads (>20% of body mass) birds flew faster and also increased wingbeat frequency (Hambly et al., 2004).

Increased loading is also expected to influence maneuvering abilities. In a simple, glided turn, minimum turning radius is a function of WL (see eqn. 3). Thus, animals carrying loads are expected to decreased maneuverability with respect to unloaded flight because of the increased WL . Despite the theoretical effect of WL on maneuvering capabilities has been extensively discussed in the literature (e.g., Hedenström, 1992; Webb et al., 1992; Norberg, 1995; Stern et al., 1997; McLean and Speakman, 2000), few empirical tests have evaluated how WL affects maneuvering performance. To date, experimental work has found a negative relationship between WL and the ability to

navigate an obstacle course (Aldridge, 1986a, b; Aldridge and Rautenbach, 1987; Aldridge and Brigham, 1988; Stockwell, 2001). This correlation is believed to reflect differences in habitat use among and within species (e.g., McKenzie and Rolfe, 1986; Norberg and Rayner, 1987; Crome and Richards, 1988; Norberg, 1994; Kalcounis and Brigham, 1995; McKenzie et al., 2002), but only few studies have correlated experimentally correlated maneuvering performance and the ability to use cluttered environments (Aldridge, 1986b; Aldridge and Rautenbach, 1987). Differences in maneuverability among species, however, cannot be uncoupled from differences in turning styles, and different turning mechanisms employ wings in different ways, hence it may prove difficult to adequately predict maneuvering performance from morphology alone (Aldridge, 1987; Iriarte-Díaz and Swartz, in review). It is possible or even likely that the performance burden produced by temporary, large-scale external or internal loading may be alleviated by fine-scale adjustments in wing kinematics to enable a species to maintain a necessary level of maneuvering performance. Further study in laboratory-controlled conditions combined with field observations of natural flight performance will be necessary to successfully answer this question.

Conclusions

Studies associating wing morphology with flight patterns, foraging habits, and habitat use (e.g., Aldridge and Rautenbach, 1987; Norberg and Rayner, 1987) have provided researchers with a broad view of the ecomorphology of flight in bats. These studies are extremely useful to generate testable new hypothesis about the function of

morphological traits, about the structuring of communities, and about the evolution of bats. There is much to do yet. New findings on the aerodynamics of bat wings and the effect of behavioral compensation on flight performance indicate that the relationship between wing morphology, flight performance, and ecology of bats is more complex than previously thought. Future studies must expand our understanding of the relative importance of unsteady aerodynamics on flight performance during different locomotory tasks. In the same vein, we expect that integration of laboratory and field studies will be required to be able to answer questions about aerodynamic mechanisms used during natural activities. In the meantime, we hope that new information drawn from detailed kinematic and aerodynamic studies of the flight of bats will help ecologists to consider functionally relevant aspects of bats' morphology and thereby to further improve our knowledge of the use of the natural environment by bats. Conversely, we envision that future studies of bat ecology can help guide functional morphologists to focus on ecologically relevant morphological traits to be studied in detail in the lab.

Many studies have emphasized the importance of interpreting interspecific variation in morphology in the context of well-defined phylogenies (reviewed in Losos and Miles, 1994). Although Norberg and Rayner (1987) cautioned about adaptive interpretations of differences in wing morphology among bats, in practice, many researchers have assumed that observed wing morphologies are adaptations to the environment bats inhabit. Some authors have suggested that is not always necessary to have a phylogeny to produce significant ecomorphological conclusions, and that might be the case with the study of flight in bats, where “interpretations [of the aerodynamic consequences of wing morphology] and their implications for flight performance and

possible habitat and food use can be expected to hold true regardless of the specific evolutionary history of wing design in bats. Physics offers an absolute scale with which to gauge the consequences of wing design.” (Wainwright and Reilly, 1994, p. 7). Even if this were true, the development of new, comprehensive phylogenies (e.g., Teeling et al., 2000; Springer et al., 2001; Jones et al., 2002; Teeling et al., 2002; Teeling et al., 2005) now allows to test hypotheses about the adaptive nature of wing morphology of bats that inhabit different environments.

We believe that advances in kinematics, aerodynamics, phylogenetic history, and ecology of bats are going to produce new insights into the relationship between morphology, behavior, flight performance, and ecology in bats.

References

- Aldridge, H. D. J. N.** (1986a). Manoeuvrability and ecological segregation in the little brown (*Myotis lucifugus*) and Yuma (*M. yumanensis*) bats (Chiroptera: Vespertilionidae). *Can. J. Zool.* **64**, 1878-1882.
- Aldridge, H. D. J. N.** (1986b). Manoeuvrability and ecology in British bats. *Myotis* **23-24**, 157-160.
- Aldridge, H. D. J. N.** (1987). Turning flight of bats. *J. Exp. Biol.* **128**, 419-425.
- Aldridge, H. D. J. N. and Brigham, R. M.** (1988). Load carrying and maneuverability in an insectivorous bat: a test of the 5% "rule" of radio-telemetry. *J. Mammal.* **69**, 379-382.
- Aldridge, H. D. J. N. and Rautenbach, I. L.** (1987). Morphology, echolocation and resource partitioning in insectivorous bats. *J. Anim. Ecol.* **56**, 763-778.
- Altringham, J. D.** (1996). Bats: biology and behaviour. New York: Oxford University Press.
- Altshuler, D. L. and Dudley, R.** (2003). Kinematics of hovering hummingbird flight along simulated and natural elevational gradients. *J. Exp. Biol.* **206**, 3139-3147.

- Altshuler, D. L., Dudley, R. and McGuire, J. A.** (2004). Resolution of a paradox: Hummingbird flight at high elevation does not come without a cost. *Proc. Natl. Acad. Sci. USA* **101**, 17731-17736.
- Arnold, S. J.** (1983). Morphology, performance and fitness. *Amer. Zool.* **23**, 347-361.
- Brigham, R. M., Grindal, S. D., Firman, M. C. and Morissette, J. L.** (1997). The influence of structural clutter on activity patterns of insectivorous bats. *Can. J. Zool.* **75**, 131-136.
- Campbell, P., Schneider, C. J., Zubaid, A., Adnan, A. M. and Kunz, T. H.** (2007). Morphological and ecological correlates of coexistence in Malaysian fruit bats (Chiroptera: Pteropodidae). *J. Mammal.* **88**, 105-118.
- Chai, P., Chen, J. S. C. and Dudley, R.** (1997). Transient hovering performance of hummingbirds under conditions of maximal loading. *J. Exp. Biol.* **200**, 921-929.
- Chai, P. and Dudley, R.** (1995). Limits to vertebrate locomotor energetics suggested by hummingbirds hovering in heliox. *Nature* **377**, 722-725.
- Chai, P. and Dudley, R.** (1996). Limits to flight energetics of hummingbirds hovering in hypodense and hypoxic gas mixtures. *J. Exp. Biol.* **199**, 2285-2295.
- Chai, P. and Dudley, R.** (1999). Maximum flight performance of hummingbirds: capacities, constraints, and trade-offs. *Am. Nat.* **153**, 398-411.
- Chai, P., Harrykisson, R. and Dudley, R.** (1996). Hummingbird hovering performance in hyperoxic heliox: effects of body mass and sex. *J. Exp. Biol.* **199**, 2745-2755.
- Crome, F. H. J. and Richards, G. C.** (1988). Bats and gaps: microchiropteran community structure in a Queensland rain forest. *Ecology* **69**, 1960-1969.
- Davis, R. and Cockrum, E. L.** (1964). Experimentally determined weight lifting capacity in individuals of five species of western bats. *J. Mammal.* **45**, 643-644.
- Dudley, R. and Chai, P.** (1996). Animal flight mechanics in physically variable gas mixtures. *J. Exp. Biol.* **199**, 1881-1885.
- Dudley, R. and Winter, Y.** (2002). Hovering flight mechanics of neotropical flower bats (Phyllostomidae: Glossophaginae) in normodense and hypodense gas mixtures. *J. Exp. Biol.* **205**, 3669-3677.
- Fenton, M. B.** (1972). The structure of aerial feeding bat faunas as indicated by ears and wing elements. *Can. J. Zool.* **50**, 287-296.
- Fenton, M. B.** (1982). Echolocation, insect hearing, and feeding ecology of insectivorous bats. In *Ecology of bats* (ed. T. H. Kunz), pp. 261-285. New York: Plenum Press.

- Findley, J. S.** (1976). The structure of bat communities. *Am. Nat.* **110**, 129-139.
- Findley, J. S. and Black, H.** (1983). Morphological and dietary structuring of a Zambian insectivorous bat community. *Ecology* **64**, 625-630.
- Findley, J. S., Studier, E. H. and Don, E. W.** (1972). Morphologic properties of bat wings. *J. Mammal.* **53**, 429-444.
- Garland, T., Jr. and Carter, P. A.** (1994). Evolutionary physiology. *Annu. Rev. Physiol.* **56**, 579-621.
- Garland, T., Jr. and Losos, J. B.** (1994). Ecological morphology of locomotor performance in squamate reptiles. In *Ecological Morphology: Integrative Organismal Biology* (eds. P. C. Waingright and S. M. Reilly), pp. 240-302. Chicago: The University of Chicago Press.
- Gatz, A. J., Jr.** (1979). Community organization in fishes as indicated by morphological features. *Ecology* **60**, 711-718.
- Hambly, C., Harper, E. J. and Speakman, J. R.** (2004). The energy cost of loaded flight is substantially lower than expected due to alterations in flight kinematics. *J. Exp. Biol.* **207**, 3969-3976.
- Hayward, B. and Davis, R.** (1964). Flight speeds in Western bats. *J. Mammal.* **45**, 236-242.
- Hedenström, A.** (1992). Flight performance in relation to fuel load in birds. *J. Theor. Biol.* **158**, 535-537.
- Hedenström, A., Johansson, L. C., Wolf, M., von Busse, R., Winter, Y. and Spedding, G. R.** (2007). Bat flight generates complex aerodynamic tracks. *Science* **316**, 894-897.
- Ho, S., Nassef, H., Pornsinsirak, N., Tai, Y. C. and Ho, C. M.** (2003). Unsteady aerodynamics and flow control for flapping wing flyers. *Prog. Aerospace Sci.* **39**, 635-681.
- Hodgkison, R., Balding, S. T., Zubaid, A. and Kunz, T. H.** (2004). Habitat structure, wing morphology, and the vertical stratification of Malaysian fruit bats (Megachiroptera : Pteropodidae). *J. Trop. Ecol.* **20**, 667-673.
- Hughes, P. M. and Rayner, J. M. V.** (1991). Addition of artificial loads to brown long-eared bats *Plecotus auritus* (Chiroptera: Vespertilionidae): handicapping flight performance. *J. Exp. Biol.* **161**, 285-298.
- Hughes, P. M. and Rayner, J. M. V.** (1993). The flight of pipistrelle bats *Pipistrellus pipistrellus* during pregnancy and lactation. *J. Zool.* **230**, 541-555.

- Iriarte-Díaz, J. and Swartz, S. M.** (in review). Kinematics of the slow turning maneuvering in the fruit bat *Cynopterus brachyotis*. *J. Exp. Biol.*
- Irschick, D., Bailey, J. K., Schweitzer, J. A., Husak, J. F. and Meyers, J. J.** (2007). New directions for studying selection in nature: studies of performance and communities. *Physiol. Biochem. Zool.* **80**, 557-567.
- Irschick, D. J.** (2002). Evolutionary approaches for studying functional morphology: examples from studies of performance capacity. *Int. Comp. Biol.* **42**, 278-290.
- Irschick, D. J. and Garland, T.** (2001). Integrating function and ecology in studies of adaptation: Investigations of locomotor capacity as a model system. *Annu. Rev. Ecol. Syst.* **32**, 367-396.
- Irschick, D. J., Herrel, A. V., Vanhooydonck, B., Huyghe, K. and Van Damme, R.** (2005). Locomotor compensation creates a mismatch between laboratory and field estimates of escape speed in lizards: A cautionary tale for performance-to-fitness studies. *Evolution* **59**, 1579-1587.
- Irschick, D. J., Meyers, J. J., Husak, J. F. and Le Galliard, J. F.** (2008). How does selection operate on whole-organism functional performance capacities? A review and synthesis. *Evol. Ecol. Res.* **10**, 177-196.
- Irschick, D. J., Ramos, M., Buckley, C., Elstrott, J., Carlisle, E., Lailvaux, S. P., Bloch, N., Herrel, A. and Vanhooydonck, B.** (2006). Are morphology-performance relationships invariant across different seasons? A test with the green anole lizard (*Anolis carolinensis*). *Oikos* **114**, 49-59.
- Jones, K. E., Purvis, A., MacLarnon, A., Bininda-Emonds, O. R. P. and Simmons, N. B.** (2002). A phylogenetic supertree of the bats (Mammalia: Chiroptera). *Biol. Rev.* **77**, 223-259.
- Kalcounis, M. C. and Brigham, R. M.** (1995). Intraspecific variation in wing loading affects habitat use by little brown bats (*Myotis lucifugus*). *Can. J. Zool.* **73**, 89-95.
- Karr, J. R. and James, F. C.** (1973). Ecomorphological configurations and convergent evolution in species and communities. In *Ecology and evolution of communities* (eds. M. L. Cody and J. M. Diamond), pp. 258-291. Cambridge: Belknap Press.
- Kullberg, C.** (1998). Does diurnal variation in body mass affect take-off ability in wintering willow tits? *Anim. Behav.* **56**, 227-233.
- Kullberg, C., Fransson, T. and Jakobsson, S.** (1996). Impaired predator evasion in fat blackcaps (*Sylvia atricapilla*). *Proc. R. Soc. Lond. B* **263**, 1671-1675.
- Kullberg, C., Jakobsson, S. and Fransson, T.** (1998). Predator-induced take-off strategy in great tits (*Parus major*). *Proc. R. Soc. Lond. B* **265**, 1659-1664.

- Lauder, G. V. and Reilly, S. M.** (1996). The mechanistic basis of behavioral evolution: comparative analysis of musculoskeletal function. In *Phylogenies and the comparative method in animal behavior* (ed. E. Martin), pp. 105-137. Oxford: Oxford University Press.
- Lawlor, T. E.** (1973). Aerodynamic characteristics of some Neotropical bats. *J. Mammal.* **54**, 71-78.
- Lee, S. J., Witter, M. S., Cuthill, I. C. and Goldsmith, A. R.** (1996). Reduction in escape performance as a cost of reproduction in gravid starlings, *Sturnus vulgaris*. *Proc. R. Soc. Lond. B* **263**, 619-624.
- Lentink, D., Muller, U. K., Stamhuis, E. J., de Kat, R., van Gestel, W., Veldhuis, L. L. M., Henningson, P., Hedenstrom, A., Videler, J. J. and van Leeuwen, J. L.** (2007). How swifts control their glide performance with morphing wings. *Nature* **446**, 1082-1085.
- Lian, Y., Shyy, W., Viieru, D. and Zhang, B.** (2003). Membrane wing aerodynamics for micro air vehicles. *Prog. Aerospace Sci.* **39**, 425-465.
- Losos, J. B., Creer, D. A. and Schulte, J. A. I.** (2002). Cautionary comments on the measurement of maximum locomotor capabilities. *J. Zool.* **258**, 57-61.
- Losos, J. B. and Miles, D. B.** (1994). Adaptation, constraint, and the comparative method: phylogenetic issues and methods. In *Ecological morphology: integrative organismal biology* (eds. P. C. Wainwright and S. M. Reilly), pp. 60-98. Chicago: The University of Chicago Press.
- Mackey, R. L. and Barclay, R. M. R.** (1989). The influence of physical clutter and noise on the activity of bats over water. *Can. J. Zool.* **67**, 1167-1170.
- Macleod, R.** (2006). Why does diurnal mass change not appear to affect the flight performance of alarmed birds? *Anim. Behav.* **71**, 523-530.
- McKenzie, N. L. and Rolfe, J. K.** (1986). Structure of bat guilds in the Kimberley mangroves, Australia. *J. Anim. Ecol.* **55**, 401-420.
- McKenzie, N. L., Start, A. N. and Bullen, R. D.** (2002). Foraging ecology and organization of a desert bat fauna. *Aust. J. Zool.* **50**, 529-548.
- McLean, J. A. and Speakman, J. R.** (2000). Morphological changes during postnatal growth and reproduction in the brown long-eared bat *Plecotus auritus*: implications for wing loading and predicted flight performance. *J. Nat. Hist.* **34**, 773-791.
- McNab, B. K.** (1971). The structure of tropical bat faunas. *Ecology* **52**, 352-358.

- Metcalf, N. B. and Ure, S. E.** (1995). Diurnal variation in flight performance and hence potential predation risk in small birds. *Proc. R. Soc. Lond. B* **261**, 395-400.
- Miles, D. B., Ricklefs, R. E. and Travis, J.** (1987). Concordance of ecomorphological relationships in three assemblages of passerine birds. *Am. Nat.* **129**, 347-364.
- Moreno, C., Arita, H. and Solis, L.** (2006). Morphological assembly mechanisms in Neotropical bat assemblages and ensembles within a landscape. *Oecologia* **149**, 133-140.
- Moss, C. F., Bohn, K., Gilkenson, H. and Surlykke, A.** (2006). Active Listening for Spatial Orientation in a Complex Auditory Scene. *PLoS Biology* **4**, e79.
- Muijres, F. T., Johansson, L. C., Barfield, R., Wolf, M., Spedding, G. R. and Hedenstrom, A.** (2008). Leading-edge vortex improves lift in slow-flying bats. *Science* **319**, 1250-1253.
- Norberg, U. M.** (1981). Allometry of bat wings and lengs and comparison with bird wing. *Philos. Trans. R. Soc. B* **292**, 359-398.
- Norberg, U. M.** (1986). Evolutionary Convergence in Foraging Niche and Flight Morphology in Insectivorous Aerial-Hawking Birds and Bats. *Ornis Scan.* **17**, 253-260.
- Norberg, U. M.** (1987). Wing form and flight mode in bats. In *Recent advances in the study of bats* (eds. M. B. Fenton P. A. Racey and J. M. V. Rayner), pp. 43-56. Cambridge: Cambridge University Press.
- Norberg, U. M.** (1990). Vertebrate flight. Berlin: Springer-Verlag.
- Norberg, U. M.** (1994). Wing design, flight performance, and habitat use in bats. In *Ecological morphology: integrative organismal biology* (eds. P. C. Wainwright and S. M. Reilly), pp. 205-239. Chicago: University of Chicago Press.
- Norberg, U. M.** (1995). How a long tail and changes in mass and wing shape affect the cost for flight in animals. *Funct. Ecol.* **9**, 48-54.
- Norberg, U. M. and Rayner, J. M. V.** (1987). Ecological morphology and flight in bats (Mammalia; Chiroptera): wing adaptations, flight performance, foraging strategy and echolocation. *Philos. Trans. R. Soc. B* **316**, 335-427.
- Pennycuick, C. J.** (1968). Power requirements for horizontal flight in the pigeon *Columba livia*. *J. Exp. Biol.* **49**, 527-555.
- Pennycuick, C. J.** (1971a). Gliding flight of the dog-faced bat *Rousettus aegyptiacus* observed in a wind tunnel. *J. Exp. Biol.* **55**, 833-845.

- Pennycuik, C. J.** (1971b). Gliding flight of the white-backed vulture *Gyps africanus*. *J. Exp. Biol.* **55**, 13-38.
- Pennycuik, C. J.** (1975). Mechanics of flight. In *Avian Biology*, vol. 5 (eds. D. S. Farner J. R. King and K. C. Parkes), pp. 1-75. New York: Academic Press.
- Poole, E. L.** (1936). Relative wing ratios of bats and birds. *J. Mammal.* **17**, 412-413.
- Rayner, J. M. V.** (1979a). A new approach to animal flight mechanics. *J. Exp. Biol.* **80**, 17-54.
- Rayner, J. M. V.** (1979b). A vortex theory of animal flight. Part 1. The vortex wake of a hovering animal. *J. Fluid Mech.* **91**, 697-730.
- Rayner, J. M. V.** (1979c). A vortex theory of animal flight. Part 2. The forward flight of birds. *J. Fluid Mech.* **91**, 731-763.
- Reilly, S. M. and Wainwright, P. C.** (1994). Conclusion: ecological morphology and the power of integration. In *Ecological Morphology: Integrative Organismal Biology* (eds. P. C. Wainwright and S. M. Reilly), pp. 339-354. Chicago: The University of Chicago Press.
- Shyy, W., Berg, M. and Ljungqvist, D.** (1999). Flapping and flexible wings for biological and micro air vehicles. *Prog. Aerospace Sci.* **35**, 455-505.
- Shyy, W., Jenkins, D. A. and Smith, R. W.** (1997). Study of adaptive shape airfoils at low Reynolds number in oscillatory flow. *AIAA Journal* **35**, 1545-1548.
- Simmons, N. B.** (2005a). Chiroptera. In *The rise of placental mammals* (eds. K. D. Rose and J. D. Archibald), pp. 159-174. Baltimore: John Hopkins University Press.
- Simmons, N. B.** (2005b). Orden Chiroptera. In *Mammals species of the world: a taxonomic and geographic reference* (eds. D. E. Wilson and D. M. Reeder), pp. 312-529. Baltimore: John Hopkins University Press.
- Sleep, D. J. H. and Brigham, R. M.** (2003). An experimental test of clutter tolerance in bats. *J. Mammal.* **84**, 216-224.
- Song, A., Tian, X., Israeli, E., Galvao, R., Bishop, K., Swartz, S. M. and Breuer, K.** (in press). Aeromechanics of membrane wings with implications for animal flight. *AIAA Journal*.
- Springer, M. S., Teeling, E. C., Madsen, O., Stanhope, M. J. and de Jong, W. W.** (2001). Integrated fossil and molecular data to reconstruct bat echolocation. *Proc. Natl. Acad. Sci. USA* **98**, 6241-6246.

- Stern, A. A., Kunz, T. H. and Bhatt, S. S.** (1997). Seasonal wing loading and the ontogeny of flight in *Phyllostomus hastatus* (Chiroptera: Phyllostomidae). *J. Mammal.* **78**, 1199-1209.
- Stockwell, E. F.** (2001). Morphology and flight manoeuvrability in New World leaf-nosed bats (Chiroptera : Phyllostomidae). *J. Zool.* **254**, 505-514.
- Strickler, T. L.** (1978). Allometric relationships among the shoulder muscles in the Chiroptera. *J. Mammal.* **59**, 36-44.
- Struhsaker, T. T.** (1961). Morphological factors regulating flight in bats. *J. Mammal.* **42**, 152-159.
- Swartz, S. M.** (1998). Skin and bones: functional, architectural, and mechanical differentiation in the bat wing. In *Bat: biology and conservation* (eds. T. H. Kunz and P. A. Racey), pp. 109-126. Washington: Smithsonian Institution Press.
- Swartz, S. M., Bishop, K. L. and Ismael-Aguirre, M.-F.** (2005). Dynamic complexity of wing form in bats: implications for flight performance. In *Functional and evolutionary ecology of bats* (eds. Z. Akbar G. McCracken and T. H. Kunz), pp. 110-130. Oxford: Oxford University Press.
- Swartz, S. M., Groves, M. D., Kim, H. D. and Walsh, W. R.** (1996). Mechanical properties of bat wing membrane skin. *J. Zool.* **239**, 357-378.
- Swartz, S. M., Iriarte-Diaz, J., Riskin, D. K., Song, A., Tian, X., Willis, D. J. and Breuer, K. S.** (2007). Wing structure and the aerodynamic basis of flight in bats. In *AIAA Aerospace Science Meeting*. Reno, NV: AIAA.
- Teeling, E. C., Madsen, O., van den Bussche, R. A., de Jong, W. W., Stanhope, M. J. and Springer, M. S.** (2002). Microbat paraphyly and the convergent evolution of a key innovation in Old World rhinolophoid microbats. *Proc. Natl. Acad. Sci. USA* **99**, 1431-1436.
- Teeling, E. C., Scally, M., Kao, D. J., Romagnoli, M. L., Springer, M. S. and Stanhope, M. J.** (2000). Molecular evidence regarding the origin of echolocation and flight in bats. *Nature* **403**, 188-192.
- Teeling, E. C., Springer, M. S., Madsen, O., Bates, P., O'Brien, S. J. and Murphy, W. J.** (2005). A molecular phylogeny for bats illuminates biogeography and the fossil record. *Science* **307**, 580-584.
- Thabah, A., Li, G., Wang, Y., Liang, B., Hu, K., Zhang, S. and Jones, G.** (2007). Diet, echolocation calls, and phylogenetic affinities of the great evening bat (*Ia io*; Vespertilionidae): another carnivorous bat. *J. Mammal.* **88**, 728-735.
- Thollesson, M. and Norberg, U. M.** (1991). Moments of inertia of bat wings and body. *J. Exp. Biol.* **158**, 19-35.

- Tian, X., Iriarte-Diaz, J., Middleton, K., Galvao, R., Israeli, E., Roemer, A., Sullivan, A., Song, A., Swartz, S. and Breuer, K.** (2006). Direct measurements of the kinematics and dynamics of bat flight. *Bioinspiration & Biomimetics* **1**, S10-S18.
- van der Veen, I. T. and Lindström, K. M.** (2000). Escape flights of yellowhammers and greenfinches: more than just physics. *Anim. Behav.* **59**, 593-601.
- Vaughan, T. A.** (1966). Morphology and flight characteristics of molossid bats. *J. Mammal.* **47**, 249-260.
- Veasey, J. S., Metcalfe, N. B. and Houston, D. C.** (1998). A reassessment of the effect of body mass upon flight speed and predation risk in birds. *Anim. Behav.* **56**, 883-889.
- Voigt, C. C. and Winter, Y.** (1999). Energetic cost of hovering flight in nectar-feeding bats (Phyllostomidae: Glossophaginae) and its scaling in moths, birds and bats. *J. Comp. Physiol. B* **169**, 38-48.
- Wainwright, P. C.** (1991). Ecomorphology: experimental functional anatomy for ecological problems. *Amer. Zool.* **31**, 680-693.
- Wainwright, P. C.** (1994). Functional morphology as a tool in ecological research. In *Ecological morphology: integrative organismal biology* (eds. P. C. Wainwright and S. M. Reilly), pp. 42-59. Chicago: University of Chicago Press.
- Wainwright, P. C. and Reilly, S. M.** (1994). Introduction. In *Ecological morphology: integrative organismal biology* (eds. P. C. Wainwright and S. M. Reilly), pp. 1-9. Chicago: University of Chicago Press.
- Webb, P. I., Speakman, J. R. and Racey, P. A.** (1992). Inter- and intra-individual variation in wing loading and body mass in female pipistrelle bats: theoretical implications for flight performance. *J. Zool.* **228**, 669-673.
- Winter, Y.** (1998). Energetic cost of hovering flight in a nectar-feeding bat measured with fast-response respirometry. *J. Comp. Physiol. B* **168**, 434-444.
- Winter, Y.** (1999). Flight speed and body mass of nectar-feeding bats (Glossophaginae) during foraging. *J. Exp. Biol.* **202**, 1917-1930.
- Winter, Y., von Helversen, O., Norberg, U. M., Kunz, T. H. and Steffensen, J. F.** (1993). Flight cost and economy of nectar-feeding in the bat *Glossophaga soricina* (Phyllostomidae: Glossophaginae). In *Animal-plant interactions in tropical environments* (eds. W. Barthlott C. M. Naumann K. Schmidt-Loske and K.-L. Schuchman), pp. 167-174. Bonn: Museum Koenig.

- Witter, M. S., Cuthill, I. C. and Bonser, R. H. C.** (1994). Experimental investigations of mass-dependent predation risk in the European starling, *Sturnus vulgaris*. *Anim. Behav.* **48**, 201-222.
- Zhang, L., Liang, B., Parsons, S., Wei, L. and Zhang, S.** (2007). Morphology, echolocation and foraging behaviour in two sympatric sibling species of bat (*Tylonycteris pachypus* and *Tylonycteris robustula*) (Chiroptera: Vespertilionidae). *J. Zool.* **271**, 344-351.
- Zook, J.** (2007). Somatosensory adaptations of flying mammals. In *Evolution of nervous systems: a comprehensive reference. Volume 3: Mammals* (eds. J. H. Kaas and L. Krubitzer), pp. 215-226. Boston: Elsevier Academic Press.
- Zook, J. M. and Fowler, B. C.** (1986). A specialized mechanoreceptor array of the bat wing. *Myotis* **23-24**, 31-36.